Membrane-bound IL-6R is Upregulated on Th17 Cells and Inhibits Treg Cell Migration in Autoimmune Arthritis

Inaugural Dissertation

zur

Erlangung des Doktorgrades
Dr. nat. med.

der Medizinischen Fakultät
und
der Mathematisch-Naturwissenschaftlichen Fakultät
der Universität zu Köln

vorgelegt von

Shuaifeng Yan

Aus Henan, China

Hundt Druck GmbH, Köln

2022

Membrane-bound IL-6R is Upregulated on Th17 Cells and Inhibits Treg Cell Migration in Autoimmune Arthritis

Inaugural Dissertation

zur

Erlangung des Doktorgrades
Dr. nat. med.

der Medizinischen Fakultät
und
der Mathematisch-Naturwissenschaftlichen Fakultät
der Universität zu Köln

vorgelegt von

Shuaifeng Yan

Aus Henan, China

Hundt Druck GmbH, Köln

2022

Betreuer:	PD Dr. David Kofler
Referent*innen	Prof. Dr. Sabine Eming
	Prof. Dr. Niels Gehring
Datum der mündlichen Prüfung:	12.09.2022

This thesis was performed at the Department I of Internal Medicine at the University Hospital Cologne under the supervision of PD Dr. David M. Kofler.

“纸上得来终觉浅，绝知此事要躬行”

陆游

“The paper is not shallow until you learn and do it by yourself”

Lu You

ACKNOWLEGEMENT

Firstly, I would like to sincerely thank my supervisor PD Dr. David Kofler, who provided me with the opportunity to join his lab in order to work on a project that I am particularly interested in. I greatly appreciate his support, attention, discussion, patience, and kindness during my stay in Germany. Without the time and great effort he put into this project, I would not have been able to finish it.

My sincere appreciation also goes to my tutors from the IPMM Graduate School, Prof. Dr. Manolis Pasparakis and Prof. Dr. Sabine Eming. I want to thank them for taking the time to provide constructive discussions regarding this project, as well as sharing their experiences for scientific thinking development and the thesis review.

I would also like to thank everyone in AG Kofler for their kind support during my Ph.D. in Cologne. I will always remember the happy moments I spent here. A special thanks to Viktoria, Konstantin, Mara, Eva, Jan, Shela, and Thom who always treated me like family and always helped me in the lab. I would like to express my gratitude to Ph.D. student Qu Jiang from AG Herling, Ph.D. Lisa Rusyn, Ph.D. Anastasia Nikiforov from AG Seeger for their methodical advice and helpful discussions for this project. A big thanks goes to the technician Martina and Ph.D. Nasrin from AG Heildel for their excellent technical support in histology, which was important for this project.

I am very grateful for the support which I got from my friends Jintao, Rulin, Mujie, Eva, Lydia, Joanna, Caro, Ruth, and Marcel. Thank you so much for your help, kindness, patience, and encouragement to pursue my goal.

The greatest appreciation I owe to my wife Shuya, who always encourages, supports and believes in me, as well as respecting every decision I made. I feel extremely lucky to have your by my side during my stay in Germany. It is you who filled the challenging life in Germany with of good memories!!!

Last but not least, my greatest thanks go out to my parents, my elder brother and my sister for all their love. They always believed and encouraged me. It was them who gave me the courage to challenge myself and pursue my dreams abroad.

DANKSAGUNG

Zunächst möchte ich mich bei meinem Betreuer PD Dr. David Kofler aufrichtig bedanken, der mir die Möglichkeit gab, bei ihm an einem Projekt zu arbeiten, das mich besonders interessiert. Ich weiß es sehr zu schätzen, dass er mich während meines Aufenthaltes in Deutschland voll und ganz unterstützte, mir Aufmerksamkeit schenkte, mit mir diskutierte und mir viel Geduld und Freundlichkeit entgegenbrachte. Ohne die Zeit und die große Mühe, die er in dieses Projekt gesteckt hat, hätte ich es nicht zu Ende führen können.

Mein aufrichtiger Dank geht auch an meine beiden Tutoren der IPMM Graduate School, Prof. Dr. Manolis Pasparakis und Prof. Dr. Sabine Eming. Ich danke ihnen dafür, dass sie sich die Zeit genommen haben, konstruktive Diskussionen für dieses Projekt zu führen und ihre Erfahrungen bei der Entwicklung des wissenschaftlichen Denkens sowie bei der Überprüfung der Arbeit zu teilen.

Ich möchte auch allen Mitarbeitern der AG Kofler für ihre freundliche Unterstützung während meiner Promotion in Köln danken. Ich werde mich immer an jeden glücklichen Moment erinnern, den ich hier verbracht habe. Ein besonderer Dank geht an Viktoria, Konstantin, Mara, Eva, Jan, Shela und Thom, die mich immer wie ein Familienmitglied behandelt haben und mir im Labor immer geholfen haben. Ich möchte mich bei Ph.D studentin Qu Jiang von der AG Herling, Dr. Lisa Rusyn und Dr. Anastasia Nikiforov von der AG Seeger für ihre methodischen Ratschläge und hilfreichen Diskussionen für dieses Projekt bedanken. Ein großer Dank geht an die Technikerin Martina und Ph.D. Nasrin von der AG Heildel für ihre hervorragende technische Unterstützung in der Histologie, die für dieses Projekt wichtig war.

Ich bin sehr dankbar für die Unterstützung meiner Freunde, die ich von Jintao, Rulin, Mujie, Eva, Lydia, Joanna, Caro, Ruth und Marcel erhielt. Vielen Dank für eure Hilfe, eure Freundlichkeit, eure Geduld und eure Ermutigung, mein Ziel zu verfolgen.

Die größte Wertschätzung schulde ich jedoch meiner Frau Shuya, die mich immer ermutigt, mich unterstützt, an mich glaubt und jede meiner Entscheidungen respektiert. Ich fühle mich sehr glücklich, dass ich sie während meines Aufenthalts in Deutschland an meiner Seite hatte. Ihr seid es, die das herausfordernde Leben in Deutschland mit schönen Erinnerungen gefüllt haben!!!

Nicht zuletzt gilt mein großer Dank meinen Eltern, meinem älteren Bruder und meiner Schwester für ihre Liebe. Sie haben immer an mich geglaubt und mich ermutigt. Sie waren es, die mir den Mut gaben, mich selbst herauszufordern und meinen Traum im Ausland zu verfolgen.

ABSTRACT

Currently, our understanding of membrane-bound IL-6R (mIL-6R) mediated IL-6 signaling in Th17 cells as well as the interaction between Treg and Th17 cells during the course of rheumatoid arthritis (RA) is limited. Th17 cells are a highly inflammation-inducing cell population in the pathogenesis of RA. The induced inflammation is thought to be closely associated with the activation and the recruitment of many different types of cells, including monocytes, neutrophils, macrophages, and osteoclasts. In addition, reduced regulatory T (Treg) cells frequencies with impaired suppressive properties were also found in RA. In this study, we assessed dynamic changes in membrane-bound IL-6 receptor (IL-6R) expression levels on Th17 cells by means of flow cytometry during the development of collagen-induced arthritis (CIA) in mouse. Subsequently, bioinformatics analysis based on proteomics was performed to evaluate potential pathways affected by altered IL-6R signaling in autoimmune arthritis. Our analysis shows that membrane-bound IL-6R is upregulated on Th17 cells and is inversely correlated with IL-6 serum levels in experimental autoimmune arthritis. Moreover, IL-6R expression is significantly increased on Th17 cells from untreated patients with RA. Interestingly, $CD4^+$ T cells from CIA mice and from RA patients show reduced phosphorylation of vasodilator-stimulated phosphoprotein (VASP). Bioinformatics analysis based on proteomics of $CD4^+$ T cells with low or high phosphorylation levels of VASP revealed that integrin signaling and the related pathways are significantly enriched in cells with low phosphorylation of VASP. Specific inhibition of p-VASP reduces the migratory function of Treg cells but has no influence on effector $CD4^+$ T cells. Importantly, IL-6R blockade restores the phosphorylation level of VASP, thereby improving the migratory function of Treg cells from RA patients. Thus, our results establish a link between IL-6R signaling and phosphorylation of VASP, which controls Treg cell migration in autoimmune arthritis.

ZUSAMMENFASSUNG

Derzeit wissen wir nur wenig über die Rolle der mIL-6R-vermittelten IL-6-Signalübertragung auf Th17 Zellen im Verlauf der rheumatoiden Arthritis (RA) und die Interaktion zwischen Treg-Zellen und Th17-Zellen. Th17-Zellen sind eine stark entzündungsauslösende $CD4^+$ T-Zell-Population in der Pathogenese der RA, von der man annimmt, dass sie eng mit der Aktivierung und Rekrutierung vieler Zelltypen wie Monozyten, Neutrophilen, Makrophagen, Osteoklasten u.a. verbunden ist. Gleichzeitig wurde bei RA eine Beeinträchtigung der Häufigkeit von Treg-Zellen und ihrer suppressiven Eigenschaften festgestellt. In dieser Studie untersuchten wir die dynamischen Veränderungen des membrangebundenen IL-6-Rezeptors (IL-6R) auf Th17-Zellen mittels Durchflusszytometrie während der Entwicklung der kollageninduzierten Arthritis (CIA). In einem nächsten Schritt wurde eine bioinformatische Analyse auf der Grundlage der Proteomik durchgeführt, um potenzielle Signalwege zu bewerten, die von der veränderten IL-6R-Signalgebung bei Autoimmunarthritis betroffen sind. Unsere Analyse zeigt, dass membrangebundenes IL-6R auf Th17-Zellen hochreguliert wird und negativ mit den IL-6-Serumspiegeln bei experimenteller Autoimmunarthritis korreliert. Außerdem ist die Expression von IL-6R auf Th17-Zellen von unbehandelten RA-Patienten deutlich erhöht. Interessanterweise zeigen $CD4^+$ T-Zellen von CIA-Mäusen und RA-Patienten eine verminderte Phosphorylierung von vasodilator-stimuliertem Phosphoprotein (VASP). Eine bioinformatische Analyse auf der Grundlage der Proteomik von $CD4^+$ T-Zellen mit niedriger oder hoher Phosphorylierung von VASP ergab, dass die Integrin-Signalisierung und verwandte Signalwege in Zellen mit niedriger Phosphorylierung von VASP deutlich angereichert sind. Die spezifische Hemmung von p-VASP reduziert die Migrationsfunktion von Treg-Zellen, hat aber keinen Einfluss auf die $CD4^+$ T-Effektorzellen. Wichtig ist, dass eine IL-6R-Blockade das Phosphorylierungsniveau von VASP wiederherstellt und dadurch die Migrationsfunktion der Treg-Zellen von RA-Patienten verbessert. Unsere Ergebnisse belegen somit einen Zusammenhang zwischen der IL-6R-Signalübertragung und der Phosphorylierung von VASP, die die Migration von Treg-Zellen bei Autoimmunarthritis steuert.

TABLE OF CONTENTS

LIST OF FIGURES

LIST OF TABLES

LIST OF ABBREVIATIONS

3D reconstruction	Three dimensional reconstruction
AA	Adjuvant arthritis
Ab	Antibody
Abl	Tyrosine kinase Ab1
ACPA	Anti-citrullinated protein antibody
ACR	American college of rheumatology
ACT	Adoptive cell therapy
ADAM10	A disintegrin and metalloproteinase domain-containing protein 10
ADAM17	A disintegrin and metalloproteinase 17
AIA	Antigen-induced arthritis
AMPK	AMP-activated protein kinase
APCs	Antigen-presenting cells
APS	Ammoniumpersulfat
bDMARDs	Biological disease-modifying anti-rheumatic drugs
BMI	Body mass index
BSA	Bovine serum albumin
BV	Brilliant Violet
CAA	Chloroacetamide
CCL20	Chemokine ligand 20
CCR6	Chemokine receptor 6
CD	Cluster of differentiation
CD127	IL-7 receptor a-chain
CD25	IL-2 receptor a-chain
CFA	Complete Freund's adjuvant
CIA	Collagen-induced arthritis
CO_2	Carbon dioxid
COX-2	Cyclooxygenase-2
CRP	c-reactive protein
CS	Clinical score
csDMARDs	Conventional synthetic DMARDs
CT	Computed tomography
CTF	C-terminal fragment
CTLA-4	Cytotoxic T-lymphocyte-associated protein 4
DAS28	Disease activity score (determined by 28 joint count)
DCs	Dendritic cells
DEPs	Differential expressed proteins

DMARDs	Disease-modifying anti-rheumatic drugs
DMSO	Dimethysulfoxide
DNA	Deoxyribonucleic acid
DTT	Dithiothreitol
EDTA	Ethlenediaminetetraacetic acid
ELISA	Enzyme-linked immunosorbent assay
ESR	Erythrocyte sedimentation rate
EU	European Union
EULAR	European League Against Rheumatism
EVB	Epstein-Barr virus
EVH1	N-terminal homology domain 1
EVH2	C-terminal homology domain
EVs	Extracellular vesicles
FACS	Fluorescence-activated cell sorting
Fc	Fragment crystallizable
FELASA	Federation of European Laboratory Animal Science Association
FITC	Fluorescein isothiocyanate
FoxP3	Forkhead box protein3
Gcs	Glucocorticoids
GO	Gene ontology
GSEA	Gene set enrichment analysis
H&E staining	Hematoxylin and eosin staining
HC	Healthy individuals
HLA	Human leukocyte antigen
HLs	Hindlimbs
IC	Intracellular
IFA	Incomplete Freund’s adjuvant
IFNr	Interferon gamma
Ig	Immunoglobulin
IL-17	Interleukin-17
IL-1R	Interleukin-1 receptor
IL-1β	Interleukin-1 β
IL-23	Interleukin-23
IL-6	Interleukin-6
IL-6R	Interleukin-6 receptor
IL-6Ri	Interleukin-6 receptor inhibitors
ITAM	Immunoreceptor tyrosine-based activation motif
IBD	Inflammatory bowel disease

iTregs	induced regulatory T cells
JAK	Janus kinase
JAKi	Janus kinase inhibitor
KEGG	Kyoto Encyclopedia of Genes and Genomes
mAb	Monoclonal antibody
MACS	Magnetic-activated cell sorting
MAP	Mycobacterium avium paratuberculosis
MAPK	Mitogen-activated protein kinase
mBSA	Methylated bovine serum albumin
MHC	Major histocompatibility complex
mIL-6R	Membrane-bound IL-6 receptor
MMPs	Matrix metallo proteinases
mRNA	Messenger ribonucleic acid
MS	Mass spectrometry
MS	Multiple sclerosis
NES	Normalized enrichment score
NK	Natural killer
NOD	Non-obese diabetic
NSAIDs	Nonsteroidal anti-inflammatory drugs
nTregs	Natural regulatory T cells
PADI4	Peptidy1 arginine deiminase 4
PBMC	Peripheral blood mononuclear cells
PBS	Phosphate buffered saline
PBS-T	Phosphate buffered saline with tween20
PE	Phycoerythrin
PGE2	Prostagliandin E2
PGIA	Proteoglycan-induced arthritis
pH	Potetntia Hidrogenii
PKA	cAMP-dependent protein kinase
PKD1	Protein kinase D1
PKG	Protein kinase G
PRR	Proline rich region
PTPN22	Protein tyrosine phosphatase, non-receptor type 22
pTregs	peripheral regulatory T cells
p-VASP(Ser157)	Vasodilator-stimulated phosphoprotein phosphorylated at site Serine 157
qPCR	Quantitative real-time PCR
RA	Rheumatoid arthritis

RANKL	Receptor activator of nuclear factor kappa-B lignad
RA un	Rheumatoid arthritis untreated
RhF	Rheumatoid factor
RORrt	Retinoic acid receptor-related orphan receptor gamma
RNA	Ribonucleic acid
rpm	Revolutions per minute
SHP2	JAK-SH2 domain tyrosine phosphatases
sIL-6R	Soluble interleukin-6 receptor
SLE	Systemic lupus erythematosus
SSZ	Sulfasalazine
STAT	Signal transducer and activator of transcription
STAT4	Signal transducer and activator of transcription 4
TAE	Tris-acetate-EDTA
TCR	T cell receptor
TGF-β	Transforming growth factor β
Th	T helper
TNF	Tumor necrosis factor
Treg	Regulatory T cells
Tris	Tris(hydroxymethyl)aminomethane
tsDMARDs	Targeted synthetic DMARDs
U	Unit
UNG	Uracil-N glycosylase
VASP	Vasodilator-stimulated phosphoprotein
WB	Western blot
WT	Wide type
X-vivo	Serum free, haematopoietic media

1 INTRODUCTION

1.1 Rheumatoid arthritis

1.1.1 Etiology

Rheumatoid arthritis (RA) is the most common form of autoinflammatory arthritis characterized by chronic inflammation in multiple joints, leading to synovitis, cartilage destruction, as well as bone erosion (Smolen, Aletaha, and McInnes 2016; Chang and Nigrovic 2019). Joint destruction can lead to disability, a reduction in quality of life as well as life expectancy, and an increased burden for the healthcare system. RA affects about 1% of the global population, can occur at any age and affects women two to three times more often than men (Almutairi et al. 2021; Cross et al. 2014; Helmick et al. 2008). So far, intensive research has been done and important progress has been made to define the cause of RA, leading to an improved understanding of the involved pathogenic mechanisms (Su et al. 2019; Noack and Miossec 2014; Wang et al. 2015). However, the etiology of RA remains in part unclear. At present, it is believed that the disruption of self-tolerance is essential for the initiation and development of RA, the immune system cannot distinguish bewteen microbial- and self-antigens, resulting in the targeting of healthy tissue.

The risk of developing RA is thought to be related to a combination of hereditary, environmental and other factors (Scherer, Häupl, and Burmester 2020), which are shown in Table 1. Genome sequencing has been used for RA research during the past 10 years and more than 300 genes have been identified as genetic risk variants for RA (Okada et al. 2014). These genes include human leukocyte antigen (HLA), non-receptor type 22 (PTPN22), chemokine receptor 6 (CCR6), peptidy1 arginine deiminase 4 (PADI4), protein tyrosine phosphatase, signal transducer and activator of transcription 4 (STAT4), and CTLA4 (Stastny 1978; Verpoort et al. 2005; Huizinga et al. 2005; Hammer et al. 1995). In addition, the analysis of RA-associated genes revealed the top three pathways involved in the pathogenesis of RA: JAK-STAT singnaling, NF-κB signaling, and T-cell receptor signaling pathways. Interestingly, most of these genes are not specific to the development of RA. They are reported to also be associated with other autoimmune diseases, such as systemic lupus erythematosus (SLE), type 1 diabetes and Graves' disease. Targeting risk genes is a promising approach for the treatment of RA, as shown by the success of JAK inhibitors.

Environmental factors are thought to be important contributors to the break of immune tolerance and have been associated with the development of RA-associated autoantibodies.

These environmental factors include cigarette smoking (Terao et al. 2014; Ospelt et al. 2017; van Wesemael et al. 2016). Moreover, meta-analysis revealed an association between obesity and RA, particularly among women with a high body weight index (BMI) (Zhou and Sun 2018), but the underlying mechanism remains unknown (Dar et al. 2018). Furthermore, children whose mothers smoked have a two-fold increased risk of developing RA due to early cigarette smoke exposure. Evidence also shows that Epstein-Barr virus (EBV) and Mycobacterium avium paratuberculosis (MAP) may be involved in the pathogenesis of RA, which is thought to have a cross-talking relationship with autoantibodies (Bo et al. 2018).

The incidence of RA reaches its peak in the sixth decade of life, even though the onset it can occur at any age. It has been reported that ACPA in healthy, first-degree relatives of RA patients was elevated with age, especially in postmenopausal women (Alpizar-Rodriguez et al. 2017). Interestingly, a significant gender difference was observed, with a higher incidence of RA for females as compared to males. The underlying mechanism for this sex-discrepancy remains unknown, but reproductive load may play a role in altering susceptibility to autoimmunity in females. To sum up, these factors are thought to disrupt the interactions between components of both the adaptive and the innate immune system in the occurrence of RA (Scherer, Häupl, and Burmester 2020).

Table 1 The factors involved in the etiology of RA

Gene factors	Environmental factors	Others factors
HLA-DR	Infections	Age
PTPN 22	Smoking	Gender
CTLA4	Obesity	Reproductive load
PADI4	Dust exposure	
CCR6	Early life exposure to cigarette smoke	
STAT4		

1.1.2 Clinical manifestation

The classical clinical manifestation of RA include early morning stiffness and pain in small joints such as the wrists as well as metacarpophalangeal and proximal interphalangeal joints of the hands,however, large joints including knees and hips can also be affected. This morning stiffness and pain can last for more than one hour in the morning. An important indicator of disease progression is the number of tender or swollen joints (DAS28 score). Plain X-rays can provide radiological evidence of bone erosion caused by RA, although it may be absent in the early stage of the disease. However, the combination of C-reactive protein (CRP) serum concentration, rheumatoid factor and ACPA provides more sensitivity and specificity for RA

diagnosis. Therefore, the clinical features, serological examination and radiological scan should be considered for RA diagnose. The detailed diagnostic criteria for RA diagnosis are listed in Table 2, as published by the American College of Rheumatology and the European League Against Rheumatism (EULAR). Patients that have a total score of more than 6 in four categories including joint involvement, acute-phase reactants, serology, and symptoms duration will be diagnosed with RA.

Table 2 The 2010 American College of Rheumatology/European League Against Rheumatism classification criteria for rheumatoid arthritis

	Score		Score
A. joint involvement		**C. Acute-phase reactants**	
1 large joint	0	Normal CRP& ESR	0
2-10 large joints	1	Abnormal CRP & ESR	1
1-3 small joints	2	**D. Duration of symptoms**	
4-10 small joints	3	＜6 weeks	0
＞10 joints (at least 1 small joint)	5	＞6 weeks	1
B. Serology			
Negative RF & ACPA	0	Add score of categories A-D	
Low positive RF/ACPA	2	≥6/10=definite RA	
High positive RF/ACPA	3		

This table was modified from Aletaha et al, 2010.

1.1.3 Current options for treatment

Currently, conventional synthetic disease modifying antirheumatic drugs (DMARDs), targeted synthetic DMARDs and biological DMARDs are widely used in clinical practice. If no signs and symptoms of inflammatory activity are found, the patient is considered to be in remission (Smolen et al. 2010). Even though the current treatment strategies for RA based on suppression of autoimmune inflammation, have significantly improved clinical symptoms and postponed destructive progress (Maini et al. 1998; Feldmann and Maini 2003), approximately 30% of RA patients still don't show an adequate response to the currently available treatments well (Feldmann and Maini 2003). Table 3 shows the current treatment options available for RA.

Conventional synthetic DMARDs (csDMARDs) are recommended as the first line treatment approach for RA by the European League Against Rheumatism (EULAR) as they provide a significant improvement of disease activity or are able to induce remission (Emery, Breedveld, et al. 2008; Nandi, Kingsley, and Scott 2008; Plosker and Croom 2005; Dougados et al. 2003). There are several choices available in this category, such as MTX, Leflunomide, Sulfasalazine (SSZ), and others. Certain enzymes involved in DNA formation, repair, as well as

development can be blocked by csDMARDs. Additionally, csDMARDs combined with GCs show better clinical results (Goekoop-Ruiterman et al. 2007; Möttönen et al. 1999), this has to be weighed against side effects caused by long-term GC use (Hoes et al. 2009). Following the EULAR guidelines, any delay in starting the treatment of RA patients could lead to a worse outcome as compared to an early intervention which is started as soon as the diagnosis is established (Gaffo, Saag, and Curtis 2006; Lard et al. 2001).

Table 3 Main available medication for RA treatment

Category	Mechanism	Generic name
Conventional synthetic DMARDs (csDMARDs)	Inhibit DNA formation, repair and development	Methotrexate, Leflunomide, Sulfasalazine, Hydroxychloroquine
Targeted synthetic DMARDs (tsDMARDs)	JAK inhibitor	Baricitinib, Tofacitinib, Upadacitinib, Filgotinib
Biological originator DMARDs	TNF inhibitor	Adalimumab, Certolizumab, Etanercept, Golimumab, Infliximab
	IL-6R inhibitor	Tocilizumab, Sarilumab
	IL-6 inhibitor	Sirukumab, Olokizumab, Situximab, Clazakizumab,
	IL-1R inhibitor	Anakinra
	Co-stimulation (CTLA-4) inhibitor	Abatacept
	Anti-CD20	Rituximab

JAK inhibitors are considered to be targeted synthetic DMARDs (tsDMARDs) and have been used for the treatment of RA in the EU over the last five years. Their safety and efficacy has been studied in long-term clinical trials as well as through the analysis of real-world data (Wollenhaupt et al. 2019; Keystone et al. 2018; Taylor et al. 2019). Therefore, tsDMARD have been included in the EULAR/ACR recommendations for patients with a limited or no response to csDMARDs treatment.

TNF-α leads to the production of a series of pro-inflammatory cytokines and is thought to be able to activate osteoblasts and effector cells. Therefore, it is involved in the cartilage damage and bone erosion in RA. Considering the role of TNF-α in RA pathogenesis, TNF-α inhibitors were tested in clinical trials and showed promising outcomes. The clinical application proved successful for the treatment of RA, especially in combination with MTX (Klareskog et al. 2004; Breedveld et al. 2006).

The inhibitors targeting IL-6 signaling consist of IL-6 inhibitors including sirukumab, olokizumab, situximab, and IL-6 receptor inhibitors including tocilizumab and sarilumab. Tocilizumab is shown to be more effective when compared to a DMARD monotherapy (Jones

et al. 2010). Combined with MTX, IL-6 receptor inhibitors show superior efficacy in reducing disease activity after 4 months as compared to MTX monotherapy. Importantly, Tocilizumab is particularly effective for patients who respond poorly to TNF-α inhibitors (Emery, Keystone, et al. 2008).

Even though the number of clinical trials with IL-1R inhibitor anakinra is limited (Cohen et al. 2002; Gartlehner et al. 2006), the anakinra shows a significant improvement in persistent active RA patients when compared to MTX alone. Abatacept binds to CD80/CD86 on the surface of antigen-presenting cells, which inhibit the activation of T lymphocytes. Rituximab can lead to the depletion of B cells by specifically binding to the antigen CD20.

Apart from the above mentioned treatments, nonsteroidal anti-inflammatory drugs (NSAIDs) are also widely used as an additional treatment of RA. Nevertheless, about 30% of patients who respond poorly to all current management approaches and it is necessary to develop new treatments for RA (Smolen et al. 2020).

1.2 T cells and their roles in rheumatoid arthritis

1.2.1 T cells development and $CD4^+$ T cell differentiation

1.2.1.1 Intrathymic T cell development

T lymphocytes are generated from bone marrow progenitors cells which then migrate to the thymus. The developing progenitors in the thymus are also known as thymocytes. They interact with stromal cells in the thymus, which is necessary for their maturation and selection, finally the matured T cells will be transferred to the periphery (Kumar, Connors, and Farber 2018). The thymus consists of the cortex (outer region) and medulla region (inner region). In the earliest stage of developing thymocytes, neither CD4 nor CD8 is not expressed and T cells are classified as double-negative (DN) cells. There are four subpopulations of DNs, classified by the expression of CD44 and CD25 as follows: $CD44^+CD25^-$ cells, $CD44^+CD25^+$ cells, $CD44^-CD25^+$ cells, and $CD44^-CD25^-$ cells. A process called β-selection occurs in the $CD44^-CD25^+$ subset of cells, selecting for the successful rearrangement of the TCR-β chain locus. Cells that failed to undergo β-selection die by apoptosis. TCR-β chain contributes to the pre-TCR complex which binds to CD3 and results in the survival and differentiation by upregulating CD4 and CD8. In the cortex, $CD4^+CD8^+$ cells (DPs) rearrange and produce αβ-TCR, therefore further undergoing positive selection. These cells then migrate to the medulla for future negative selection. After maturation and a series of selections, only naive $CD4^+$ or

$CD8^+$ cells that have a proper affinity to antigens or APCs finally survive, exit the thymus and circulate to the periphery (Zúñiga-Pflücker 2004).

1.2.1.2 $CD4^+$ T cell differentiation in the periphery

Human $CD4^+$ T cell development, differentiation and maintenance are variable throughout the course of a lifetime. Naïve $CD4^+$ T cells in the peripheral blood can respond to new antigens and memory T cells subsequently differentiating into different subsets (Kumar, Connors, and Farber 2018). Moreover, $CD4^+$ T cells have the potential to develop into different T helper (Th) subpopulations dependent on environmental factors the cells are exposed to. Normally, naive $CD4^+$ T cells are relatively quiescent cells and their TCR is inactive due to a lack of stimulation. With the cytokines IL-6 and TGF-β, antigen-presenting cells can stimulate high expression of the transcription factor retinoic acid receptor-related orphan receptor gamma (RORγt), promoting the differentiation of naïve $CD4^+$ T cells into Th17 cells (Park et al. 2005). However, TGF-β alone induces the differentiation of Treg cells by upregulating the expression of transcription factor Forkhead box protein3 (Foxp3) (Chen et al. 2003). In the presence of IL-12, naive $CD4^+$ T cells differentiate into Th1 cells, driven by activated STAT4 (Hsieh et al. 1993). Th22 cell differentiation is poorly understood. It is suspected that IL-6 and tumor necrosis factor (TNF) are important in this process (Raphael et al. 2015). The activation of STAT6 by IL-4 is reported to be important for the differentiation of Th2 cells (Sokol et al. 2008). Furthermore, naïve $CD4^+$ T cells differentiate into Th9 cells in the presence of IL-4 and TGF-β (Tripathi and Lahesmaa 2014).

1.2.2 Th17 cell subset in physiology and pathology

In healthy individuals, the frequency of Th17 cells is limited in the peripheral blood as they mainly locate on the mucosal surface of the intestine and lung in a microbiota-dependent manner (Stockinger and Omenetti 2017). Th17 cells are reported to participate in the defense against pathogenic microbes and maintain tissue homeostasis by producing IL-17. The differentiation of Th17 cells is initiated from naive $CD4^+$ cells by APCs and certain cytokines (Park et al. 2005). Importantly, excessive activation of Th17 cells can lead to inflammation and autoimmune disease.

In RA, Th17 cells are significantly increased both in peripheral and inflamed synovial fluid, and they are thought to be correlated with disease activity in RA (Leipe et al. 2010; Penatti et al. 2017; van Hamburg et al. 2011; Zizzo et al. 2011). In addition, they are involved in the development of fibroblast-like tissue, which contributes to synovitis, cartilage damage and

bone erosion (van Hamburg and Tas 2018). Th17 cells were shown to recruit many different types of cells at inflammatory sites including neutrophils and activate B cells, furthermore Th17 cells also promote osteoclastogenesis (Azizi, Jadidi-Niaragh, and Mirshafiey 2013; Kaplan 2013). Th17 cells secret the pro-inflammatory cytokine IL-17, which has a strong effect in recruiting leukocytes, activating many types of cells which are involved in the pathogenesis of RA as well as inducing pro-inflammatory cytokines production in stromal cells. Moreover, Th17 cells also produce other pro-inflammatory cytokines including IL-22, TNF-α, GM-CSF, and IFN-γ. These molecules can further induce the production of IL-6, IL-8, IL-1β, PGE2, and MMPs, which contributes to the pathology of RA (van Hamburg and Tas 2018).

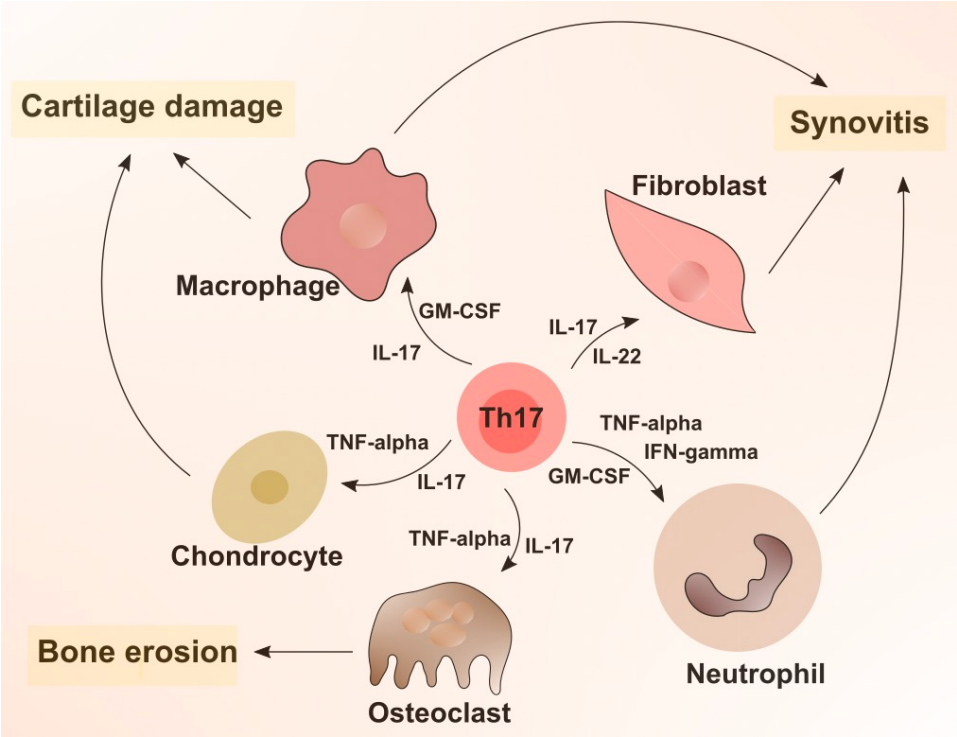

Figure 1 The role of Th17 cells in the pathology of RA

Schematic view of the inflammatory roles of Th17 cells in the pathogenesis of RA. Th17 cells secret a series of pro-inflammatory cytokines: IL-17, IL-22, TNF-α, GM-CSF, and co-express IFN-γ, which contribute to synovitis, cartilage damage and bone erosion by interacting with macrophages, fibroblasts, neutrophils, osteoclasts, and chondrocytes in the inflamed synovial tissue.

1.2.3 The regulatory T cell subset in physiology and pathology

Treg cells are most abundant in the early stages of life, after which they decrease in frequency throughout childhood then reach a stable low level of frequency in adults (Thome et al. 2016). Treg cells only account for approximately 5-10% of $CD4^+$ T cells (Okeke and Uzonna 2019)

and are classically comprised of three different subsets: natural Treg cells (nTregs) derived from the thymus, peripheral Treg cells (pTregs) generated in vivo in peripheral lymphoid organs, and induced Treg cells (iTregs) that are differentiated ex vivo (Campbell and Koch 2011). Each of the subgroups has protective properties and prevents autoimmunity by inhibiting immune cell overactivation and proliferation (Okeke and Uzonna 2019).

Treg cells are characterized by the transcriptional factor Foxp3 and by cell surface expression of CD25 (IL-2 receptor) as well as a low expression level of the cell surface marker CD127. FoxP3 is the major transcription factor maintaining Treg cell stability and function (Zheng et al. 2010). It is reported that deficiency of Tregs or mutations in FoxP3 can lead to autoimmune disorders both in mice and in humans (Huter et al. 2008). The suppressive activity of Treg cells is mediated through different mechanisms, including cytokine production, direct cell-cell contact suppression and the regulation of antigen presenting cells (APCs) which induces effector T cell apoptosis and immunosuppression (Wing and Sakaguchi 2012; Shevach 2009; Putnam et al. 2009; Okeke and Uzonna 2019; Thornton and Shevach 1998). High levels of IL-10 and TGF-β are expressed by Treg cells once they are stimulated, and these cytokines are reported to exert important functions in suppressing the proliferation and activation of effector T cells in both human and murine models (Nakamura, Kitani, and Strober 2001; Vignali, Collison, and Workman 2008). In addition, TGF-β is thought to contribute to Treg cell development and maintenance of function (Marie et al. 2005). Cytotoxic T-lymphocyte-associated antigen 4 (CTLA-4) is highly expressed on Treg cells (Wing et al. 2008) and can decrease the co-stimulation level of CD80 as well as CD86 on APCs, thereby reducing the activation level as well as proliferation of naive T cells both *in vivo* and *in vitro* (Onishi et al. 2008). Like CTLA-4, the transmembrane protein lymphocyte activation gene-3 (LAG-3) binds major histocompatibility complex class II (MHC II) on antigen presenting cells and inhibits dendritic cells (DCs) activation through an immunoreceptor tyrosine-based activation motif (ITAM) mediated inhibitory signaling pathway (Liang et al. 2008). Moreover, Treg cells also disrupt the metabolism of target cells through a strong expression of CD25. As a ligand of CD25, IL-2 is important for the activation and proliferation of effector T cells. Therefore, the competitive consumption of IL-2 by Treg cells has been thought to suppress the effector T cells' function and mediate disruption of effector T cells' metabolism, leading to immunosuppression and effector T cells death (de la Rosa et al. 2004; Thornton and Shevach 1998). Treg cells also mediate immunosuppression by the ectonucleotidases CD39 and CD73. CD39 is constitutively expressed on Treg cells and can hydrolyze ATP and ADP (Bours et al. 2006). It also acts together with CD73 to produce adenosine (Borsellino et al. 2007). Once

bound to the adenosine receptor A2A on activated T cells (Ohta and Sitkovsky 2001), adenosine can induce metabolic disruption through the following mechanism: cyclic adenosine monophosphate (cAMP) in Treg cells drives the inhibition of T cell proliferation and promotes the synthesis of IL-2 by gap junction formation, which prevents the production of proinflammatory cytokines in effector T cells (Bopp et al. 2007). Furthermore, the CD28 superfamily member PD-1 binds to its ligands, thereby preventing the proliferation and IFN-γ production in T cells (Fife and Pauken 2011). Importantly, granzyme B expressing Treg cells have cytotoxic effects on effector T cells (Grossman et al. 2004), in addition the apoptosis of effector T cells can be induced by Treg cells in a cell-cell contact dependent manner (Gondek et al. 2005). These suppressive pathways work together to mediate the cell contact-dependent suppressive function of Treg cells (Figure 2).

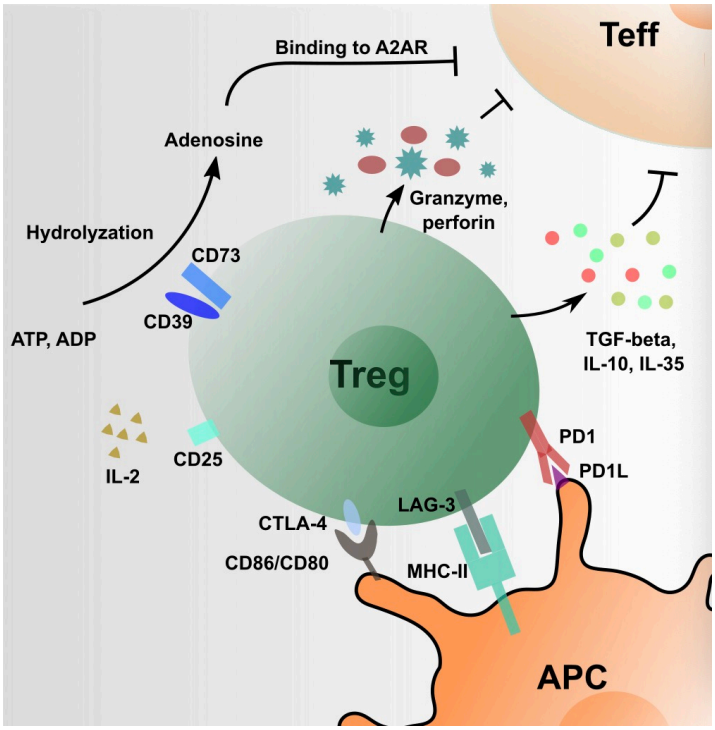

Figure 2 The mechanisms of immunosuppressive function mediated by Treg cells

Treg cells secrete the cytokines TGF-β, IL-10 and IL-35 to directly inhibit the activation and proliferation of effector T cells. CTLA-4, LAG-3 and PD1 on Treg cells mediate the downregulation of APC cell functions, which prevents the activation of naïve T cells and effector T cells. CD25 expressed on Treg cells sequesters IL-2 that is necessary for T cell in the periphery, thereby preventing their activation and proliferation. Adenosine produced by the hydrolyzation of CD39 and CD73 from ATP or ADP binds to the A2A receptor on effector T cells, thereby inhibiting proliferation and the production of inflammatory cytokines. Treg cells also mediate the cytolysis of effector T cells through granzymes and perforin. This diagram was modified from Yan et al. (manuscript under revision).

In RA, Treg cell frequencies in the periphery and in the synovial fluid remain controversial (van Amelsfort et al. 2004; Jiao et al. 2007; Möttönen et al. 2005). This might be caused by different approaches used in identifying Treg cells. In the early stages of RA onset, Treg cells seem to be significantly decreased in the peripheral blood (Lawson et al. 2006). Treg cells are reported to accumulate in the synovial fluid and synovial membrane of inflamed joints (Moradi et al. 2014). The altered distribution of Treg cells in the synovium and synovial tissue, as well as in the periphery might affect the cell contact mediated immunosuppressive properties of Treg cells in RA (Behrens et al. 2007). In addition, Treg cells are shown to have limited suppressive function at inflammatory sites due to IL-6 overexpression (Flores-Borja et al. 2008). These FoxP3$^+$ cells lose their inhibitory activity in the synovial fluid (Li et al. 2017). Therefore, the decrease of Treg cells in the peripheral blood and the dysregulation of Treg cell function is thought to be important for the disruption of immune tolerance, leading to autoimmunity.

1.2.4 Interplay between Th17 and Treg cells in rheumatoid arthritis

The balance between Th17 cells and Treg cells is important in maintaining immune tolerance under physiologic conditions. A Th17 superiority, disrupted Treg cell frequency or disrupted Treg cell function is linked to autoimmune disorders, for example, multiple sclerosis (Viglietta et al. 2004), psoriasis (Martin et al. 2013), RA (Kaneko et al. 2018), inflammatory bowel disease (IBD) (Skroza et al. 2013) and SLE (Martin, Baeten, and Josien 2014). Normally, Th17 cells are important in maintaining tissue homeostasis as well as combatting foreign substances, however, overactivation of this subset leads to autoimmunity. Similarly, a lack of Treg cells can induce a disruption of self-tolerance and lethal autoimmunity in humans.

TGF-β is essential for the induction of the transcription factors RORγt and FoxP3 and is therefore important in the differentiation of Th17 cells and Treg cells, respectively. TGF-β itself drives naive CD4$^+$ T cells to differentiate into Treg cells in the presence of IL-2, while it promotes the differentiation of Th17 cells in the presence of IL-6 (Bettelli et al. 2006; Veldhoen et al. 2006; Zhou et al. 2007). Therefore, TGF-β, IL-2 as well as IL-6 can influence the balance between Th17 cells and Treg cells in the immune system (Knochelmann et al. 2018). In addition, both subsets show dynamic plasticity following the influences of the external environmental factors, which makes the interplay between both subsets complex (Knochelmann et al. 2018). It is reported that with exposure to IL-6, with or without IL-1β and IL-23 present, FoxP3$^+$ Treg cells can downregulate their expression of FoxP3 and express more Th17 genes including but not limited to IL-17, IL-23 receptor and RORγt. These Treg

cells are characterized by an impaired ability to suppress Th17 cells and cytotoxic T cells in autoimmune arthritis. Of note is that infiltrating T cells in ovarian tumor which express IL-17 show the ability to transdifferentiate into FoxP3$^+$ T cells, and this phenomenon is thought to be independent of prostaglandin E_2 (PGE_2) and TGF-β (Downs-Canner et al. 2017). Therefore, modulating the immunological balance between both subsets may represent a promising option in restoring self-tolerance. However, it still remains unclear how both cell populations interact with one another in RA. In addition, the underlying mechanisms of IL-6 signaling inhibitors provided improvement in RA patients, as well as the role of IL-6 signaling. However, mIL-6R mediated IL-6 signaling in T cell specific subsets in the pathogenesis of RA remains unclear. More investigations are required to better understand these mechanisms. Figure 3 shows the relationship between Th17 and Treg cells.

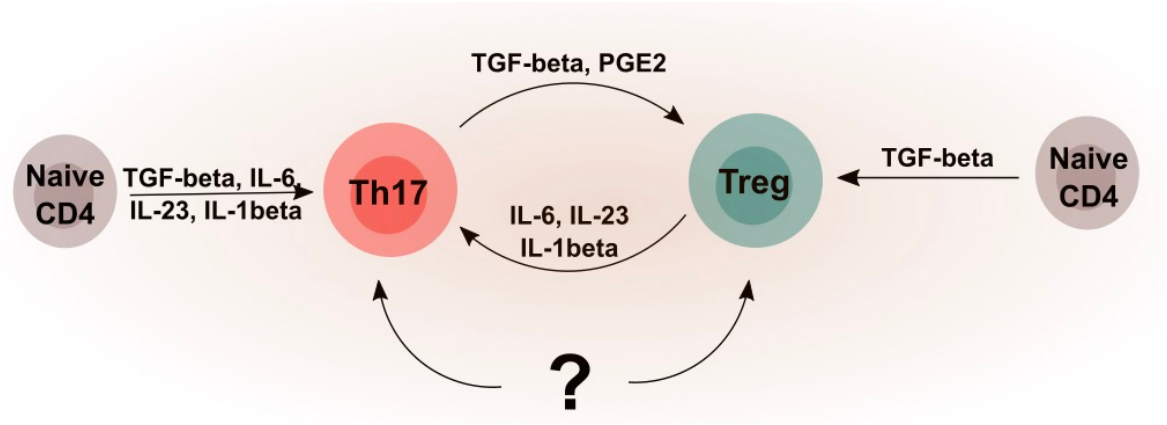

Figure 3 The balance between Treg cells and Th17 cells.
Th17 cells and Treg cells can differentiate from naïve CD4$^+$ T cells under different cytokines conditions. Both subsets have the potential to transdifferentiate to the other CD4$^+$ T subsets. Shown here are the conditions and interactions involved in Th17 and Treg differentiation. Given the importance of both subsets in autoimmunity, further research on the interactions of both subpopulations is warranted.

1.3 Interleukin-6 signaling

1.3.1 Interleukin-6 and its pleiotropic effects

IL-6 is a 26 kDa secreted cytokine with pleiotropic effects in many biological and pathological processes (Arnold et al. 2020). It is secreted by various types of cells including monocytes, B cells, fibroblasts, and other types of cells. IL-6 is synthesized for tissue repair during the innate immune response, and it plays an important role in naïve CD4$^+$ T cell differentiation, proliferation as well as antibody production by plasma cells in the adaptive immune response

(Bettelli et al. 2006). IL-6 is crucial for maintaining of the balance between osteoblasts and osteoclasts (De Benedetti et al. 2006). IL-6 has also been found to play a protective role in liver injury and intestinal epithelial-cell proliferation (Gewiese-Rabsch et al. 2010; Taniguchi et al. 2015). Emerging data also suggests that IL-6 is involved in the regulation of metabolism, for example though anti-obesity effects in lipid metabolism and insulin resistance (Timper et al. 2017; Kraakman et al. 2015). In the early stage of infection and tissue injury, IL-6 is rapidly produced to maintain immune defense. However, over-production and dysregulation of IL-6 receptor signaling can be involved in disease pathogenesis.

1.3.2 Interleukin-6 receptors

As the ligand of IL-6, IL-6 receptor has two forms, the 80 kDa transmembrane protein and the 50-55 kDa soluble form (sIL-6R) (Hibi et al. 1990). Membrane-bound IL-6 receptor is mainly found on lymphocytes as well as hepatocytes, whereas sIL-6R can travel anywhere by circulating in the peripheral blood. Furthermore, the sIL-6R can bind to cells that do not express the mIL-6 receptor. sIL-6R is shed from membrane-bound IL-6R by adamalysin proteases ADAM metalloproteinase 17 (ADAM17) and ADAM metalloproteinase 10 (ADAM10) (Nishimoto et al. 2007). The plasma level of sIL-6R is increased in a multitude of inflammatory states. However, the sIL-6R form enables the cells which lack mIL-6R on the cell surface to respond to the IL-6, subsequently activating associated downstream signals in targeted cells. The sIL-6R is thought to be important to contribute to the broad biological functions of IL-6.

Currently, three different modes of IL-6 signaling have been revealed: the classic signaling mode, trans-signaling mode and trans-presentation signaling mode (Nowell et al. 2009). The combination of IL-6 and IL-6 receptor requires gp130, a transmembrane protein which serves as a signal transducer to initiate IL-6 signaling (Kishimoto, Akira, and Taga 1992). As the subunit of the complex of IL-6 and IL-6 receptor, gp130 is expressed ubiquitously in the human body. Classic signaling is mediated by mIL-6R and gp130, therefore it only occurs in cells expressing the mIL-6 receptor. Trans-signaling is mediated by the binding of sIL-6R, the complex of sIL-6R and IL-6 can then activate the cells that do not express IL-6 receptor on the cell surface. The third IL-6 signaling model which is termed as IL-6 trans-presentation is observed in the interplay between Th17 cells and DCs (Heink et al. 2017). It is reported that the complex of IL-6 and mIL-6r on DCs can be functioned as a ligand for gp130 on pathological Th17 cells. It was reported that Th17 cell-driven inflammation by means of IL-17 production can be enhanced by increased IL-6 receptor levels on $CD4^+$ T cells in autoimmune diseases (Saini et al. 2020). Recently, another IL-6 signaling model has been reported, which

is mediated by mIL-6R on extracellular vehicles (EVs). These mIL-6R can be transported and fused with cells that do not express IL-6R, therefore initiating the downstream signaling (Arnold et al. 2020). Figure 4 shows the three different modes of IL-6 signaling.

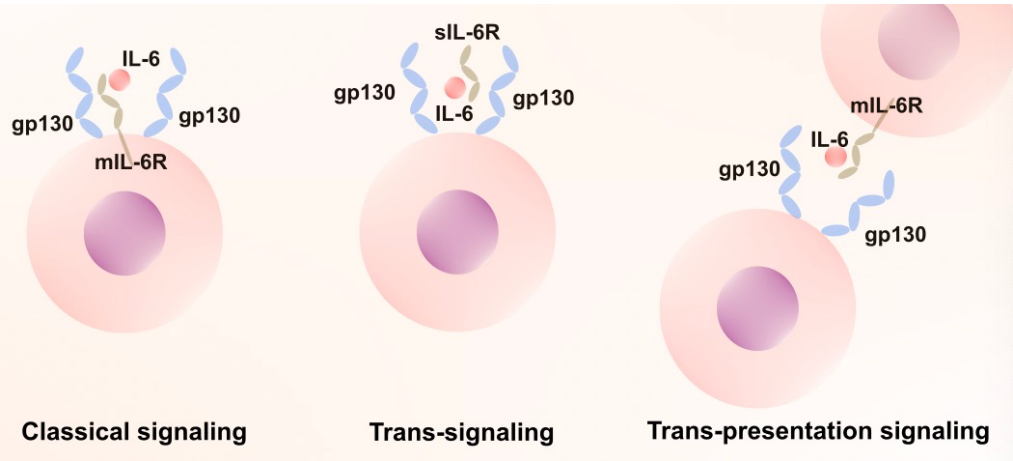

Figure 4 Three modes of IL-6 signaling

Three modes of IL-6 signaling: Classic signaling, Trans-signaling, and Trans-presentation. Classical signaling occurs in a limited number of cells that express membrane-bound IL-6R. Trans-signaling makes it possible for those cells that only express gp130 to activate IL-6 signaling pathways through soluble IL-6R. Trans-presentation signaling provides an alternative approach to activate IL-6 signaling by presenting the complex of IL-6 and mIL-6R to cells. All of the three different modes of IL-6 signaling can activate the downstream signal pathways in the cells. This diagram was modified from Hodes et al, 2016.

1.3.3 The downstream pathways of Interleukin-6 signaling

Once activated, IL-6 signaling leads to the phosphorylation of tyrosine kinases of the Janus kinase (JAK) family, and signal transducer and activator transcription 3 (STAT3) with subsequent recruitment and activation (Kimura and Kishimoto 2010). The JAK-SH2 domain tyrosine phosphatases (SHP2) mitogen-activated protein kinase (MAPK) pathway is also activated, making them the two main IL-6 mediated signaling pathways.

1.3.4 Interleukin-6 signaling in RA

IL-6 and sIL-6R are elevated in both the serum and synovial fluid of affected joints in RA and correlate with disease activity and joint destruction (Madhok et al. 1993; Sack et al. 1993). IL-6 is rapidly elevated in human serum in response to TNF, IL-1β, prostaglandins, and stress mediators (Hunter and Jones 2015). In RA-like disease models including antigen-induced arthritis (AIA) mouse model and collagen II-induced arthritis (CIA) mouse model, IL-6 is crucial for arthritis development (Ohshima et al. 1998). IL-6 plays a crucial role in RA, involves the

JAK/STAT3 signaling pathway and drives the differentiation of pathologic Th17 cell from naïve $CD4^+$ T cells together with other cytokines including IL-1β, TGF-β and IL-23 (Weaver et al. 2007; O'Shea and Paul 2010). IL-6 deficient mice are resistant to arthritis and blockade of IL-6 improves joint swelling as well as inhibiting the infiltration of inflammatory cells into inflamed joints (Fujimoto et al. 2008). IL-6 increases synoviocyte proliferation thereby promoting osteoclastogenesis in the presence of sIL-6R by inducing receptor activator of nuclear factor kappa-B lignad (RANKL) expression (Hashizume, Hayakawa, and Mihara 2008). It also increases the production of matrix metalloproteinases (MMPs), which contributes to cartilage damage in RA (Suzuki et al. 2010).

The elevated level of IL-6 and its dysregulation in RA makes IL-6 an interesting therapeutic target. Two approaches make blocking IL-6 feasible, either by directly blocking the cytokine IL-6 itself or by targeting its receptor. Blocking IL-6 leads to the accumulation of the complex of IL-6 and antagonist in the serum, which causes fever and fatigue in patients. The IL-6 receptor inhibitors also block IL-1 (a cytokine belonging to IL-6 family), which also finds importance in the pathology of RA (Avci, Feist, and Burmester 2018). Interestingly, IL-6 blockade is very effective and improves the overall response especially in RA patients who respond poorly to anti-TNF-α antibodies. Blockade of IL-6 signaling for the treatment of RA has proven successful in clinical practice. Taking the numerous pleiotropic functions of IL-6 into consideration there are concerns for adverse effects, especially infections in response to IL-6 signaling blockade (Hennigan and Kavanaugh 2008; Maini et al. 2006). The prevalence of severe infections was reported to be as high as 6.98/100 patient-years in RA patients who received treatment with tocilizumab (one of the IL-6R inhibitors). It is observed that treatment with tocilizumab leads to neutropenia in RA (Nishimoto et al. 2004), in contrast to the treatment with TNF-α inhibitors. Recently, Harbour et al. reported the importance of continued classical IL-6 signaling for both Th17 cells development and the transcriptional and functional identity in different mouse models of colitis (Harbour et al. 2020). Although the role of IL-6 signaling in Th17 cell induction has been clarified (Harrington et al. 2005; Bettelli et al. 2006), it remains poorly understood how mIL-6R-mediated signaling in Th17 cells affects Treg cells in RA.

1.4 Vasodilator-stimulated phosphoprotein (VASP)

1.4.1 Introduction of VASP

Vasodilator-stimulated phosphoprotein (VASP) belongs to Ena/VASP family, consisting of N-terminal homology domain 1 (EVH1), C-terminal homology domain 2 (EVH2), and a central proline-rich region (PRR) (Blume et al. 2007) (Figure 5). It was first detected in platelets and endothelial cells (Halbrügge and Walter 1989), after which high expression were found in the spleen, stomach, intestine, and other organs (Gambaryan et al. 2001). The phosphorylation of VASP is an important post-translational modification, shown to control all aspects of VASP functioning (Döppler and Storz 2013). For example, it reduces its association with actin thereby inhibiting actin polymerization, and finally results in reduced motility of cells. It is also found to have a regulatory role in fibroblasts and cancer cells migration (Krause and Gautreau 2014; Sechi and Wehland 2004; Trichet, Sykes, and Plastino 2008). Five phosphorylation sites have been reported: Tyr 39, Ser157, Ser239, Thr278, and Ser322 (Döppler and Storz 2013). VASP serves as a substrate for several serine/threonine kinases including PKA, PKG, AMPK, PKD1, and Abl.

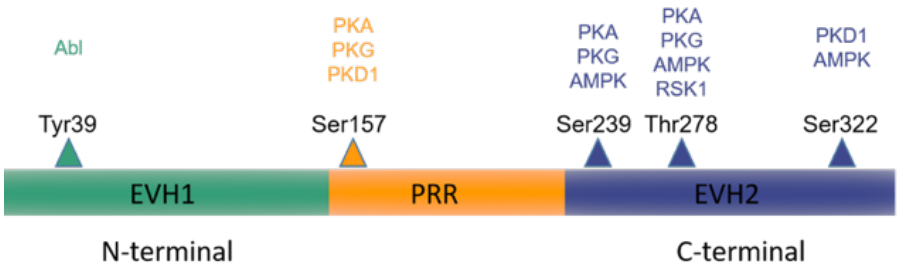

Figure 5 VASP structure

VASP consists of three main domains, the EVH1 domain, EVH2 domain and PRR region. VASP can be phosphorylated at 5 different sites by different kinases. Briefly, Abl leads to the phosphorylation at Tyr39; PKA, PKG and PKD1 can lead to VASP phosphorylation at Ser157; PKA, PKG, AMPK can phosphorylate Ser239; PKA, PKG AMPK and RSK1 result in the phosphorylation at Thr278; VASP phosphorylated at Ser322 is mediated by PKD1 and AMPK. This diagram was modified from Döppler et al, 2013.

1.4.2 The role of VASP in disease

Henes et al. showed that the expression level of VASP was decreased *in vitro* by IL-6 in endothelial HMEC-1 cells (Henes et al. 2009). This observation links cell migration with IL-6 signaling because VASP has been identified as a major regulator of cell mobility in fibroblasts and cancer cell lines (Krause and Gautreau 2014; Sechi and Wehland 2004; Trichet, Sykes, and Plastino 2008; Laban, Weigert, Zink, Elgheznawy, Schurmann, et al. 2018). Hebatullah

et al. reported that VASP is an important regulator of leukocyte recruitment in post-ischemic revascularization (Laban, Weigert, Zink, Elgheznawy, Schürmann, et al. 2018). However, there is a gap of knowledge regarding its role in RA. A full understanding of the function of VASP phosphorylation will be beneficial for our comprehension of how phosphorylation of VASP affects cell motility and how it may contribute to the pathology, as well as the treatment of RA.

1.5 Mouse models of rheumatoid arthritis-like disease

Due to ethical limitations, the pathogenesis of RA as well as the safety and efficiency of certain drugs can not be studied in humans. Therefore, it is difficult to directly study certain topics in RA, such as the dynamic characteristics of RA in the early stage of disease. This makes it important to develop mouse models of RA which can accurately mimic the disease. To tackle this issue, the first mouse models of RA were developed more than 40 years ago in order to gain insights into the pathogenesis of RA and to perform tests on the efficiency of different drugs (Hegen et al. 2008). These animal models share important clinical manifestations with RA patients, such as the swelling of joints, synovitis, cartilage damage, and bone erosion (McNamee, Williams, and Seed 2015). Currently, several RA-like disease mouse models exist that mimic different characteristics of RA (Vincent et al. 2012). Importantly, even though it has been reported that the murine immune system is different from humans both in the components and organization of immune responses, a lot of important conclusions have been drawn from these mouse models. One prominent example, is the conception that $CD4^+$ T cells as well as B cells play a necessary role in RA development (Kadowaki et al. 1994). The discovery of anti-self-antigen antibodies (Rosloniec et al. 1997) and the role of pro-inflammatory cytokines have been identified using arthritis mouse models (Horai et al. 2004). These RA-like disease models can be categorized into induced moue models and spontaneous mouse models according to the distinct mechanisms used to induce arthritis in mice joints.

1.5.1 Induced mouse models of arthritis

The collagen type II induced arthritis (CIA) mouse model is widely used for RA research and was first reported more than forty years ago (Trentham, Townes, and Kang 1977). In 2007, Brand reported the standard method to induce arthritis by the method of immunization of emulsion including collagen II in the presence of complete Freund's adjuvant (CFA), which is characterized by a high concentration of anti-collagen auto-antibodies thereby causing severe

joint inflammation (Brand, Latham, and Rosloniec 2007). DBA1/J is the “gold standard” line of this induction method for RA-like disease research because of its high susceptibility resulting from the level of MHC class II (Holmdahl 2006). Moreover, Th17 cells plays an essential role in CIA joint inflammation (Murphy et al. 2003).

Adjuvant arthritis (AA), characterized by multiple joint arthritis and rapid onset of manifestations, is triggered by an injection of CFA in the tail of rats or repetitive intra-articular CFA injection in mice (Gauldie et al. 2004; McNamee, Williams, and Seed 2015). Like in CIA, $CD4^+$ T cells play a crucial role in the initiation of murine arthritis and AA is also susceptible on the level of MHC and non-MHC genes (Holmdahl et al. 1992; Kim and Moudgil 2009). The interesting point of this model is that bone erosion occurs at an early disease stage with limited damage to cartilage, making it different to RA in human patients (van den Berg 2009).

Proteoglycan-induced arthritis (PGIA) can be induced in susceptible strains by injecting human cartilage proteoglycan aggrecan. The subsequent inflammation in the joints is progressive and characterized by a high concentration of autoantibodies (Glant et al. 1987). It was shown that PGIA is dependent on B cells that produce autoantibodies as well as $CD4^+$ T cells. The successful induction of arthritis is also characterized by the presence of Th17 cells (Glant et al. 1987).

Antigen-induced arthritis (AIA) is induced through the intra-articular injection of the antigen of methylated bovine serum albumin (mBSA). This method is distinct from other induced arthritis mouse model because it gets remove the need for susceptibility genes, which means it can induce destructive arthritis regardless of the genetic background of the mouse (van den Berg 2009). T cells have been shown to be involved in the local inflammation of this mouse model as well as immune complexes.

1.5.2 Spontaneous mouse models of arthritis

Spontaneous arthritis mouse models are different from induced mouse models regarding the mechanisms to induce arthritis, disease onset, chronicity, and specific autoimmunity. Spontaneous RA-like disease mouse models were found in several transgenic mouse lines, for example, SKG, K/BxN, human TNF, and IL-1 receptor knockout mouse. SKG mouse was found to carry a missense mutation in ZAP70, a TCR signaling adaptor molecule, which contributes to a disrupted selection and release of autoreactive cells in the thymus and subsequent onset of spontaneous arthritis (Sakaguchi et al. 2003). TNF transgenic mouse develops spontaneous destructive arthritis which is similar to RA and which is prevented by

specifically blocking of TNF by anti-TNF monoclonal antibody (Butler et al. 1997). Both the IL-1 receptor knockout and IL-1 overexpression can induce polyarthritis in mice. What is very interesting is that it seems the mechanisms are different, because T cells are the main driver of arthritis in IL-1 receptor knockout mouse whereas arthritis is mainly mediated by macrophages and neutrophiles in the IL-1 overexpression mouse line (Niki et al. 2001; Horai et al. 2000). K/BxN mice are found to develop spontaneous arthritis coincidently when crossing KRN mice and non-obese diabetic (NOD) mice.

1.6 Aim of the study

Currently, our understanding of mIL-6R mediated IL-6 signaling on Th17 cells in the course of RA and the interaction between Treg cells and Th17 cells is limited. Th17 cells are an important inflammation-inducing population in the pathogenesis of RA, which is thought to be closely associated with the activation of many distinct cell types including monocytes, neutrophils, macrophages, and osteoclasts. Meanwhile, impaired Treg cell frequencies and impaired suppressive properties were found in RA. Here, we wanted to decipher the dynamic characteristics of membrane-bound IL-6R on Th17 cells, dynamic regulations of Treg cells and possible interactions in the development of autoimmune arthritis *in vivo*.

To achieve this goal, we addressed the following questions:

- What are the *in vivo* dynamic characteristics of mIL-6R expression on Th17 cells during the course of CIA?
- How do *in vivo* Treg cell frequency and related cytokines vary during the course of CIA?

mIL-6R is increased on Th17 cells and downregulates the expression in p-VASP (Ser157) in the CIA mouse model. To verify these findings in humans, we performed flow cytometry and western blot in human samples. Furthermore, we identified the role of excessive IL-6 signaling in the downregulation of p-VASP (Ser157) using a transgenic mouse (IL-6 overexpression mouse) strain.

Next, we addressed the following questions:

- How is membrane-bound IL-6R expressed on Th17 subset in RA patients and healthy individuals?
- Is the excessive IL-6 signaling specifically responsible for the downregulation of p-VASP (Ser157) in humans, CIA mice or transgenic mice?

mIL-6R mediated IL-6 signaling specifically regulates the expression level of p-VASP (Ser157) in CIA and RA. VASP is a protein that is involved in cell motility in many types of cells. Whether p-VASP (Ser157) is involved in the migration of autoimmune suppression subset Treg cells remains unknown. To identify the role of p-VASP (Ser157) in the pathology of RA, we performed proteomics analysis based on the expression level of p-VASP (Ser157) and transwell migration assay to evaluate the effects of specifically blocking p-VASP (Ser157) in Treg cells migration ability.

In this part, we addressed the following questions:

- What pathways are specifically involved in the decreased p-VASP (Ser157) expression level in RA patients?
- Is the migration ability of Treg cells modified by a specific inhibition of p-VASP (Ser157)?

In the thesis, I show for the first time that the mIL-6 receptor is upregulated dynamically on Th17 cells *in vivo* during the development of CIA and inhibits Treg cell migration by downregulation of post-translation modification of VASP. These findings may help to improve our understanding of how mIL-6R participates in the pathogenesis of RA and identify VASP as a promising potential target for the treatment of RA.

2 MATERIALS

2.1 Chemicals

Table 4 List of chemicals used in this study

Chemicals	Company
Agarose Basic	AppliChem GmbH, Darmstadt, Germany
Albumin (BSA)	AppliChem GmbH, Darmstadt, Germany
Ampuwa sterile water	Fresenius Kabi Deutschland GmbH
Ammoniumpersulfat (APS)	Invitrogen, ThermoFisher Scientific, Carlsbad, USA
Bromophenol Blue	AppliChem GmbH, Darmstadt, Germany
EDTA (Ethylenediaminetetraacetic acid disodium salt dihydrate)	Sigma-Aldrich, Saint Louis, USA
Ethanol	Carl Roth GmbH, Karlsruhe, Germany
Ethanol Absolute for Molecular Biology	AppliChem GmbH, Darmstadt, Germany
Formaldehyde solution, 10%	Carl Roth GmbH, Karlsruhe, Germany
Glycin	Carl Roth GmbH, Karlsruhe, Germany
HCl 37%	VWR chemicals, Langenfeld, Germany
10% neutral buffered formalin	Carl Roth GmbH, Karlsruhe, Germany
Ionomycin, Calcium Salt	Cell Signaling Technology, Massachusetts, USA
Isofluran-Piramal	Piramal Citical Care, Hellbergmoos, Germany
Methanol	AppliChem GmbH, Darmstadt, Germany
Milk poder, blotting grade	Carl Roth GmbH, Karlsruhe, Germany
NaCl	Carl Roth GmbH, Karlsruhe, Germany
PMA, PKC activator	Abcam, Cambridge, UK
SDS	Applichem GmbH, Darmstadt, Germany
Sodium Hydroxide	Sigma-Aldrich, Saint Louis, USA
TEMED	Applichem GmbH, Darmstadt, Germany
Tris	Carl Roth GmbH, Karlsruhe, Germany
Tween 20	Bio-rad, Hercules, USA
Xylene	Carl Roth GmbH, Karlsruhe, Germany
2-Propanol	Carl Roth GmbH, Karlsruhe, Germany

2.2 Kits

Table 5 List of kits used in this study

Kit	Cat. Nr.	Company
BD Cytofix/Cytoperm Kit	554714	BD Bioscience, Heidelberg, Germany
$CD4^+$ T Cell Isolation Kit, human	130-096-533	Miltenyi Biotec GmbH, Bergisch Gladbach, Germany
$CD4^+$ T Cell Isolation Kit, mouse	130-104-454	Miltenyi Biotec GmbH, Bergisch Gladbach, Germany
Cyto-Fast TM Fix/Perm Buffer Set	426803	BioLegend, San Diego, USA

Kit	Cat. Nr.	Company
DAB Substrate Kit	AB64238	Abcam, Cambridge, UK
DoubleStain IHC Kit: R&Rt on human/mouse tissue (Green/HRP & AP/Red)	Ab183285	Abcam, Cambridge, UK
FoxP3 Fix/Perm Buffer Set	421403	BioLegend, San Diego, USA
KAPA2G Fast HotStart PCR Kit with dNTPs & Mg-free buffers	KK5512079610 14001	KAPA Biosystems, Massachusetts, USA
Quantikine ELISA mouse IFNr (MIF00)	P265983	R&D System, Minneapolis, MN, USA
Quantikine ELISA mouse IL-17 (M1700)	P284984	R&D System, Minneapolis, MN, USA
Quantikine ELISA mouse IL-6 (MR6000B)	P275725	R&D System, Minneapolis, MN, USA
Quantikine ELISA mouse IL-6Ra (MR600)	P283888	R&D System, Minneapolis, MN, USA
Quantikine ELISA mouse TGF-β1 (DB100B)	P300320	R&D System, Minneapolis, MN, USA
Quantitect Reverse	205313	Qiagen, Hilden, Germany
Rneasy Mini Kit	74104	Qiagen, Hilden, Germany
T Cell Activation/Expansion Kit	130-091-441	Miltenyi Biotec GmbH, Bergisch Gladbach, Germany
True Nuclear™ Transcription Factor Buffer Set	424401	BioLegend, San Diego, USA

2.3 Buffers and gels

Table 6 List of buffers and gels used in this study

Buffers and gels	Composition/Company
1.5M Tris-HCl	90.75g Tric, adjust PH8.8 with HCl to final volume 500ml with H_2O_{dd}
10% APS solution	1g APS in 10ml H_2O_{dd}
10% SDS	10g SDS in 100ml H_2O_{dd}
1M Tris-HCl	60g Tric, adjust PH6.8 with HCl to final volume 500ml with H_2O_{dd}
Agarose gel for genotyping	1.5g Agarose, 100ml 1×TAE buffer, 8ul INTAS HD Green Plus DNA Stain
Alkaline lysis buffer	25nM NaOH, 0.2mM EDTA, H_2O_{dd}, PH12
AutoMACS Running Buffer	Miltenyi Biotec GmbH, Bergisch Gladbach, Germany
Complete C stock	1 tablet in 1ml H_2O_{dd}, use 1:50
EDTA Decalcifying buffer	200g EDTA disodium salt, 50ml 10N NaOH, H_2O_{dd}, PH8.0

Buffers and gels	Composition/Company
Laemmli buffer 5× (10ml)	0.875ml 1 M Tris-HCl, 0.35M SDS, 4.5ml 30% Glycerol, 0.5ml 0.25% Brompphenol Blue, 1.25ml 5% β-Mercaptoethanol
Mini-PROTEAN TGX Gels, 4-15%	Bio-Rad Laboratories GmbH, Feldkirchen, Germany
Mini-PROTEAN TGX Gels, 4-20%	Bio-Rad Laboratories GmbH, Feldkirchen, Germany
Neutralization buffer	40mM Tris-HCl, adjust PH4.0 with HCl to final volume 500ml with H_2O_{dd}
PhophoStop stock	1 tablet in 1ml H_2O_{dd}, use 1:50
Polyacrylamid-Gel (Mini-Gel)	1.5M Tris-HCl PH8.8, 10% SDS (w/v), 30% Acrylamid, 10% APS, TEMED, H_2O_{dd}
Running buffer 10×	250Mm Tris, 1.92 M Glycine, 35Mm SDS, H_2O_{dd}, PH8.3
TAE buffer 50×	2M Tris, 1M acetic acid, 50ml 0.5M EDTA, H_2O_{dd}, PH7.6-7.8
TBS 10×	137Mm NaCl, 20Mm Tris, PH7.6
TBST	1ml Tween-20 (20%), 1L 1×TBS
Transfer buffer	100ml 10× transfer buffer, 200ml Methanol, 700ml H_2O_{dd}

2.4 Reagents

Table 7 List of reagents used in this study

Reagent	company
Aquatex (aqueous mounting agent) for microscopy	Merck, Darmstadt, Germany
AutoMACS Washing Buffer	Miltenyi Biotec GmbH, Bergisch Gladbach, Germany
Bovine type II collagen, 5ml×2mg/ml	Chondrex, Redmond, USA
Cell lysis buffer10×	Cell Signaling Technology, Massachusetts, USA
Cell Staining Buffer	Biolegend, San Diego, USA
Chicken type II collagen, 5ml×2mg/ml	Chondrex, Redmond, USA
Citrate Buffer, PH6.0, 10×	Sigma-Aldrich, Saint Louis, USA
Complete Freund's Adjuvant, 5ml×1mg/ml	Chondrex, Redmond, USA
DNA ladder Gene Ruler^{TM} 1kb	Fermentas, St. Leon-Rot, Germany
DNA loading dye 6×	Fermentas, St. Leon-Rot, Germany
Dulbeccos Phosphate Buffered Saline 1×	Gibco Lifetechnologies, Bleiswijk
FlowCheck Pro Fluoropheres	Beckman Counter, Krefeld, Germany
Hematoxylin Solution (Mayer's, Modified)	Abcam, Cambridge, UK
Human Serum	Sigma-Aldrich, Saint Louis, USA
Goat serum (Normal), control unconjugated, whole serum	Dako, Hamburg, Germany
Fast enzyme	Zytomed Systems, Berlin, Germany
Fluorescence mounting medium	Dako, Hamburg, Germany

Reagent	company
Super PAP Pen liquid blocker mini new	Science Services, München, Germany
Target retrieval solution, PH 9 (10 ×)	Dako, Hamburg, Germany
Incomplete Freund's Adjuvant, 5ml	Sigma-Aldrich, Saint Louis, USA
Hydrogen peroxide, 30%	Carl Roth GmbH, Karlsruhe, Germany
Brefeldin A	Invitrogen, ThermoFisher Scientific, Carlsbad, USA
IsoFlow Sheath Fluid	Beckman Counter, Krefeld, Germany
Pancoll	Pan biotech GmbH, Aidenbach, Germany
Phosphate Buffered Saline (PBS-20×)	Cell Signaling Technology, Massachusetts, USA
RBC Lysis Buffer (10 ×)	Biolegend, San Diego, USA
RPMI Medium 1640 (1×) + GlutaMAX™-1	Gibco, Life Technologies Europe, Bleiswijk, Netherlands
TaqMan Fast Adcanced Master Mix	Applied Biosystems, ThemoFisher Scientific, Carlsbad, USA
Trypan Blue stain 0.4%	Life Technologies Corporation, Oregon
X-Vivo 15, medium	Lonza, Verviers, Belgium

Table 8 List of cytokines used for *in vitro* assay

Reagent	Cat. Nr.	Company
Recombinant Human CCL20 (MIP-3a) (carrier free)	583802	BioLegecarrier-freeo, USA
Recombinant Human IL-1β	130-093-895	Miltenyi Biotec GmbH, Bergisch Gladbach, Germany
Recombinant Human IL-23	20-23	PeproTech, Rocky Hill, USA
Recombinant Human IL-6	130-095-365	Miltenyi Biotec GmbH, Bergisch Gladbach, Germany
Recombinant Human TGF-β1	100-21C	PeproTech, Rocky Hill, USA

2.5 Consumables

Table 9 List of consumables used in this study

Consumables	company
8 microtubes PCR, 0.2ml	BRAND, Werthelm, Germany
Cell counting chamber slide	Invitrogen, Thermo Fisher Scientific,
Corning Cell Strainer 70um Nylon	Corning, Durham, USA
LS Column	Miltenyi Biotec GmbH, Bergisch Gladbach, Germany
Micro tube 1.5 protein LB	SARSTEDT, Nuembrecht, Germany
MicroAmp™ Optical Adhesive Film	Applied Biosystems, ThermoFisher Scientific, Carlsbad, USA
Microtest plate 96 well	SARSTEDT, Nuembrecht, Germany
Microvette 100LH	Sarstedt, Nuembrecht, Germany
PVDF blotting membrane, 0.2µm	GE Healthcare Life Scieces, Germany

Consumables	company
SafeSeal micro tube 0.5ml	SARSTEDT, Nuembrecht, Germany
SafeSeal micro tube 1.5ml	SARSTEDT, Nuembrecht, Germany
SafeSeal micro tube 2ml	SARSTEDT, Nuembrecht, Germany
Serological pipette 10ml	SARSTEDT, Nuembrecht, Germany
Serological pipette 25ml	SARSTEDT, Nuembrecht, Germany
Serological pipette 5ml	SARSTEDT, Nuembrecht, Germany
Tanswell 5µm	Corning, Durham, USA
TC Plate 24 well	SARSTEDT, Nuembrecht, Germany
TC Plate 48 well	SARSTEDT, Nuembrecht, Germany
TC Plate 96 well	SARSTEDT, Nuembrecht, Germany

2.6 Antibodies

Table 10 List of antibodies used in the study

Antibody	Clone	Species/isotype	Cat. Nr.	Company
APC αnti-Human IFN gamma	4S.B3	Mouse IgG1, k	17-7319-82	Affymetrix eBioscience
PerCP-Cyanine5.5 αnti-Human IL-17A	eBio64DEC17	Mouse IgG1, k	457179-42	Affymetrix eBioscience
APC anti-human IL-17A Antibody	BL168	Mouse IgG1, k	512334	Biolegend, San Diego, USA
APC/Cy7 anti-mouse IL-17A Antibody	TC11-18H10.1	Rat IgG1, k	506940	Biolegend, San Diego, USA
β-Actin Antibody	AC-15	IgG1	NB600-501H	Novus Biologicals, Centennial, USA
Brilliant Violet 421 anti-human CD127 (IL-7Rα) Antibody	A019D5	Mouse IgG1, k	351310	Biolegend, San Diego, USA
Brilliant Violet 421 anti-human IL-17A Antibody	BL168	Mouse IgG1, k	512322	Biolegend, San Diego, USA
DyLight 405 IL-6R Antibody (B-6R)	B-6R	Mouse IgG1	NB 100-64770V	Novus Biologicals USA, Littleton, USA
FITC anti-human CD127 (IL-7Ra) Antibody	A019D5	Mouse IgG1, k	351312	Biolegend, San Diego, USA
FITC anti-human FoxP3 Antibody	206D	Mouse IgG1, k	320105	Biolegend, San Diego, USA
FITC anti-human IL-17A Antibody	BL168	Mouse IgG1, k	512304	Biolegend, San Diego, USA

Antibody	Clone	Species/isotype	Cat. Nr.	Company
GAPDH XP Rabbit mAb (HRP Conjugate)	D16H11	Rabbit IgG	8884	Cell Signaling Technology, Massachusetts, USA
LIVE/DEAD Fixable Dead Cell Stain Kits	Not applicable	Not applicable	L23101	Invitrogen, ThermoFisher Scientific, Carlsbad, USA
Pacific Blue anti-human CD4 Antibody	OKT4	Mouse IgG2b, k	317424	Biolegend, San Diego, USA
Pacific Blue mouse IgG2b, k Isotype Control	MPC-11	Mouse IgG2b, k	400627	Biolegend, San Diego, USA
Pacific Blue TM anti-mouse CD4 Antibody	GK1.5	Rat IgG2b, k	100428	Biolegend, San Diego, USA
PE anti-human CD25 Antibody	M-A251	Mouse IgG1, k	356103	Biolegend, San Diego, USA
PE anti-human CD4 Antibody	A161A1	Rat IgG2b, k	357404	Biolegend, San Diego, USA
PE anti-mouse IL-17A Antibody	TC11-18H10.1	Rat IgG1, k	506903	Biolegend, San Diego, USA
PE Mouse Anti-human IFNr	4S.B3	Mouse IgG1, k	554552	BD Bioscience, Heidelberg, Germany
PE Mouse IgG1, k Isotype Control	MOPC-21	Mouse IgG1, k	550617	BD Bioscience, Heidelberg, Germany
PE/Cy7 anti-mouse IFNr Antibody	XMG1.2	Rat IgG1, k	505825	Biolegend, San Diego, USA
Phospho-VASP (Ser157) Antibody	/	Rabbit IgG	3111	Cell Signaling Technology, Massachusetts, USA
PE mouse anti-STAT3	/	Mouse IgG1,	560391	BD Bioscience, Heidelberg, Germany
Alexa Fluor 647 mouse anti-STAT3 (pY705)	/	Mouse IgG2a, k	557815	BD Bioscience, Heidelberg, Germany
VASP Antibody	/	Rabbit IgG	3112	Cell Signaling Technology, Massachusetts, USA
VASP Antibody	OTI4D6	Mouse IgG	NBP2-00555	Novus Biologicals, Centennial, USA
VASP Antibody Blocking Peptide	LS-E48840		197287	LSBio, Eching, Germany

Antibody	Clone	Species/isotype	Cat. Nr.	Company
FITC FoxP3 mAb	FJK-16s	Rabbit IgG2a, Kappa	11-5773-82	Invitrogen, ThermoFisher Scientific, Carlsbad, USA
TGF-β1 mAb	TB21	Mouse IgG1	MA1-21595	Invitrogen, ThermoFisher Scientific, Carlsbad, USA
Goat Anti-mouse IgG H&L (Alexa Fluor 594)	/	Goat polyclonal secondary antibody	Ab150116	Abcam, Cambridge, UK

2.7 ELISA Kits

Table 11 R & D Quantikine™ Elisa for mouse IL-6

Part	Part #	Storage	Company
Mouse IL-6 Microplate	892369	4°C	
Mouse IL-6 Standard	892371	≤20 °C	
Mouse IL-6 Control	892372	≤20 °C	
Mouse IL-6 Conjugate	892665	4°C	
Assay Diluent RA1-14	895180	4°C	R & D Systems,
Calibrator Diluent RD5T	895175	4°C	Minneapolis,
Wash Buffer Concentrate	895003	4°C	USA
Color Reagent A	895000	4°C	
Color Reagent B	895001	4°C	
Stop Solution	895174	4°C	
Plate Sealers	N/A	4°C	

Table 12 R & D Quantikine™ Elisa for mouse IL-17

Part	Part #	Storage	Company
Mouse IL-17 Microplate	890669	4°C	
Mouse IL-17 Standard	890670	≤20 °C	
Mouse IL-17 Control	890672	≤20 °C	
Mouse IL-17 Conjugate	890671	4°C	
Assay Diluent RD1-38	895301	4°C	R & D Systems,
Calibrator Diluent RD5T	895175	4°C	Minneapolis,
Wash Buffer Concentrate	895003	4°C	USA
Color Reagent A	895000	4°C	
Color Reagent B	895001	4°C	
Stop Solution	895174	4°C	
Plate Sealers	N/A	4°C	

Table 13 R & D Quantikine™ Elisa for mouse TGF-β1

Part	Part #	Storage	Company
TGF-β1 Microplate	891124	4°C	
TGF-β1 Standard	891126	≤20 °C	
TGF-β1 Conjugate	890671	4°C	
Assay Diluent RD1-21	895215	4°C	
Assay Diluent RD1-73	895541	4°C	R & D
Calibrator Diluent RD53 Concentrate	895175	4°C	Systems,
Wash Buffer Concentrate	895003	4°C	Minneapolis,
Color Reagent A	895000	4°C	USA
Color Reagent B	895001	4°C	
Stop Solution	895174	4°C	
Plate Sealers	N/A	4°C	

2.8 PCR primer

Table 14 List of primers used in this study

Target	Sequence	Company
B2M	FW: TGTCCACCTTCCAGCAGATGT;	Applied Biosystems,
	RV: AGCTCAGTA ACAGTCCGCCTAG.	ThermoFisher Scientific,
IL-6R	FW: CGTCAGCTCCACATCTGATAGTG;	Carlsbad, USA
	RV: CCTTTGGAGCCCCTTTCTG	
Internal Positive	FW: AGAGAGCTCCCCTCA ATTATGT	
Control		The Jackson Laboratory,
Internal Positive	RV: AGCCACTTCTAGCACAAAGAACT	Bar Harbor, ME USA
Control		
IL-6 Transgene	FW: ACCTCTTCAGAACGAATTGACAAA	
IL-6 Transgene	RV:AGCTGCGCAGAATGAGATGAGTTGT	

2.9 Software

Table 15 List of software in this study

Software	Company
GraphPad Prism	GraphPad Software, Inc, San Diego, USA
GSEA	Broad institute, Inc, Massachusetts, USA
Inkscape	The Inkscape Project, /
Kaluza Analysis	Beckman Coulter, Carifornia, USA
Microsoft Excel	Microsoft, Redmond, USA
Microsoft Word	Microsoft, Redmond, USA
PCR machine	Applied Biosystems, ThermoFisher Scientific, Carlsbad, USA
Powerpoint	Microsoft, Redmond, USA
Tbtools	/(Written by CJ-Chen)
Olympus BX53 microscope	Olympus Corp, Tokyo, Japan

3 METHODS

3.1 Mouse experiments

3.1.1 Mouse lines in the study

The DBA1/J mouse strain is the “gold standard” for the establishment of a rheumatoid arthritis-like mouse model. Immunization with type II collagen of bovine origin or from chickens results in the inflammation of multiple joints ultimately leading to arthritis similar to autoimmune rheumatoid arthritis as seen in humans. The CIA mice develop arthritis with characteristics similar to those of arthritis in humans, including inflammation in synovial tissue, cartilage damage and bone erosion in multiple joints. Furthermore, the use of this mouse line is advantageous in establishing an arthritis mouse model as the DBA1/J line is highly susceptible to the established disease induction method. It is reported that the arthritis incidence is as high as 80-100% when using this mouse strain with the aforementioned induction method (Brand, Latham, and Rosloniec 2007). Immune-mediated glomerulonephritis, nephritis and tubulointerstitial disease may also occur due to the collagen induction (Xie et al., 2004).

In the C57BL/6-Tg (H2-L-IL-6) Kish/J mouse line, human IL-6 protein is highly expressed in different organs as confirmed by ELISA as well as a high expression of IL-6 mRNA by PCR. The human IL-6 gene, which is located on chromosome 9, is inserted under the direction of the mouse histocompatibility 2, D region (H-2LD) promoter. There are homozygous and heterozygous phenotypes of this transgenic mouse line. Although it is feasible for the homozygotic phenotype to survive and retain its fertility, the heterozygous phenotype is kept for subsequent experiments to avoid the early occurrence of plasma cell tumor (The details of this mouse line are available at the website of The Jackson Laboratory). Shown below is the genotyping information of this mouse line: DNA is isolated from ear tags by alkaline lysis buffer for 60 minutes at room temperature. The same volume of neutralization buffer was added to the lysis buffer and stored at -20^{O}C for further use. Then PCR and electrophoresis were performed. The protocol and reagents for standard PCR were provided by The Jackson Laboratory. The primer sequences for the genotyping primers were listed as follows: Internal Positive Control Forward for genotyping: AGAGAGCTCCCCTCA ATTATGT; Internal Positive Control for genotyping: AGCCACTTCTAGCACAAAGAACT; IL-6 Transgene Forward for genotyping: ACCTCTTCAGAACGAATTGACAAA; IL-6 Transgene Reverse for genotyping: AGCTGCGCAGAATGAGATGAGTTGT. The reagents used for the genotyping PCR are listed in Table 16.

Table 16 The list of reagents used for for Genotyping

Reagents	Stock	Final	Volume
H_2O_{dd}	/	Up to final volume (25µl)	6.35µl
Kapa 2G HotStart buffer	/	1.3×	6.5µl
$MgCl_2$	/	2.6	2.6µl
dNTP Kapa	/	0.26	0.65µl
Primer internal control IL-6 forward	10µM	0.5µM	1.25µl
Primer internal control IL-6 reverse	10µM	0.5µM	1.25µl
Transgene IL-6 forward	10µM	0.5µM	1.25µl
Transgene IL-6 reverse	10µM	0.5µM	1.25µl
Kapa 2G HotStart taq polymerase	5U/µl	0.03U/µl	0.15µl
DNA	/	50-200ng	5.00µl

We used the following PCR cycler program as shown in Table 17 for transgenic mouse genotyping.

Table 17 The PCR reaction conditions used for genotyping

Steps	Temperature	Time	Cycles
Denaturation	94ºC	120 sec	1
Denaturation	94ºC	20 sec	10
Annealing	65 ºC	15 sec	10
Elongation	68 ºC	10 sec	10
Denaturation	94 ºC	15 sec	28
Annealing	60 ºC	15 sec	28
Elongation	72 ºC	10 sec	28
Final elongation	72 ºC	120 sec	1
Final hold	10 ºC	Hold	N/A

Figure 6 shows the representative genotyping of mice. The samples with two bands (transgene=451bp and internal positive control=253bp) are identified as mice that carry the human IL-6 target gene. This assay does not distinguish hemizygous phenotype from homozygous transgenic animals, which is why we always crossed the male mouse which carries the human IL-6 gene with a wild-type female mouse to achieve the heterozygous phenotype for further experimentation.

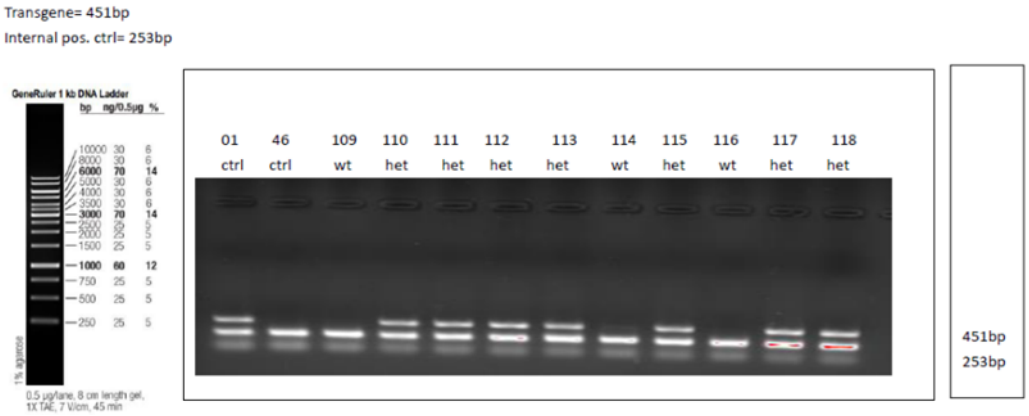

Figure 6 Example of identification of transgenic representative mouse

The samples with two bands (transgene=451bp and internal positive control=253bp) are identified as mice that carry the target gene. Therefore, in this representative figure, mice 110,111, 112, 113, 115, 117, and 118 are heterozygous phenotypes whereas mice 109, 114, and 116 are wild-type mice.

3.1.2 Collagen-induced mouse model establishment

3.1.2.1 General description

Mice of the DBA/1J strain were used for the induction of CIA. Experiments for establishing CIA were conducted as previously decribed elsewhere *(Brand, Latham, and Rosloniec 2007).* Briefly, all mice were kept under specific pathogen-free conditions, 8-12 weeks old mice were age and gender matched for the control and CIA group. Immunization of bovine type II collagen (Chondrex Inc, Woodinville, USA) with complete Freund's adjuvant (CFA, Chondrex, Redmond, USA) containing a final concentration of 0.5 mg/ml of inactivated Mycobacterium tuberculosis (Chondrex Inc, Woodinville, USA) was prepared by the Ika T8 Ultra Turrax homogenizer (IKA-Werke GmbH & Co, Baden-Württemberg, Germany), next the stability of the emulsion was tested by adding one drop of the emulsion into a bottle of water (Yan, Golumba-Nagy, et al. 2021). Only the highly stable emulsions were used for subsequent experiments. The emulsion was kept on ice and quickly transferred to the animal facility for the immunization injection (Yan, Golumba-Nagy, et al. 2021).

The mice were injected subcutaneously at the base of the tail with a total emulsion volume of 100µl at the beginning of the induction and a second injection of 100µl of CII mixed with incomplete Freund's adjuvant (IFA, Chondrex, Redmond, USA) was done in the CIA group at day 21 while the mice in the control group were injected with same volume Dulbecco's phosphate-buffered saline, all animal procedures included in this study were approved by the local authorities and animal protection committee (LANUV NRW, approval no. 81-02.04.2018

A161) and were performed according to the recommendations of the Federation of European Laboratory Animal Science Association (FELASA) (Yan, Golumba-Nagy, et al. 2021). The workflow for the induction of CIA is shown below (Figure 7).

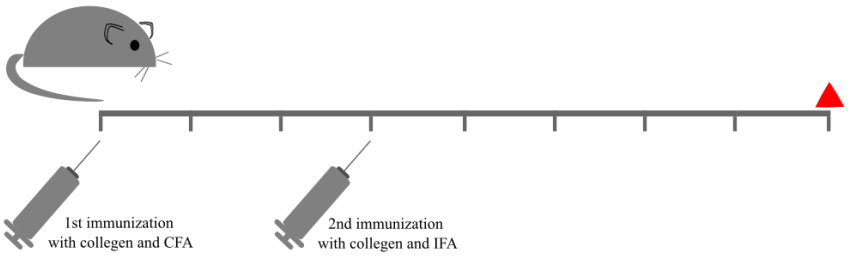

Figure 7 Workflow of establishing CIA mouse model in DBA1/J strain

Displayer here is the process of establishing the CIA mouse model. It takes 8 weeks for the establishment in total. The time points shown are for the first immunization (Day 0), booster immunization (Day 21), and the end time point (Day 56) in the establishment of the CIA mouse model. This diagram was adapted from the publication of Yan et al, 2021.

3.1.2.2 Measurement of paw thickness

The mouse paw thickness was monitored regularly. It was measured once a week with a digital caliper for the first three weeks after which it was measured every three days for the next five weeks (Yan, Golumba-Nagy, et al. 2021).

3.1.2.3 Clinical score collection

The frequency of mouse paw clinical score collection was the same as paw thickness measurement. The clinical score of arthritis was graded as shown in Table 18 (Howe 2004). Each limb was scored independently.

Table 18 Clinical scores of mouse joints inflammation

Score	Clinical manifestations
0	No evidence of erythema and swelling
1	Erythema and mild swelling confined to the tarsals or ankle joint
2	Erythema and mild swelling extending from the ankle to the tarsals
3	Erythema and moderate swelling extending from the ankle to metatarsal joints
4	Erythema and severe swelling encompass the ankle, foot and digits, or ankylosis of the limb

The table is taken from the publication of Brand et al, 2007.

Figure 8 shows the visual representation of different clinical scores. As the onset of arthritis varies in different mice, a clinical score was necessary to supplement the evaluation of mouse arthritis.

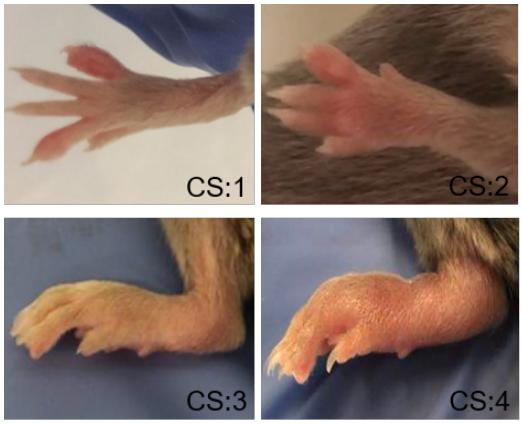

Figure 8 Mouse arthritis clinical score evaluation example

This figure shows the representative images of mouse arthritis clinical score collection for a clinical score (CS) of 1-4. The details of the score criteria are shown in Table 18.

3.1.3 Mouse serum collection

At day 56 of CIA induction, mice were anesthetized using 4% isoflurane (Piramal Critical Care, Hellbergmoos, Germany) in the air for blood collection. Blood was collected in serum separator tubes by cheek punch as recommended by the animal health carer. The samples were left to clot for 30 minutes at room temperature. Centrifugation was then performed for 20 minutes at 1000Xg centrifugation. The serum was removed immediately, aliquoted in EP tubes, and stored at -80^{o}C. Repeated freeze-thaw cycles were prevented prior to performing assays.

3.1.4 Mouse organs harvest

The mice were sacrificed by cervical dislocation in order to harvest organs. The spleens, limbs, and lymph nodes were removed immediately and stored in ice cold PBS for subsequent fixation or splenic lymphocytes isolation by MACS.

3.1.5 Mouse splenic CD4^{+} T cells isolation

Mouse spleens were pooled with a 70µm strainer and 1ml Syringe (BD Plastipak) handle to get a single-cell suspension, the suspensions were then filtered twice with strainers (Corning,

Durham, USA) to filter doublets, blood cells from the splenic suspensions were subsequently lysed with 1x erythrocytes lysing buffer (Biolegend, San Diego, USA), and density gradient centrifugation was used to isolate primary mouse monocytes from single-cell suspensions (Yan, Golumba-Nagy, et al. 2021). Mouse $CD4^+$ T cells were enriched from mice splenic single-cell suspension using the mouse specific $CD4^+$ T cell isolation kit (Miltenyi Biotec GmbH, Bergisch Gladbach, Germany), the purity of the isolated cells was verified by flow cytometry, and only the samples with a purity of more than 95% were used for subsequent experiments (Yan, Golumba-Nagy, et al. 2021).

3.1.6 Histologic staining

3.1.6.1 Hematoxylin & Eosin staining

For histological analysis, limbs were collected after the mice were sacrificed and fixed in 10% neutral buffered formalin (Carl Roth GmbH, Karlsruhe, Germany) for 24 hours at 4 degrees with subsequent decalcification in 20% EDTA solution on a shaking bed (Major Science) at 4 degrees for 4-6 weeks, and the limbs were then embedded in paraffin (Yan, Golumba-Nagy, et al. 2021). Sections (5μm thickness) were cut from the paraffin blocks and mounted on silanized slides. Then sections were then deparaffinized in xylene (Carl Roth GmbH, Karlsruhe, Germany), dehydrated with graded ethanol, and stained with hematoxylin and eosin (H&E staining) (Yan, Golumba-Nagy, et al. 2021), Histopathological scores were scored by two independent researchers in a blinded manner as previously described (Camps et al. 2005).

3.1.6.2 Immunohistochemistry staining

For immunohistochemistry staining, tissue peroxidase was blocked with 3.0% hydrogen peroxide (Carl Roth GmbH, Karlsruhe, Germany) in methanol (AppliChem GmbH, Darmstadt, Germany) for 20 min at room temperature; for antigen retrieval, the citric acid buffer was used and the slides were heated at 100°C for 20 min and then cooled for 30 min at room temperature, and after washing the slides were incubated with goat serum to reduce unspecific protein binding after deparaffinization and dehydration (Yan, Golumba-Nagy, et al. 2021). IL-17 expression was measured with a polyclonal rabbit anti-IL-17 antibody, and rabbit AP Polymer was added to each section for 30min in a moist chamber after washing, then permanent Red Working Solution was applied to completely cover the tissue for 10min, finally the sections were then counterstained with Meyer’s hematoxylin, dehydrated, and mounted

(Yan, Golumba-Nagy, et al. 2021). Human tonsil tissue was used as a positive control. The slides were protected from drying out in a moist box if not specially stated.

3.1.6.3 Immunofluorescence staining

Lymph nodes from mice were collected and fixed in 10% neutral buffered formalin for 24 hours at 4 degrees, then stored in 70% alcohol at 4 degrees for further embedding in paraffin. 5µm sections were cut from the paraffin blocks. After deparaffinization and dehydration, the sections were incubated with normal goat serum to reduce unspecific protein binding after antigen retrieval. A PAP Pen was used to block liquid to save antibodies. For Treg cells immunofluorescence, a fast enzyme was used for antigen retrieval for 5 minutes at room temperature. FoxP3 in mouse lymph nodes was detected in green with the rat anti-mouse FITC-conjugated FoxP3 antibody (1:100) at 4 degrees overnight, and TGF- β1 was stained with the use of mouse anti-mouse antibodies (1:150) followed by Alexa Fluor 594-conjugated goat anti-mouse antibody (1:500). The slides were washed three times for five minutes each with PBS after each antibody incubation. 4', 6-diamidino-2-phenylindole (DAPI) was used to label cell nuclei. After three times of washing cycles with PBS, the slides were covered with Fluorescence mounting medium and a cover glass. For imaging, the Olympus BX53 microscope (Olympus, Münster, Germany) was used. The sections were protected from drying out in a moist box if not specified otherwise.

3.2 Human samples

3.2.1 Patient samples involved in this study

All RA patients involved in the study fulfilled the criteria of the 2010 ACR/ EULAR classification (van der Linden et al. 2011). Peripheral blood samples were collected at the outpatient clinic of the Division of Clinical Immunology and Rheumatology at the University Hospital Cologne, the patients' characteristics are shown in Table 19. Untreated RA patients were defined as either first diagnosed or patients without treatment for at least eight weeks prior to inclusion in the study, age and sex-matched healthy individuals served as controls, and blood was drawn after written informed consent was obtained as governed by the Declaration of Helsinki (Yan, Golumba-Nagy, et al. 2021). The Ethics Committee of the University Hospital Cologne has passed the study (approval no. 13-091).

Table 19 Characteristics of RA patients and healthy individuals

Samples	Number	Sex	Age	Duration (years)	DAS28	RF	ACPA	CRP	ESR
HC	33	69.7%F	58.18±3.83	N/A	0	Neg.	Neg.	Neg.	Neg.
RA	65	66.2%F	56.215±3.85	4.26±0.75	3.76±.37	188.22±64.01	391.08±64.01	21.08±5.84	27.42±5.89

Blood samples were collected from patients with rheumatoid arthritis (RA) and healthy individuals. RA untreated patients were defined as either newly diagnosed with RA or untreated for at least eight weeks. neg.: negative; n/a: not applicable. This table was taken from the publication of Yan et al, 2021.

3.2.2 Human peripheral blood $CD4^+$ T cell isolation

3.2.2.1 $CD4^+$ T cells/naïve $CD4^+$ T cell isolation

Density gradient centrifugation was performed to isolate primary human peripheral blood monocyte cells (PBMCs) from whole blood. PBMCs were used for subsequent isolation of $CD4^+$ T cells. We purified $CD4^+$ T cells by magnetic-activated cell sorting (MACS) based on the negative selection with a human $CD4^+$ T cell isolation kit. Naïve $CD4^+$ T cells were magnetically isolated with the naïve T Cell Isolation Kit for humans. The purity of the isolated cell populations was verified by flow cytometry and only the samples with a purity of more than 95% were used for subsequent experiments (Yan, Golumba-Nagy, et al. 2021). Viable cells were counted using an automated cell counter as described below.

3.2.2.2 Cell counting

Countess II FL (Invitrogen, Thermo Fisher Scientific) was used for cell counting and viability determination. Briefly, cell suspensions were diluted with PBS or medium to a total volume of 1ml. 0.4% Trypan blue (Invitrogen, Thermo Fisher Scientific) was used to dilute the suspension to identify the dead cells at a 1:1 dilution. Next, a 10µl cell suspension mixture was added to the cell counting chamber slide (Invitrogen, Thermo Fisher Scientific). The concentration of viable cells was determined by the cell counter “Countess II FL”.

3.2.2.3 Cell freezing

The purified cells (2-8 x 10^6) were centrifuged at 350×g for 5 minutes, and the supernatant was discarded. The cells were then suspended in 950µl cold PBS and centrifuged again at 350×g for 5 minutes. The supernatant was discarded and the cells were placed in a -80^{o}C freezer for long-term storage for subsequent PCR, or WB experiments.

3.2.3 Quantitative real-time polymerase chain reaction (qRT-PCR)

RNeasy Mini Kit was used for RNA isolation from $CD4^+$ T cells following conversion of RNA into cDNA using the QuantiTect Reverse Transcription Kit. Primers for the IL-6 receptor and β2-microglobulin were purchased from Applied Biosystems, all reactions were performed using the 7500 Fast Real-Time PCR System, and the values are represented as the difference in Ct values normalized to β2-microglobulin for each sample using the following formula: relative RNA expression = $(2\text{-}dCt) \times 10^3$ (Yan, Golumba-Nagy, et al. 2021). Table 20 shows a sample mixture for the qPCR reaction. The reaction cycle is listed in Table 21.

Table 20 The reagents used for qRT-PCR

Reagents	Volume
cDNA	1μl (500ng)
Primer	1μl
H_2O_{dd}	8μl
TaqMan buffer	10μl

Table 21 The reaction conditions used for qRT-PCR

Steps	Temperature	Time	Cycles
UNG incubation hold	50 °C	120 sec	1
Denaturation	95 °C	120 sec	40
Annealing	95 °C	3 sec	40
Elongation	60 °C	30 sec	40

3.3 Assays & analysis

3.3.1 Flow cytometry analysis

Purified $CD4^+$ T cells or induced Th17 cells were stimulated for six hours with PMA (500ng/ml) and ionomycin (1.5μM), Brefeldin A was added to cell culture two hours before flow cytometry staining, and the LIVE/DEAD™ Fixable Dead Cell Stain Kit was used to exclude dead and injured cells during flow cytometry (Yan, Golumba-Nagy, et al. 2021). Briefly, cells were stained with antibodies targeting cell surface antigens including CD4, CD25, and CD127, then fixed and permeabilized by the BD Cytofix/Cytoperm Kit or the True-Nuclear™ Transcription Factor Buffer Set according to the manufacturer's instructions and stained with anti-IL-17A, anti-IFN-γ, and anti-FoxP3 (Yan, Golumba-Nagy, et al. 2021). Flow cytometry was performed on the Gallios 10/3 flow cytometer and the results were analyzed using the Kaluza Analysis Software, Th17 cells were identified by IL-17A expression in purified $CD4^+$ T cells whereas

Treg cells were defined as $CD4^+CD25^+CD127^-FoxP3^+$ T cells in humans and $CD4^+FoxP3^+$ T cells in mice (Yan, Golumba-Nagy, et al. 2021).

3.3.2 Western blot analysis

Purified human and murine $CD4^+$ T cells were lysed with cell lysis buffer, and protein concentration was detected with the BCA Protein Assay Kit, lysates were run on 4–15% gradient polyacrylamide gels, and blotting was performed with the TransBlot® Turbo™ Transfer System, after that proteins were detected with the following antibodies: HRP anti-β2-Actin antibody mouse mAb, anti-VASP rabbit mAb, and anti-rabbit IgG HRP-linked antibody (Yan, Golumba-Nagy, et al. 2021). Detection was done by the ImageJ software.

3.3.3 Migration assay

Human purified $CD4^+$ T cells were transfected by the lipofection method using the Pierce Protein Transfection Reagent Kit and p-VASP blocking peptide (Lifespan Biosciences Inc., Seattle, USA) reagent as recommended by the manufacturers, briefly, the blocking peptide for p-VASP was diluted in DPBS before addition to the dried Pierce Reagent, then the mixture was pipetted up and down 3-5 times prior to vertexing to ensure a homogeneous mixture, after incubation at room temperature for 5 minutes the lipo-surrounding p-VASP blocking peptide was ready for subsequent experimentation (Yan, Golumba-Nagy, et al. 2021). The primary human $CD4^+$ T cells were transfected by lipid surrounded p-VASP blocking antibody with the antibodies from the T cell Activation/Expansion Kit for an overnight incubation in an incubator set to 5% CO_2 at 37 degrees Celsius (Yan, Golumba-Nagy, et al. 2021). The migration of Treg cells was then evaluated by a chemo-attractant transwell migration assay. 6.5mm Transwells with 5µm pore size were equilibrated for 2 hours in x-Vivo 15 media supplied with 1% human serum and 1% penicillin-streptomycin, and $1*10^6$ $CD4^+$ T cells were then seeded to the transwell and incubated for 4 hours under cell culture conditions, 50 ng/ml CCL20 was used as a chemo-attractant in the lower compartment (Yan, Golumba-Nagy, et al. 2021). Total migrated $CD4^+$ cells in the lower chamber were counted by hemocytometer and Treg cells were identified using anti-human CD25, CD127, and FoxP3 antibodies (Yan, Golumba-Nagy, et al. 2021).

3.3.4 Enzyme-linked immunosorbent assay

Mice serum preparation and IL-6, IL-17, and TGF-β1 level determination in serum were performed according to the manufacturer's instructions. The details of Elisa kits are available in Table 11, Table 12 and Table 13.

3.3.5 Proteomic identification by mass spectrometry (MS)

We assessed the expression of 3231 known proteins by performing mass spectrometry (MS) in human purified $CD4^+$ T cells from healthy individuals (n=3), RA untreated patients (n=3), and RA patients treated with IL-6 receptor blockade (n=3), all RA untreated patients were defined as being naïve to treatment with disease-modifying anti-rheumatic and biological drugs as well as being seropositive for both rheumatoid factor and anti-citrullinated protein antibodies (Yan, Golumba-Nagy, et al. 2021). For proteomic analysis, MACS- purified $CD4^+$ T cells were lysed in SP3 lysis buffer and chromatin was degraded with a Bioruptor. Samples were reduced with 5 mM Dithiothreitol (DTT) at 55°C for 30 min, alkylated with 40 mM Chloroacetamide (CAA) at room temperature for 30 min and protein amount was quantified using the Direct Detect Spectrometer. The mass spectrometer was operated at CECAD/ZMMK Proteomics Facility (Cologne, Germany), then LFQ values were log2 transformed, and T-tests were used to determine significantly changes in protein levels (Yan, Golumba-Nagy, et al. 2021). P-values of less than 0.05 as well as 1.5 fold or greater change were defined as significant differential expressed proteins (DFPs). Heat map visualization of DFPs was obtained calculating a z-score of the LFQ values for each protein by TBtools as previously described (Kotschenreuther et al. 2021).

3.3.5.1 Gene ontology (GO), KEGG pathway analysis

The proteins with the highest significance of expression (q less than 0.05) were subjected to GO, KEGG pathway analysis, GO and KEGG analyzed data was visualized using the web-based tool Weishengxin **(**http://www.bioinformatics.com.cn/) (Yan, Golumba-Nagy, et al. 2021).

3.3.5.2 Gene set enrichment analysis (GSEA)

GSEA was performed to determine whether a priori defined sets of genes have statistically significant, consistent differences between two biological states using the GSEA 4.0 software (http://www.gsea-msigdb.org/gsea/) (Yan, Golumba-Nagy, et al. 2021).

3.4 Statistics

Statistical analysis was performed using GraphPad Prism 8. Where indicated, data was analyzed by non-parametric Mann-Whitney test and are presented as the mean ± SEM. Correlation analysis was performed by the Spearman r correlation test, all other data was analyzed using unpaired two-tailed Student's t-test or one-way ANOVA as appropriate (Yan, Golumba-Nagy, et al. 2021). $p < 0.05$ was considered to be statistically significant. *$p < 0.05$, **$p < 0.01$, ***$p < 0.001$, ns: non-significant, $p > 0.05$.

A part of the experimental results is published in the following paper:

Yan S, Golumba-Nagy V, Kotschenreuther K, Thiele J, Refaian N, Shuya D, Gloyer L, Dittrich-Salamon M, Meyer A, Heindl LM, Kofler DM. Membrane-bound IL-6R is upregulated on Th17 cells and inhibits Treg cell migration by regulating post-translational modification of VASP in autoimmune arthritis. Cell Mol Life Sci. 2021 Dec 16;79(1):3. doi: 10.1007/s00018-021-04076-2. PMID: 34913099; PMCID: PMC8674172.

4 RESULTS

4.1 Characteristics of Th17 cells and Treg cells in the development of CIA and in RA patients *in vivo*

4.1.1 Establishment of the CIA model in DBA1/J mice

To identify the dynamic characteristics in the development of CIA, we firstly induced a CIA mouse model in our lab. Following the second immunization with collagen type II in combination with IFA, mice in the CIA group developed swollen paws, with no joint inflammation being found in the control group. A representative example of a swollen paw is shown in Figure 9A. During the development of CIA, the mean clinical score in the CIA group was significantly increased as compared to the control group on the 30th-day after the first immunization (Figure 9B) (Yan, Golumba-Nagy, et al. 2021). In addition, the paw thickness of mice in the CIA group was significantly different as compared to mice in the control group day 14 days after the first immunization at day 0 (Figure 9C). Furthermore, H&E staining analysis of the mouse joints revealed a significant accumulation of inflammatory cells, cartilage destruction and bone erosion in the CIA mouse model (Figure 9D). An elevated score in synovial inflammation as well as hyperplasia was observed in the CIA group as compared to the control group (Figure 9E-F).

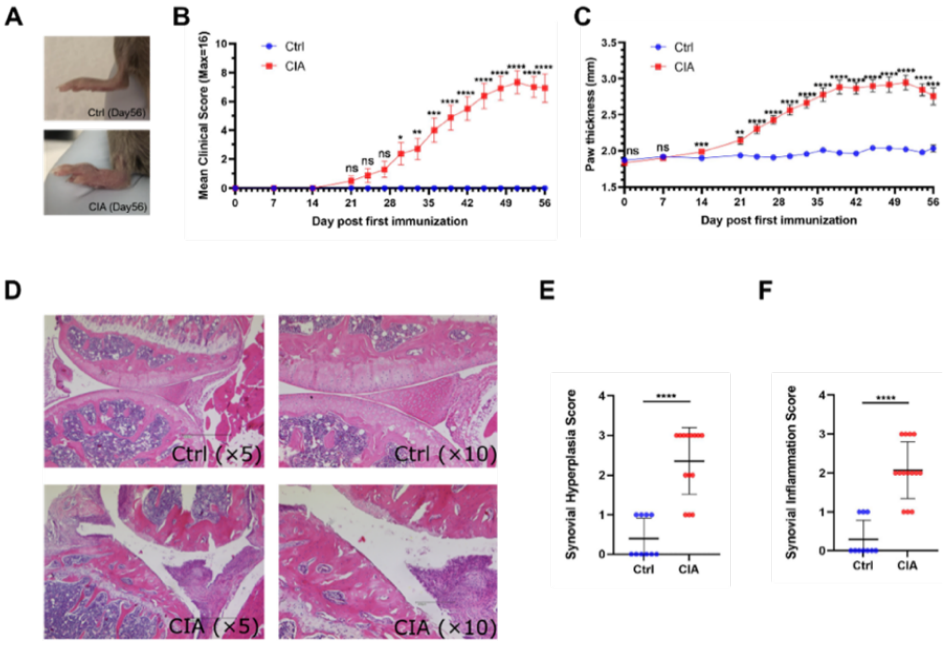

Figure 9 Establishment of CIA mouse model in DBA1/J strain

(A) Representative example of the normal hindlimb in the control group and swollen hindlimbs in CIA mice on day 56 after the first immunization. (B) The mean clinical score of control mice (n=16) and CIA mice (n=24) in the development of arthritis is shown. (C) Thickness of hindlimbs of the control mice (n=16) and CIA mice (n=24) were monitored during the course of arthritis. (D) The upper panel shows a representative example of H&E staining of hindlimbs from the control mice whereas the lower panel shows the inflamed joints staining in the CIA group. (E) Synovial hyperplasia score is shown in control mice (n=10) and CIA mice (n=14). The histopathological scores criteria are described in the Methods section. (F) Synovial inflammation score is shown in control mice (n=10) and CIA mice (n=14) is shown. Data is presented as the mean ± standard error of the mean (SEM). Statistical analysis was performed using a two-tailed Student's t-test (*$p < 0.05$, **$p < 0.01$, ***$p < 0.001$, ****$p < 0.0001$). This diagram was taken from the publication of Yan et al, 2021.

4.1.2 Th17 and Treg cells expression in CIA mice

4.1.2.1 Th17 cells are increased in CIA mouse splenocytes and accumulates in murine joints

To verify the Th17 cell's participation in the pathogenesis of RA, we performed flow cytometry to evaluate the Th17 frequency level in mouse purified $CD4^+$ T cells in splenic lymphocytes and immunochemistry staining to see the accumulation of the Th17 subset in inflamed joints. Figure 10A shows an example of the spleens collected from the CIA group and Control group, then $CD4^+$ T was enriched from single cells suspension by negative selection through MACS. A representative example of flow cytometry staining of obtained Th17 cells is shown in Figure 10B. Our results from the CIA mouse model confirm that Th17 cell frequency was significantly elevated in the CIA group as compared to the control group (Figure 10C), furthermore, IHC staining of inflamed joints revealed that Th17 cells migrated into the inflammatory sites (synovial tissue) of CIA joints whereas there was no Th17 cells accumulation in the joints of the control group (Figure 10D-E) (Yan, Golumba-Nagy, et al. 2021).

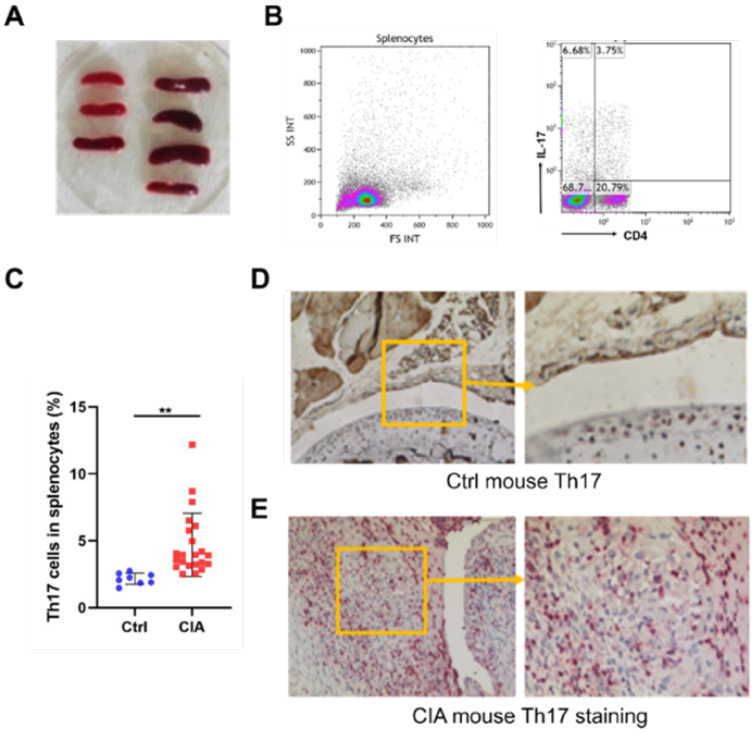

Figure 10 Th17 cells are significantly increased in CIA mouse and accumulate in mouse joints

(A) The left panel shows the spleens collected from mice in the control group, the right panel shows the spleens of in CIA mice. Single-cell suspensions were prepared from the spleens and $CD4^+$ splenic T lymphocytes were enriched by negative selection through MACS for subsequent flow cytometric analysis. (B) Representative example of flow cytometry analysis of Th17 cells from the spleen of mice with collagen II-induced arthritis (CIA). (C) Shown is the frequency of Th17 cells in purified murine $CD4^+$ splenocytes in the control group (Control, n=8) and the CIA group (n=22) as assessed by flow cytometry. (D) Representative figures of Th17 cells staining by immunohistochemistry in the joints of murine hindlimbs (HLs) in control mice. (E) Representative figures of Th17 cells staining by immunohistochemistry in the joints of murine hindlimbs (HLs) in CIA mice. Data is presented as the mean ± standard error of the mean (SEM). Statistical analysis was performed using a two-tailed Student's t-test (*$p < 0.05$, **$p < 0.01$, ***$p < 0.001$, ****$p < 0.0001$). This diagram was adapted from the publication of Yan et al, 2021.

4.1.2.2 Treg cells are decreased in CIA mouse splenocytes

To evaluate the balance between Treg cells and Th17 cells, Treg cells were stained in sorted $CD4^+$ splenic lymphocytes for flow cytometry. Treg cells in mice were defined as being positive for both CD4 and FoxP3. Figure 11A shows the flow cytometry staining of Treg cells in control mice and CIA mice at Day 56. In the CIA group, Treg cell frequency was significantly decreased as compared to the control mice (Figure 11B) (Yan, Golumba-Nagy, et al. 2021).

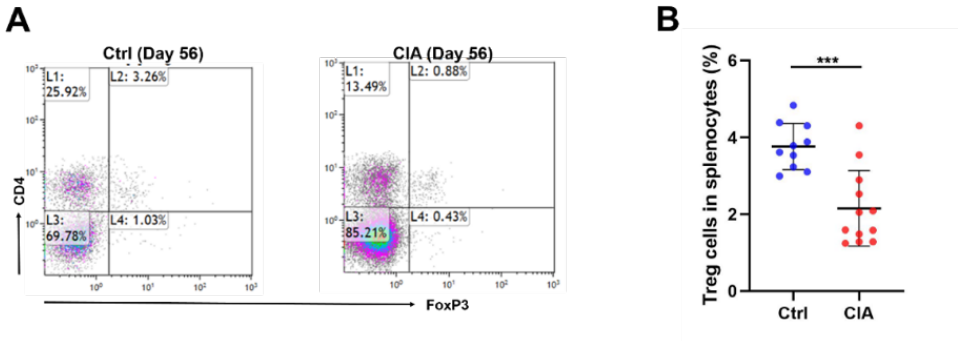

Figure 11 Treg cells are decreased in CIA mouse model and the balance between Th17 cells and Treg cells is shifted to Th17 cells

(A) Representative example of flow cytometry analysis of Treg cell frequency in $CD4^+$ T cells sorted from splenocytes in control mice and the CIA mouse model. (B) Treg cells frequency was analyzed by flow cytometry in purified murine $CD4^+$ T cells isolated from splenocytes from control mice (n=10) and CIA mice (n=12). Data is presented as the mean ± standard error of the mean (SEM). Statistical analysis was performed using a two-tailed Student's t-test (*p < 0.05, **p < 0.01, ***p < 0.001, ****p < 0.0001). This diagram was adopted from the publication of Yan et al, 2021.

4.1.2.3 Treg cell function is impaired in CIA mice

In order to see whether Treg cell function is impaired in CIA mouse joints, we performed immunofluorescence (IF) staining with mouse joint sections embedded in paraffin to determine if TGF-β1 levels in Tregs were altered. Figure 12 shows IF staining results of synovial tissue from mouse joints. We used human tonsil sections as a positive control (the upper panel). We found Treg cells ($FoxP3^+$) which express TGF-β1 and cells which only express TGF-β1 in synovial tissue in CIA mouse joints (the lower panel) whereas there were no Treg cells in the synovial tissue from the control mice (the middle panel) (Yan, Golumba-Nagy, et al. 2021). The synovial tissue in control mouse joints is rather thin and there are almost no immune cells (such as Treg cells or Th17 cells) in healthy mouse synovial tissue as compared to the CIA mouse model. Therefore, it is not possible to directly compare the TGF-β1 levels in control mouse joint and CIA mouse joints sections. In order to compare the TGF-β1 levels in Tregs, we switched to peripheral lymphatic organs in control mouse and CIA mouse models and performed IF staining with lymph nodes (LN) from each (Figure 13).

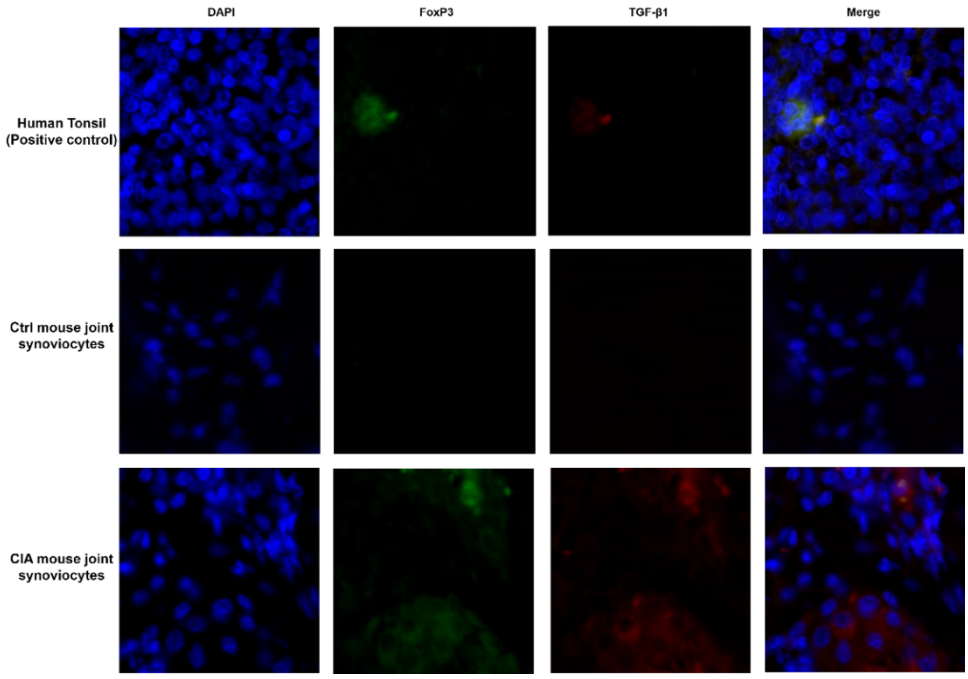

Figure 12 Representative immunofluorescence (IF) staining of TGF-β1 and FoxP3 in mouse joints
Mouse joints were stained by IHF. Human tonsil tissue served as positive control. IF staining from control mice (middle row) and CIA mice (lower row). 4', 6-diamidino-2-phenylindole (DAPI) was used to label cell nuclei (blue). FoxP3 was stained with FITC labeled antibody (green) whereas TGF-β1 was stained with Alexa Fluor 594-conjugated antibody (red). This diagram was adapted from the supplement materials of publication of Yan et al, 2021.

What we found from mouse LN staining is that Treg cells from control mouse express the transcription factor Foxp3 and produce TGF-β1 (the upper panel) whereas the Treg cells from CIA mice only express Foxp3 without producing TGF-β1 (the lower panel) (Yan, Golumba-Nagy, et al. 2021). This indicates that Treg cells functioning is impaired in CIA mice. Treg cells lost their ability to produce TGF-β1 which is important for Treg cells to exert their immunosuppressive function.

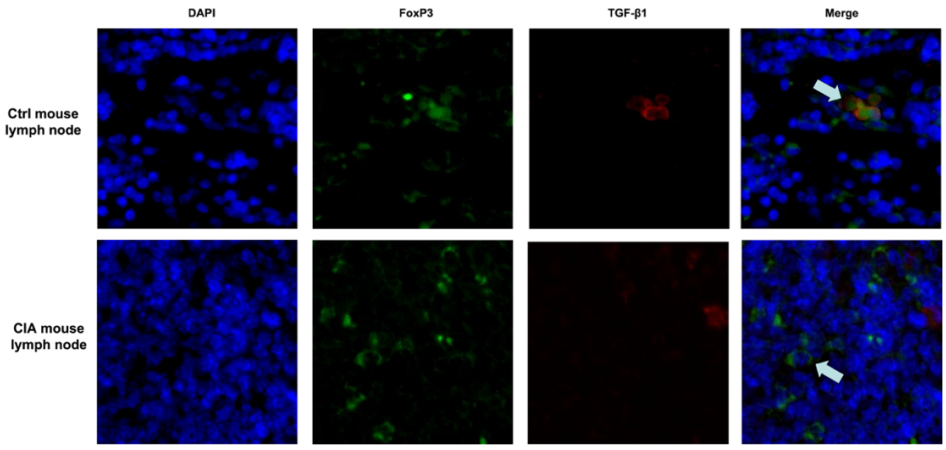

Figure 13 Representative immunofluorescence (IF) staining of TGF-β1 and FoxP3 in lymph nodes
Mouse lymph nodes were stained by IHF. IF staining from control mice (upper row) and CIA mice (lower row). Treg cells were marked with an arrow. 4', 6-diamidino-2-phenylindole (DAPI) was used to label cell nuclei (blue). FoxP3 was stained with FITC labeled antibody (green) whereas TGF-β1 was stained with Alexa Fluor 594-conjugated antibody (red). This diagram was adapted from the supplement materials of publication of Yan et al, 2021.

4.1.3 The balance between Th17 and Treg cells is shifted to Th17 cells during the course of CIA

To investigate if the balance of both subsets was affected or not, we collected $CD4^+$ T splenocytes and performed staining for flow cytometry to investigate the balance between both subsets. The flow cytometric analysis shows that the ratio of Th17/Treg is dramatically increased in CIA mice, which indicates the balance between these populations is shifted towards Th17 cells in the CIA mouse model when assessing purified $CD4^+$ splenic lymphocytes (Figure 14) (Yan, Golumba-Nagy, et al. 2021).

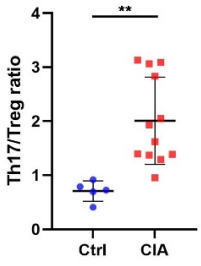

Figure 14 The Th17/Treg ratio in CIA mouse model
The ratio between Th17 cells frequencies and Treg cells frequencies is shown in purified murine $CD4^+$ splenocytes (Control, n=5; CIA, n=12). Data is presented as the mean ± standard error of the mean (SEM). Statistical analysis was performed using a two-tailed Student's t-test (*p < 0.05, **p < 0.01, ***p < 0.001, ****p < 0.0001). This diagram was adapted from the publication of Yan et al, 2021.

4.1.4 Membrane-bound IL-6R is significantly elevated on Th17 cells in the CIA mouse model

To assess mIL-6 receptor expression on Th17 cells, purified CD4$^+$ T splenic lymphocytes were stained with anti-CD4, anti-IL17, and anti-membrane-bound IL-6R antibodies. Flow cytometric results in Th17 cells stained with membrane-bound IL-6R in the control mice and at day 56 after the first immunization in the CIA group are shown (Figure 15A). A significant elevation in membrane-bound IL-6 receptor expression on Th17 cells was observed in the CIA mice (Figure 15B) (Yan, Golumba-Nagy, et al. 2021).

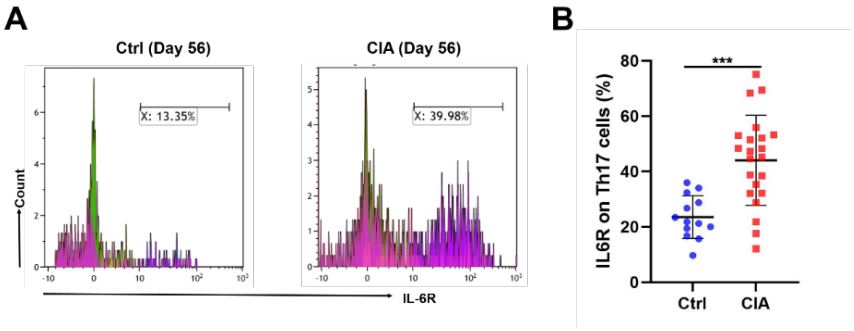

Figure 15 Membrane-bound IL-6R is elevated on Th17 cells in the CIA mouse model
(A) Representative example of flow cytometric analysis showing the membrane-bound IL-6 receptor on Th17 cells at day 56. (B) IL-6 receptor expression on Th17 cells in purified murine CD4$^+$ splenocytes is increased in the CIA mouse model as compared to mice in the control group as determined by flow cytometry (Control, n=13; CIA, n=22). Data are presented as the mean ± standard error of the mean (SEM). Statistical analysis was performed using a two-tailed Student's t-test (*p < 0.05, **p < 0.01, ***p < 0.001, ****p < 0.0001). This diagram was adapted from the publication of Yan et al, 2021.

4.1.5 Dynamic characteristics in the *in vivo* development of CIA in mice

After observing that mIL-6 receptor levels on Th17 cells was increased in purified CD4$^+$ splenic lymphocytes in CIA mice, we set out to study the underlying role of increased mIL-6 receptor expression in the CIA mouse model. Since it is not possible to directly monitor the expression level in the development of RA in the clinic due to ethical and technical limitations, a study in human subjects was not possible. Therefore, we performed experiments with the CIA mouse model to monitor the expression levels of the mIL-6 receptor on Th17 cells in the development of CIA. Figure 16 shows the workflow for monitoring the mIL-6R expression levels in the CIA mouse model. Briefly, we established six rounds of CIA mouse models in total. Mice were sacrificed at weekly intervals manner starting in the 3rd week after the first

immunization at day 0 and the expression levels of the mIL-6 receptor on the Th17 were measured from purified $CD4^+$ splenic lymphocytes by flow cytometry. Furthermore, we used flow cytometry to monitor the dynamic Th17 cells frequency, Treg cells frequency, IL-6 concentration in the serum, IL-17 concentration in the serum, as well as the ratio between both T cell subsets in the development of CIA mouse models.

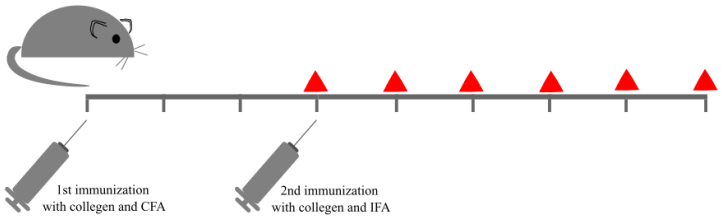

Figure 16 Workflow to monitor dynamic characteristics in the development of CIA in the mouse model
Shown here is the workflow for monitoring dynamic characteristics in the development of CIA (8 weeks in total). Two immunizations were performed on Day 0 and Day 21. Red triangles represent the end time points of each CIA induction. There were six rounds of CIA mouse models in total. This diagram was adapted from the publication of Yan et al, 2021.

4.1.5.1 Dynamic Th17 frequency in the development of CIA

Figure 17 shows the dynamic flow cytometric results of Th17 cell frequency in the course of the CIA mouse model and control mice. Analysis revealed that the Th17 cell frequency stays on a higher level as compared to the control group (Yan, Golumba-Nagy, et al. 2021). However, no statistically significant difference was found as compared to control mice during the course of CIA after the first immunization.

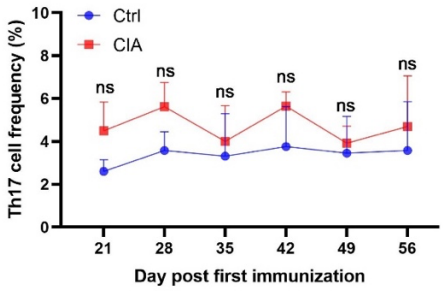

Figure 17 Dynamic Th17 cells frequency in the development of CIA
Flow cytometry analysis shows the Th17 cell frequencies in $CD4^+$ T cells isolated at different time points from splenocytes of control mice (Control, n=5) and CIA mice (n=5). Data is presented as the mean ± standard error of the mean (SEM). Statistical analysis was performed using a two-tailed Student's t-test (ns=non-significant). This diagram was adapted from the publication of Yan et al, 2021.

4.1.5.2 Dynamic IL-17 concentrations in CIA mouse model serum

Even though there was no difference regarding Th17 cells frequency during the course of CIA, we wondered whether Th17 cell functions was influenced. We collected blood serum at each time point in the development of CIA. Figure 18 shows a dramatic increase of IL-17 in blood serum throughout the development of CIA. The ELISA was performed, and the level of IL-17 started to increase 28th days after the first immunization when compared to the control group. IL-17 levels remain elevated when compared to the control group, even though Th17 cell frequency did not get increase during the development of CIA (Yan, Golumba-Nagy, et al. 2021).

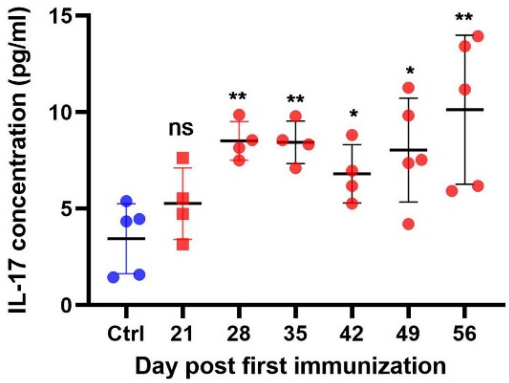

Figure 18 Dynamic serum IL-17 levels in the development of CIA by ELISA

Dynamic IL-17 concentration in serum is shown at different time points during CIA development (n=4 or 5). Data is presented as the mean ± standard error of the mean (SEM). Statistical analysis was performed using a two-tailed Student's t-test (*p < 0.05, **p < 0.01, ***p < 0.001, ****p < 0.0001, ns=non-significant).

4.1.5.3 Dynamic upregulation of mIL-6R on Th17 cell is inversely correlated with IL-6 levels in autoimmune arthritis

To evaluate the role of mIL-6R expression specifically on the Th17 subset, we monitored the mIL-6R expression level on Th17 cells in the development of CIA. Flow cytometric results revealed a significant increase in the mIL-6 receptor on Th17 cells from CIA mice starting on day 42 after the first immunization (Figure 19) (Yan, Golumba-Nagy, et al. 2021). There was no elevation of the mIL-6R on Th17 cells in the early stage of the CIA mouse model (from Day0 to Day42). After completion of CIA induction, mIL-6R reached its highest level when compared to mice in the control group. It was also found that the control group had a stable expression level of the mIL-6R on Th17 cells.

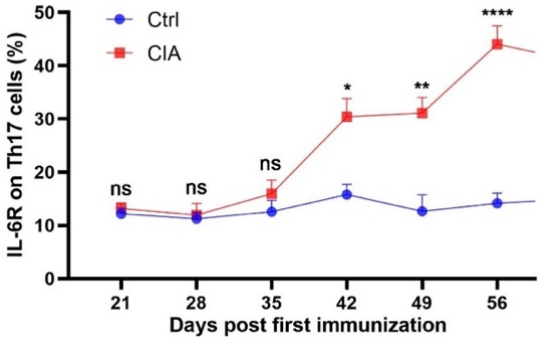

Figure 19 Dynamic mIL-6R expressions on Th17 cells in the development of CIA mice and mice in the control group by flow cytometry

Shown here is the mIL-6 receptor expression on Th17 cells as measured by flow cytometry from control mice and CIA mice (n=4 or 5 per group). Data is presented as the mean ± standard error of the mean (SEM). Statistical analysis was performed using a two-tailed Student's t-test (*p < 0.05, **p < 0.01, ***p < 0.001, ****p < 0.0001, ns=non-significant). This diagram was adapted from the publication of Yan et al, 2021.

Dynamic serum IL-6 levels were assessed by ELISA. As shown in Figure 20, we observed a significant increase in IL-6 levels after the second immunization (on day 21) until day 35 after the first immunization (Yan, Golumba-Nagy, et al. 2021). IL-6 in the serum was decreased from day 35 until day 56 after the first immunization. At day 56 of CIA induction, the IL-6 serum level was almost equivalent to that of mice in the control group. Importantly, serum IL-6 levels were increased only in the early stage of CIA induction.

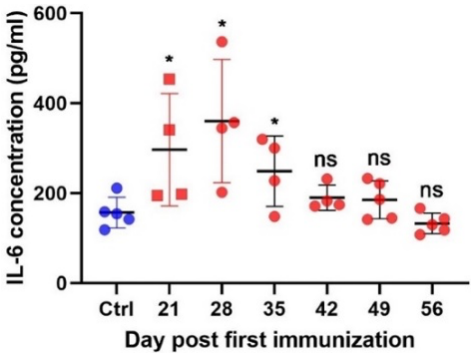

Figure 20 Dynamic serum IL-6 levels in the development of CIA mouse model as compared to mice in the control group

IL-6 serum levels at different time points were evaluated by ELISA (n=4 or 5 per group) in the development of CIA. IL-6 serum concentrations at each time point in the development were compared to the IL-6 serum concentration in the control group. Data is presented as the mean ± standard error of the mean (SEM). Statistical analysis was performed using a two-tailed Student's t-test (*p < 0.05, **p < 0.01, ***p < 0.001, ****p < 0.0001, ns=non-significant). This diagram was adapted from the publication of Yan et al, 2021.

4.1.5.4 Dynamic Treg frequency during the course of CIA

To evaluate the interaction between Th17 cells and Treg cells, we performed flow cytometric analysis to measure Treg cell frequencies during the development of CIA and in the control group. Treg cell frequency remained at a rather stable level in the control group (Figure 21). However, Treg frequency was significantly reduced in the CIA group at each time point in the development of CIA when compared to mice in the control group (Yan, Golumba-Nagy, et al. 2021).

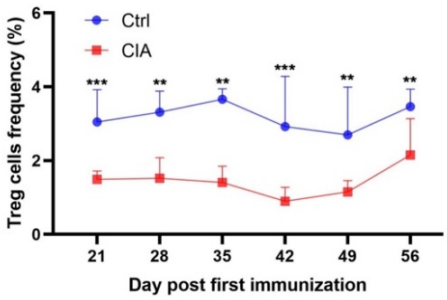

Figure 21 Dynamic Treg cells frequency in the development of CIA as compared to the control mice
Treg cells frequency was measuredin purified $CD4^+$ splenic lymphocytes using flow cytometry. Shown here are the results at different time points from splenocytes of control mice and CIA mice (n=4 or 5). Statistical analysis was performed using a two-tailed Student's t-test (**p < 0.01, ***p < 0.001). This diagram was adapted from the publication of Yan et al, 2021.

Interestingly, at the end of the experiment (day 56) Treg cells frequency was remarkably increased when compared to the Treg frequency at day 42 in Figure 22.

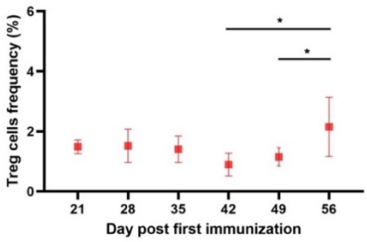

Figure 22 Dynamic Treg cells frequency in the development of CIA
Shown here is the dynamic Treg frequency in the development of the CIA. For clarity, the data from Figure 21 is presented differently to show the dynamic characteristics of Treg cell frequency in the CIA group. Treg cells were increased in the late stage of the CIA group. A significant increase was found starting on Day42. Data is presented as the mean ± standard error of the mean (SEM). Statistical analysis was performed using a two-tailed Student's t-test (*p < 0.05, **p < 0.01, ***p < 0.001, ****p < 0.0001). This diagram was adapted from the publication of Yan et al, 2021.

4.1.5.5 Dynamic dysregulation of the balance between Th17 cells and Treg cells in the development of CIA

To study the balance between Th17 cells and Treg cells, we calculated the relative differentiation of both subsets. The ratio between both subsets was elevated in CIA mice as compared to healthy control animals. The ratio peaked 42 days after the first immunization due to slightly increased Th17 cell frequencies and a mild reduction in Treg cell frequencies (Figure 17 and Figure 21) (Yan, Golumba-Nagy, et al. 2021). However, no correlation with disease score was observed.

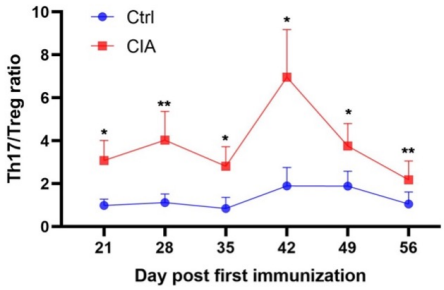

Figure 23 Dynamic dysregulation of the balance between Th17 cells and Treg cells in the development of CIA as compared to mice in the control group

Dynamic Th17/Treg cell ratios at different time points was calculated during the development of CIA in the mouse model development. Statistical analysis was performed using a two-tailed Student's t-test (*p < 0.05, **p < 0.01, ***p < 0.001, ****p < 0.0001). This diagram was adapted from the publication of Yan et al, 2021.

4.1.6 Evaluation of membrane-bound IL-6R expression in RA

4.1.6.1 Membrane-bound IL-6R expression was elevated by flow cytometry in untreated RA patients was downregulated after administration of an IL-6R inhibitor treatment

To verify the findings from the CIA mouse model experiment in humans, we performed flow cytometry to observe mIL-6 receptor expression on Th17 cells in RA patients and healthy individuals. Thus, we had three groups: healthy controls, untreated RA patients, and RA patients treated with the IL-6 receptor inhibitor tocilizumab. Figure 24A-C shows a flow cytometric analysis of the mIL-6 receptor on Th17 cells in the three groups. Consistent with what we found in $CD4^+$ T cells in CIA mice, mIL-6 receptor on Th17 cells was elevated in untreated RA patients than healthy individuals (Figure 24D), importantly, RA patients who received treatment with the IL-6 receptor blocker tocilizumab were found to have a lower level of mIL-6 receptor on Th17 cells as compared to RA patients who did not receive any treatment,

which is shown in Figure 24D. The mIL-6R expression on Th17 cells was specifically decreased after the treatment with the IL-6R inhibitor tocilizumab (Yan, Golumba-Nagy, et al. 2021).

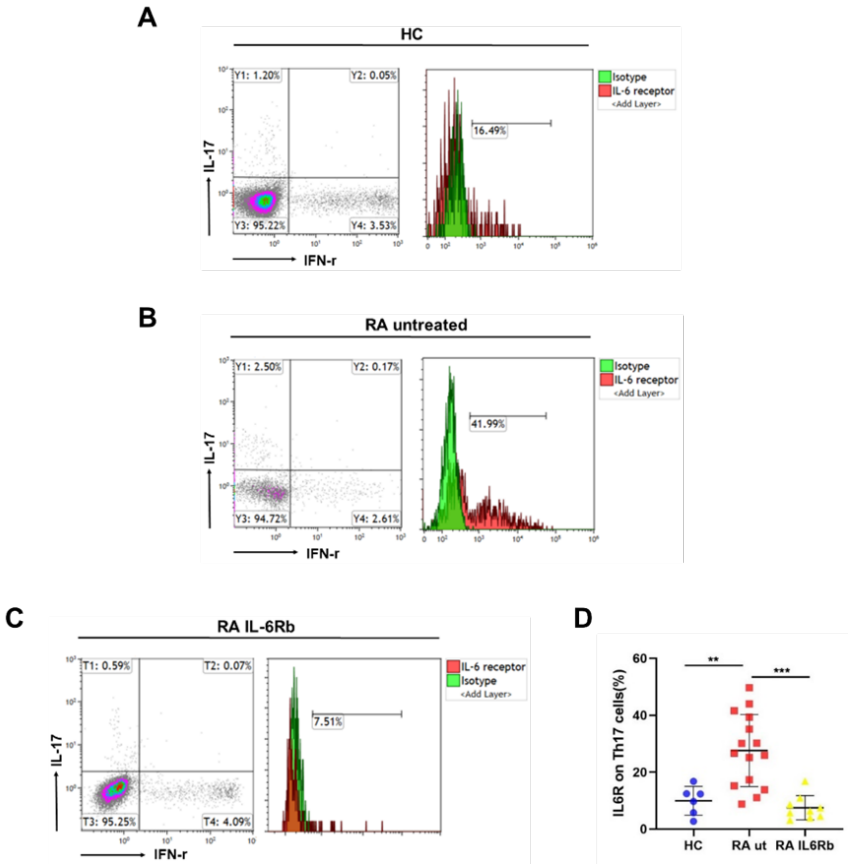

Figure 24 mIL-6R expression was increased in untreated RA patients and was downregulated after administration of an IL-6R blocking treatment

(A-C) Representative examples of flow cytometric analysis of membrane-bound IL-6 receptor on Th17 cells in healthy controls, untreated RA patients, and RA patients treated with IL-6 receptor blocking antibodies, respectively. (D) Expression levels of membrane-bound IL-6 receptor on Th17 cells from healthy controls (HC, n=6), untreated RA patients (RA ut, n=15), and RA patients treated with IL-6 receptor blocking antibodies (RA IL-6Rb, n=8) as assessed by flow cytometry. Data is presented as the mean ± standard error of the mean (SEM). Statistical analysis was performed using one-way ANOVA (*p < 0.05, **p < 0.01, ***p < 0.001, ****p < 0.0001). This diagram was adapted from the publication of Yan et al, 2021.

4.1.6.2 IL-6R mRNA is evaluated in untreated RA patients

We collected purified $CD4^+$ T cells from untreated RA patients and performed PCR. Results showed that mRNA levels of the IL-6R in $CD4^+$ T cells was significantly increased in untreated RA patients as compared to healthy individuals (Figure 25) (Yan, Golumba-Nagy, et al. 2021).

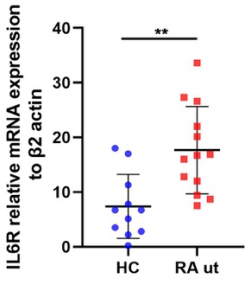

Figure 25 Membrane-bound IL-6R mRNA was evaluated in RA untreated patients

mRNA levels of the IL-6 receptor relative to β-Actin in CD4⁺ T cells from HC (n=11) and untreated RA patients (n=13). Statistical analysis was performed using a two-tailed Student's t test (*p<0.05, **p<0.01, ***p<0.001). This diagram was adapted from the publication of Yan et al, 2021.

4.2 p-VASP (Ser157) is specifically downregulated by IL-6 signaling both in mice and RA patients *in vivo*

4.2.1 p-VASP (Ser157) is downregulated in the CIA DBA1/J mouse model

IL-6 signaling is linked to a reduced phosphorylation of VASP, which is thought to be an important regulation of cell migration (Henes et al. 2009). To analyze the relationship between the expression level of p-VASP and IL-6 signaling in the CIA mouse model, we performed a western blot to see the level of VASP phosphorylation at Ser157 in CD4⁺ T splenic lymphocytes from CIA mice at day 56 after the first immunization. Western blot analysis of p-VASP (Ser157) is presented in Figure 26A (Yan, Golumba-Nagy, et al. 2021). In the CIA group, p-VASP (Ser157) expression was decreased as normalized at total VASP as compared to control mice (Figure 26B).

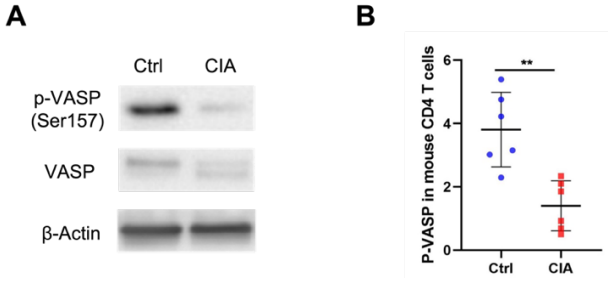

Figure 26 p-VASP (Ser157) expression was downregulated in the DBA1/J CIA mouse model

(A) Shown here is a representative exemplary western blot analysis of p-VASP (Ser157) expression in CD4⁺ T cells isolated from splenocytes of control mice and CIA mice in the DBA1/J strain. (B) p-VASP (Ser157) expression in CD4⁺ T cells isolated from splenocytes of CIA mice (n=6) was downregulated when compared to control mice (Control, n=6) by western blot. Data is presented as the mean ± standard error of mean (SEM). Statistical analysis

was performed using a two-tailed Student's t-test (*p < 0.05, **p < 0.01, ***p < 0.001, ****p < 0.0001, ns=non-significant). This diagram was adapted from the publication of Yan et al, 2021.

4.2.2 p-VASP (Ser157) is specifically downregulated and correlated with Treg cells and TGF-β downregulation in C57BL/6-Tg(H2-L-IL-6)1Kish/J mouse line

4.2.2.1 p-VASP (Ser157) is specifically downregulated in C57BL/6-Tg(H2-L-IL-6)1Kish/J mice

To see whether the lower expression of p-VASP (Ser157) was specifically regulated by IL-6 signaling, we used a transgenic mouse model of human IL-6 to detect the effects of excessive IL-6 signaling on p-VASP expression. Western blot was performed with purified $CD4^+$ T cells in mouse strain of C57BL/6-Tg(H2-L-IL-6)1Kish/J which overexpress human IL-6. Figure 27 shows the western blot results of $CD4^+$ T splenic cells. Interestingly, IL-6 overexpression not only reduced phosphorylation of VASP but also total VASP levels, which was different from Western blot results from CIA mouse $CD4^+$ T cells in the DBA/1J mouse line (Yan, Golumba-Nagy, et al. 2021). However, the high levels of IL-6 in transgenic mice lead to a significantly higher reduction of p-VASP as compared to the reduction of total VASP. p-VASP was also significantly decreased in the heterozygous mouse (Figure 27B) (Yan, Golumba-Nagy, et al. 2021).

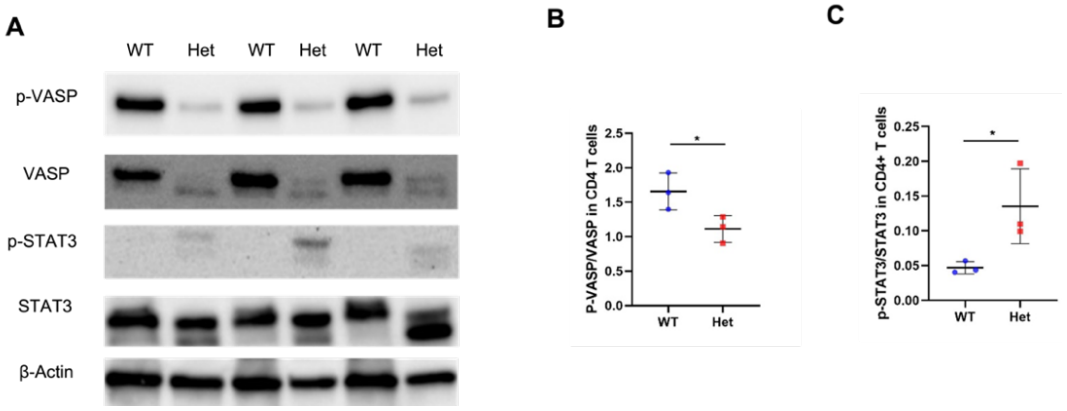

Figure 27 p-VASP (Ser157) and p-STAT3 relative expression in the C57BL/6-Tg(H2-L-IL-6)1Kish/J mouse and wild type mice

(A) Representative results of western blot analysis of total STAT3, p-STAT3, total VASP, p-VASP, and housekeeping protein β-Actin in $CD4^+$ T cells from wild-type mice (WT) and heterozygous IL-6 overexpressing mice (Het). (B) Relative expression of p-STAT3 normalized on total STAT3 expression in $CD4^+$ T cells from WT mice and Het mice (n=3 for each group). (C) Relative expression of p-VASP normalized on total VASP expression in $CD4^+$ T cells from WT mice and Het mice (n=3 each). Data is presented as the mean ± standard error of the mean (SEM). Statistical analysis is performed using a two-tailed Student's t-test. *$p < 0.05$, **$p < 0.01$, ***$p < 0.001$, ****$p < 0.0001$. This diagram was adapted from the supplement materials of publication of Yan et al, 2021.

4.2.2.2 STAT3 pathway is involved in VASP expression

To study the crosstalk between IL-6R signaling, VASP, and STAT3, we also assessed the phosphorylation status of STAT3 in $CD4^+$ T splenocytes from IL-6 overexpressing transgenic mice. In the heterozygous phenotype, phosphorylation levels of STAT3 were higher as expressed to wild-type mice. Therefore, enhanced IL-6 signaling leads to increased p-STAT3 and reduced p-VASP levels in transgenic IL-6 overexpressing mice compared to wild-type mice (Figure 27C) (Yan, Golumba-Nagy, et al. 2021).

4.2.2.3 Treg cells are decreased in C57BL/6-Tg(H2-L-IL-6)1Kish/J mice

To investigate the influence of IL-6 mediated decreased VASP phosphorylation on Treg cell polarization, we analyzed Treg cell frequencies in wild-type mice and transgenic IL-6 overexpressing mice in vivo (Figure 28). Figure 28A shows a representative flow cytometric analysis example for both groups. We observed reduced Treg cell frequencies in IL-6 overexpressing mice when compared to wild-type mice (Figure 28B) (Yan, Golumba-Nagy, et al. 2021). Therefore, reduced p-VASP seems to be related to reduced Treg cell differentiation.

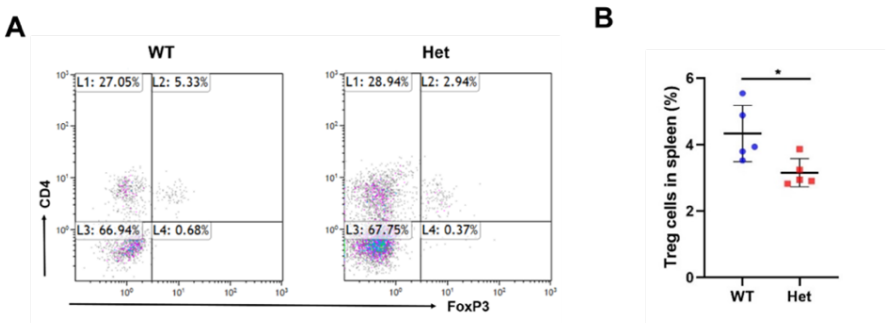

Figure 28 Treg cells are decreased in C57BL/6-Tg(H2-L-IL-6)1Kish/J mice

Treg cells frequencies in wild-type (WT) and heterozygous (Het) mice that overexpresses the IL-6 cytokine. (A) Representative example of flow cytometric staining (B) Treg cell frequencies in the spleen. Data is presented as the mean ± standard error of the mean (SEM). Statistical analysis was performed using a two-tailed Student's t-test (*$p < 0.05$). (*p < 0.05, **p < 0.01, ***p < 0.001, ****p < 0.0001, ns=non-significant). This diagram was adapted from the publication of Yan et al, 2021.

4.2.2.4 TGF-β1 is decreased in C57BL/6-Tg(H2-L-IL-6)1Kish/J mice

Furthermore, we collected blood serum from wild-type mice and IL-6 overexpressing mice and evaluated TGF-β1 expression levels in serum by ELISA. Figure 29 shows that TGF-β1

was dramatically decreased in IL-6 overexpressing mice as compared to wild-type mice (Yan, Golumba-Nagy, et al. 2021).

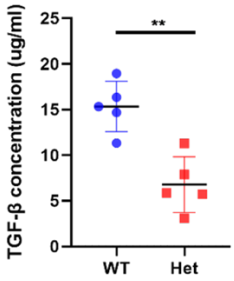

Figure 29 TGF-β1 was decreased in C57BL/6-Tg(H2-L-IL-6)1Kish/J mouse line

TGF-β1 in mouse sera from wild-type (WT) mice and heterozygous IL-6 overexpressing (Het) mice. Data is presented as the mean ± standard error of the mean (SEM). Statistical analysis was performed using a two-tailed Student's t-test (**p < 0.01). This diagram was adapted from the publication of Yan et al, 2021.

4.2.3 Relative p-VASP relative expression is negatively correlated with IL-6R expression

To reveal a possible relationship between mIL-6R on Th17 cells and VASP phosphorylation, the co-expression of mIL-6R and p-VASP was analyzed in individual samples. Interestingly, a negative correlation between IL-6R and p-VASP expression was found (p=0.0333, R^2=0.4118, Y=-9.518*X+29.27) (Yan, Golumba-Nagy, et al. 2021). The correlation analysis Is shown in Figure 30.

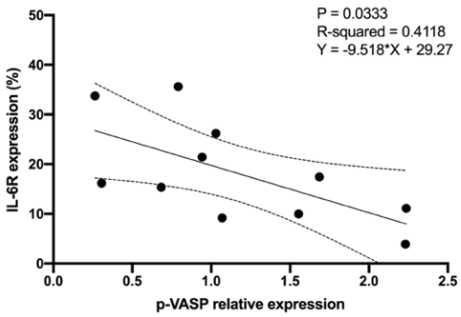

Figure 30 p-VASP relative expression is negatively correlated with IL-6R expression in human RA patients

Correlation between L-6R expression on Th17 cells and p-VASP expression. IL-6R expression was analyzed by flow cytometry and p-VASP levels by western blot. (p=0.0333, R2=0.4118, Y=-9.518*X+29.27). The statistical analysis was performed by the Spearman r correlation test (n=11). This diagram was adapted from the publication of Yan et al, 2021.

4.2.4 p-VASP (Ser157) is downregulated in untreated RA patients and is restored in RA patients reveiving IL-6R inhibitor treatment

To determine whether VASP phosphorylated at Ser157 was regulated in an IL-6 signaling-driven manner in RA patients *in vivo*, Western blot was performed with purified human $CD4^+$ T cells. Figure 31A shows the representative WB results. And p-VASP (Ser157) in $CD4^+$ T cells was significantly downregulated in untreated RA patients (Figure 31B). Importantly, RA patients treated with tocilizumab showed restored VASP's phosphorylation levels at Ser157. This indicates that the treatment of tocilizumab can specifically increase the expression level of p-VASP (Yan, Golumba-Nagy, et al. 2021).

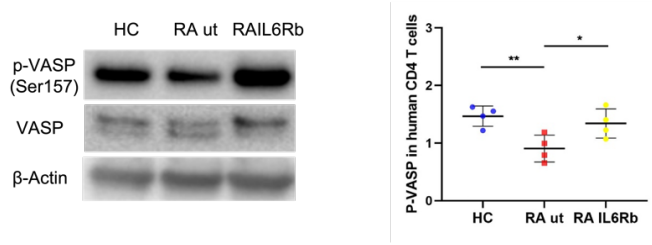

Figure 31 p-VASP (Ser157) was downregulated in untreated RA patients but gets restored in RA patients with IL-6R blocker treatment

(A) Representative example of a western blot analysis of p-VASP expression in $CD4^+$ T cells in RA patients and healthy individuals. (B) p-VASP expression analysis by western blot in $CD4^+$ T cells from HC (n=8), RA ut (n=6), and RA IL-6Rb (n=4). Data is presented as the mean ± standard error of the mean (SEM). Statistical analysis was performed using a one-way ANOVA (*p < 0.05, **p < 0.01). This diagram was adapted from the publication of Yan et al, 2021.

4.3 Integrin signaling is significantly involved in RA pathology as shown by Proteomics analysis on human RA and healthy individual samples

4.3.1 p-VASP (Ser157) expression level is associated with a distinct protein expression profile in RA

To further investigate the possible links between VASP phosphorylation at Ser157 and influenced pathways in $CD4^+$ T cells in RA patients, proteomic analysis of $CD4^+$ T cells from RA patients with low p-VASP expression, healthy individuals with higher p-VASP expression, and RA patients treated with IL-6R blocking antibody tocilizumab was performed. Among more than three thousand proteins, about one hundred proteins with a significantly altered expression (more than 1.5 fold change and $p<0.05$) were identified as shown in Figure 32 (Yan, Golumba-Nagy, et al. 2021). Table 22 shows the detailed DEPs between healthy individuals and untreated RA patients.

Figure 32 DEPs based on the different expression level of p-VASP (Ser157)

Proteomics analysis based on p-VASP (Ser157) levels in $CD4^+$ T cells. Hierarchically clustered heatmap of the relative abundance of proteins in three different types of samples (HC, left 3 columns; RA ut, 3 columns in the middle; RA IL-6Rb, right 3 columns) (n=3 per group). The expression patterns of the top 101 differentially expressed proteins are shown. Colored bars indicate the expression levels. Red blocks represent overexpressed proteins, blue blocks represent proteins with the lowest expression levels. Data is presented as the mean ± standard error of the mean (SEM). Statistical analysis was performed using a two-tailed Student's t-test. $p < 0.05$ was defined as significant. Heat map visualization of DFPs was obtained by calculating a z-score of the label-free quantification values for each protein by TB tools. This diagram was adapted from the publication of Yan et al, 2021.

Table 22 List of DEPs between healthy individuals and RA-untreated patients

DEPs between healthy individuals and RA-untreated patients	Gene names
3-phosphoinositide-dependent protein kinase 1	PDPK1
ADP/ATP translocase 3	SLC25A6
Aladin	AAAS
ATP-binding cassette sub-family D member 3	ABCD3
Beta-catenin-like protein 1	CTNNBL1
CLIP-associating protein 1	CLASP1
Coagulation factor XIII A chain	F13A1
Coiled-coil domain-containing protein 9	CCDC9
Cyclin-dependent kinase 11B	CDK11B
Cysteine-rich protein 1	CRIP1
Deoxyuridine 5-triphosphate nucleotidohydrolase, mitochondrial	DUT
E3 ubiquitin-protein ligase BRE1B	RNF40
Exocyst complex component 1	EXOC1
Fibrinogen gamma chain	FGG
Frataxin, mitochondrial	FXN
Galectin-9	LGALS9
Glutathione S-transferase theta-1	GSTT1
GPI transamidase component PIG-T	PIGT
Granzyme A	GZMA
Guanine nucleotide-binding protein subunit beta-like protein 1	GNB1L
HD domain-containing protein 2	HDDC2
Headcase protein homolog	HECA
Histone acetyltransferase KAT8	KAT8
Histone lysine demethylase PHF8	PHF8
HLA class I histocompatibility antigen, A-2 alpha chain	HLA-A
Inositol hexakisphosphate and diphosphoinositol-pentakisphosphate kinase 2	PPIP5K2
Integrator complex subunit 1	INTS1
Integrin alpha-IIb	ITGA2B
Integrin beta-3	ITGB3
Kynurenine--oxoglutarate transaminase 1	CCBL1
Methylmalonyl-CoA epimerase, mitochondrial	MCEE
Mini-chromosome maintenance complex-binding protein	MCMBP
Mitochondrial import inner membrane translocase subunit Tim10	TIMM10
Mitochondrial import receptor subunit TOM20 homolog	TOMM20
NADH dehydrogenase [ubiquinone] 1 alpha subcomplex subunit 6	NDUFA6
Nipped-B-like protein	NIPBL
Nucleoside diphosphate-linked moiety X motif 19, mitochondrial	NUDT19
Phospholysine phosphohistidine inorganic pyrophosphate phosphatase	LHPP
Protein FAM192A	FAM192A
Protein SMG9	SMG9

DEPs between healthy individuals and RA-untreated patients	Gene names
Protein TSSC4	TSSC4
Ras-related protein Rab-2A	RAB2A
Ras-related protein Rap-2b	RAP2B
Retinal rod rhodopsin-sensitive cGMP 3,5-cyclic phosphodiesterase subunit delta	PDE6D
RNA demethylase ALKBH5	ALKBH5
RWD domain-containing protein 1	RWDD1
THUMP domain-containing protein 1	THUMPD1
Trafficking protein particle complex subunit 1	TRAPPC1
Transcription initiation factor TFIID subunit 10	TAF10
Transmembrane protein 109	TMEM109
tRNA (adenine(58)-N(1))-methyltransferase non-catalytic subunit TRM6	TRMT6
Tyrosine-protein phosphatase non-receptor type 23	PTPN23
Ubiquitin-like protein 5	UBL5
Uridine phosphorylase 1	UPP1
Vacuolar protein sorting-associated protein 52 homolog	VPS52
Very-long-chain (3R)-3-hydroxyacyl-CoA dehydratase 3	HACD3
Vesicle-associated membrane protein-associated protein B/C	VAPB
WD repeat-containing protein 11	WDR11

Table 23 the DEPs between untreated patients and RA patients treated with IL-6R inhibitor Tocilizumab.

Table 23 List of DEPs between RA-untreated patients and RA patients treated with Tocilizumab

DEPs between RA-untreated patients and RA patients treated with Tocilizumab	Gene names
ADP-ribosylation factor-like protein 6-interacting protein 1	ARL6IP1
AT-rich interactive domain-containing protein 1A	ARID1A
Beta-parvin	PARVB
C2 domain-containing protein 5	C2CD5
Calcium and integrin-binding protein 1	CIB1
CD2-associated protein	CD2AP
Coagulation factor XIII A chain	F13A1
Cytoplasmic FMR1-interacting protein 1	CYFIP1
D-beta-hydroxybutyrate dehydrogenase, mitochondrial	BDH1
Dipeptidyl peptidase 9	DPP9
Embigin	EMB
Fibrinogen alpha chain	FGA
Fibrinogen gamma chain	FGG
Fructose-2,6-bisphosphatase TIGAR	TIGAR
Guanine nucleotide-binding protein G(q) subunit alpha	GNAQ

DEPs between RA-untreated patients and RA patients treated with Tocilizumab	Gene names
Guanine nucleotide-binding protein subunit beta-like protein 1	GNB1L
Histone H2B type 2-E	HIST2H2BE
HLA class I histocompatibility antigen, A-24 alpha chain	HLA-A
Integrin alpha-IIb	ITGA2B
Integrin beta-3	ITGB3
Interferon regulatory factor 2-binding protein-like	IRF2BPL
Kynurenine--oxoglutarate transaminase 1	CCBL1
Lanosterol synthase	LSS
Lysocardiolipin acyltransferase 1	LCLAT1
Lysosomal acid lipase/cholesteryl ester hydrolase	LIPA
Mitochondrial import receptor subunit TOM20 homolog	TOMM20
NEDD8-conjugating enzyme UBE2F	UBE2F
NHL repeat-containing protein 2	NHLRC2
Peptidyl-prolyl cis-trans isomerase D	PPID
PERQ amino acid-rich with GYF domain-containing protein 2	GIGYF2
Platelet basic protein	PPBP
pre-mRNA 3 end processing protein WDR33	WDR33
Pre-mRNA-splicing factor 38B	PRPF38B
Propionyl-CoA carboxylase alpha chain, mitochondrial	PCCA
Protein BUD31 homolog	BUD31
Protein MEMO1	MEMO1
Protein O-glucosyltransferase 1	POGLUT1
Protein QIL-1	QIL1
Radixin	RDX
Rap1 GTPase-GDP dissociation stimulator 1	RAP1GDS1
Serine/arginine-rich splicing factor 4	SRSF4
Splicing factor 3B subunit 6	SF3B6
Syntaxin-17	STX17
Trafficking protein particle complex subunit 1	TRAPPC1
Transformer-2 protein homolog alpha	TRA2A
Tubulin β1 chain	TUBB1
Ubiquitin-like protein 5	UBL5
YTH domain-containing family protein 3	YTHDF3
Zinc finger CCCH domain-containing protein 13	ZC3H13
Zinc finger protein 428	ZNF428
Zinc finger RNA-binding protein	ZFR

4.3.2 Integrin signaling is involved in RA

4.3.2.1 Gene ontology (GO) analysis and KEGG pathway analysis based on DEPs in healthy individuals and untreated RA patients

DEPs are enriched in various pathways including but not limited to integrin signaling, signal transduction by L1, MAP2K and MAPK activation, mitochondrial protein import, protein localization, as well as ion and integrin cell surface interactions (Figure 33). Compared to the group with low p-VASP expression group, 17 proteins were upregulated in RA patients treated with IL-6 receptor blocking antibodies (and high p-VASP expression), and 34 proteins were downregulated (more than 1.5 fold change) (Figure 34). The DEPs are involved in three functional categories, including biological processes, molecular functions, and molecular components. Interestingly, DEPs that are involved in integrin signaling were upregulated in the group with low p-VASP expression but downregulated in RA patients with high p-VASP expression treated with IL-6 receptor-blocking antibodies. Integrin signaling pathways, therefore, seem to be important pathways in RA and they are modified by treatment with IL-6 receptor-blocking antibodies. ((Yan, Golumba-Nagy, et al. 2021))

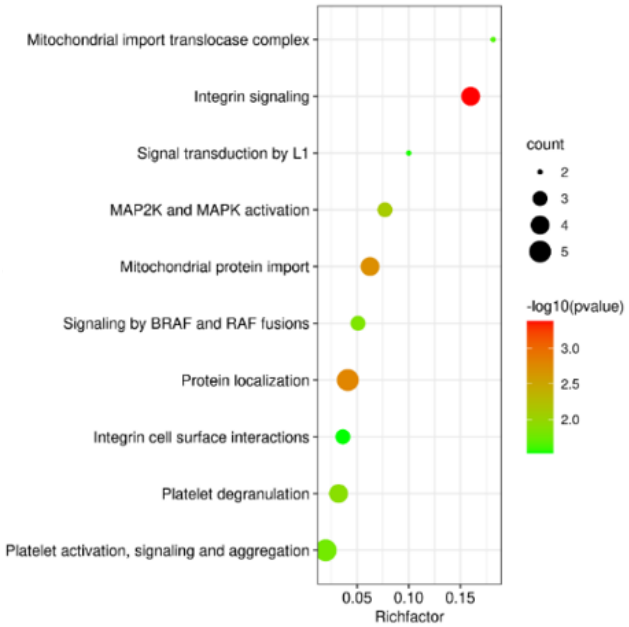

Figure 33 Bubble plot enriched on Gene Ontology (GO) and KEGG pathway in healthy individuals and RA untreated patients (n=3 per group).

The ratio between the number of different proteins in the corresponding pathways and the total number of proteins identified in the graph is higher, indicating a higher difference in protein concentration. The size of the dots represents the number of different proteins associated with the corresponding pathway. Pathways with a high difference between the groups are characterized by a larger number of proteins. The top 10 pathways are listed

below: mitochondrial import translocase complex, integrin signaling, signal transduction by L1, MAP2K activation, mitochondrial protein import, signaling by BRAF and RAF fusions, protein localization, integrin cell surface interactions, platelet degranulation, and platelet activation signaling and aggregation. A bubble diagram was created on the website: http://www.bioinformatics.com.cn/. This diagram was adapted from the publication of Yan et al, 2021.

4.3.2.2 Gene ontology (GO) analysis and KEGG pathway analysis based on DEPs in untreated RA patients and RA patients treated with an IL-6R inhibitor

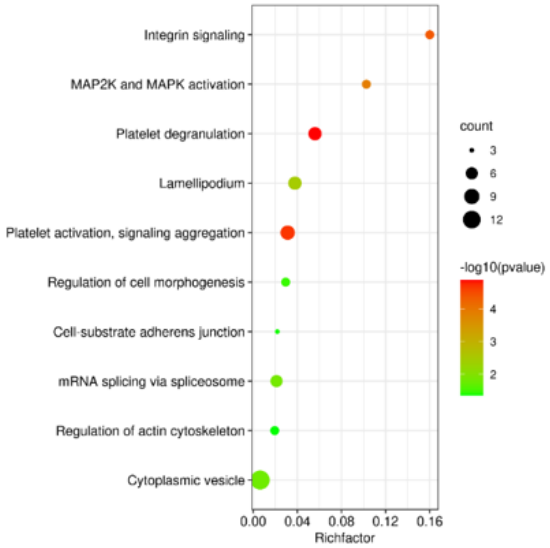

Figure 34 Bubble plot enriched on GO and KEGG pathway in CD4⁺ T cells from RA ut and RA treated with IL-6Rb patients.

The ratio between the number of different proteins in the corresponding pathways and the total number of proteins identified in the graph is higher, indicating a higher difference in protein concentration. The size of the dots represents the number of different proteins associated with the corresponding pathway. Pathways with a high difference between the groups are characterized by a larger number of proteins. The top 10 pathways are listed below: integrin signaling, MAP2K and MAPK activation, platelet degranulation, lamellipodium, platelet activation signaling aggregation, regulation of cell morphogenesis, cell-substrate adherens junction, mRNA splicing via spliceosome, regulation of actin cytoskeleton, and cytoplasmic vesicles. A bubble diagram was created on the website: http://www.bioinformatics.com.cn/. This diagram was adapted from the publication of Yan et al, 2021.

4.3.2.3 Gene set enrichment analysis (GSEA) of DEPs in healthy individuals and untreated RA patients

Gene set enrichment analysis (GSEA) was performed based on DEPs. Several pathways closely related to CD4⁺ T cell functions were significantly modified in untreated RA patients with lower p-VASP expression (Figure 35): integrin mediated signaling pathway (q= 0.0016313214, NES: 1.708097), integrin binding (q= 0.012345679, NES: 1.6539156),

leukocyte migration (q=0.006825, NES: 1.913600), cell substrate adhesion (q= 0.0, NES: 1.714524), cell matrix adhesion (q=0.019293, NES: 1.838242), positive regulation of epithelial cell migration (q= 0.011308562, NES: 1.3389298), regulation of substrate adhesion dependent cell spreading (q= 0.006102565, NES: 107215812), and regulation of tissue remodeling (q= 0.0083289262, NES: 1.7024468) (Yan, Golumba-Nagy, et al. 2021).

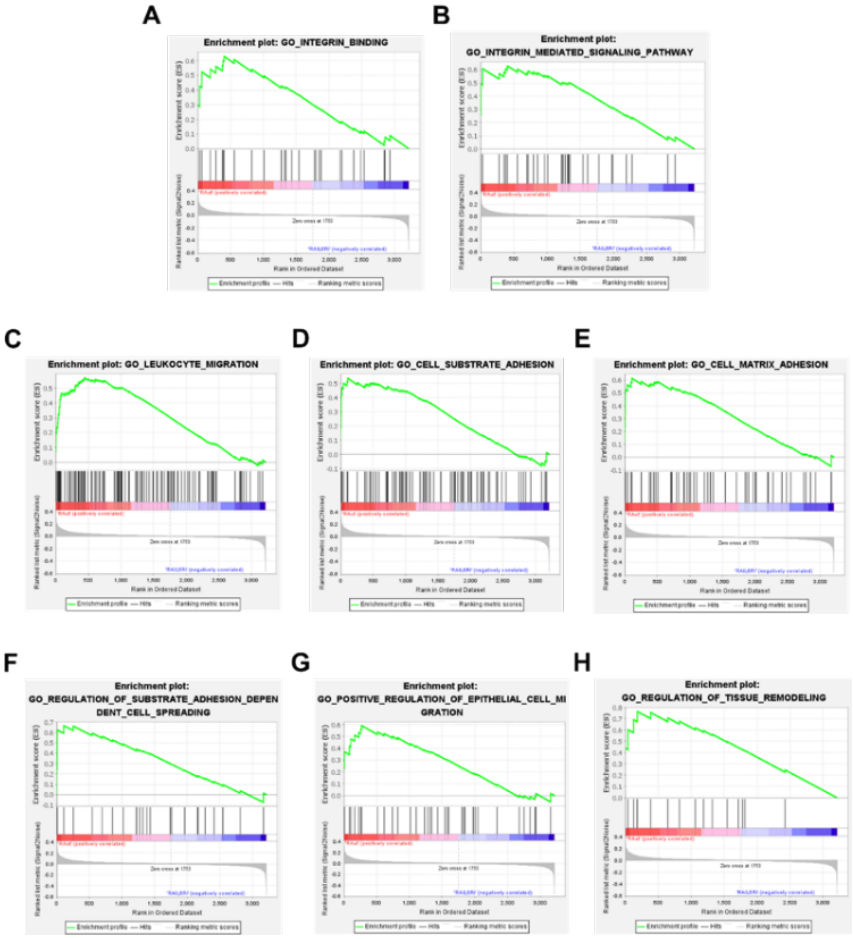

Figure 35 Gene set enrichment analysis (GSEA) score curves based on DEPs in healthy individuals and untreated RA patients

(A-H) Representative enrichment plots are shown for categories identified using GSEA as significantly enriched in positively correlated proteins in RA ut as compared to RA IL-6Rb. Black bars represent the position of members of the category in the ranked list together with the running enrichment score (plotted in green). Examples shown here are the integrin-mediated signaling pathway (q=0.0016313214, NES: 1.708097), integrin-binding (q= 0.012345679, NES: 1.6539156), leukocyte migration (q=0.006825, NES: 1.913600), cell-substrate adhesion (q=0.0, NES: 1.714524), cell-matrix adhesion (q=0.019293, NES: 1.838242), positive regulation of epithelial cell migration (q=0.011308562, NES: 1.3389298), and regulation of substrate adhesion-dependent cell spreading (q=0.006102565, NES: 107215812), regulation of tissue remodeling (q=0.0083289262, NES: 1.7024468). NES = normalized enrichment score; q = FDR (false discovery rate) q-value. Gene set enrichment was performed using GSEA 4.0 software. This diagram was adapted from the publication of Yan et al, 2021.

4.4 *In vitro* transwell migration assay

To further identify whether p-VASP (Ser 157) is crucial for the migration of immune cells in RA, we specifically blocked it and performed a transwell migration assay with purified $CD4^+$ T cells from RA patients as well as healthy individuals *in vitro*. The chemo-attractant migration assay was performed as indicated in the workflow shown in Figure 36 (Yan, Golumba-Nagy, et al. 2021). A chemo-attractant transwell assay experiment (50ng/ml CCL20 in the lower chamber) was performed to study the migration of T cells.

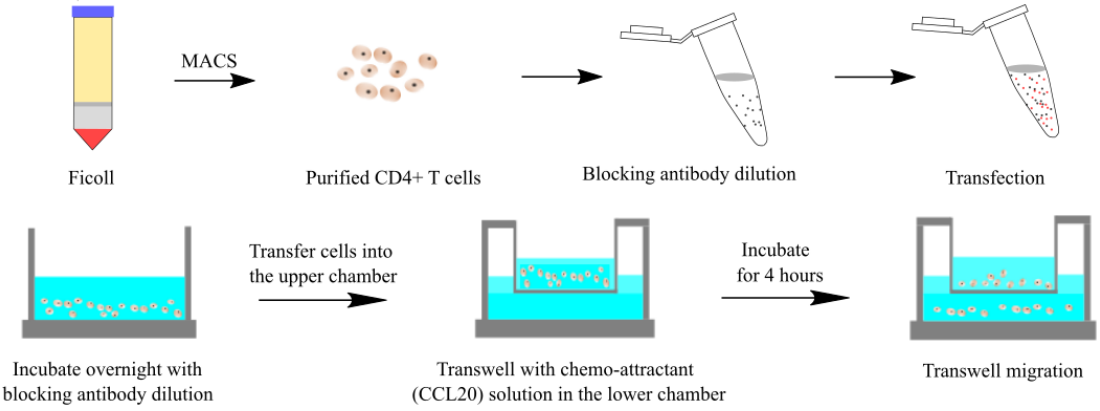

Figure 36 Schematic view of the chemoattractant transwell migration experimental setup

Schematic presentation of the distinct peripheral blood mononuclear cells (PBMCs) layer following density gradient centrifugation of blood samples. $CD4^+$ T cells were enriched through magnetic-activated cell sorting (MACS). Specific blocking peptide for p-VASP was diluted in DPBS. Blocking peptide solution was added to an EP tube containing dry film of lipofection kit for 5 minutes at room temperature. Incubate purified $CD4^+$ T cells and lipo-decorated p-VASP blocking antibody overnight with T cell receptor (TCR) activated. The infected human $CD4^+$ T cells were seeded in the transwell (The upper chamber), and in the lower chamber, which contained a medium with a chemo-attractant (50ng/ml CCL20). Migrated Treg cells in the lower chamber were collected for flow cytometric staining after 4 hours of incubation. This diagram was adapted from the publication of Yan et al, 2021.

4.4.1 Effector T cell migration ability does not alter in response to the p-VASP blockade

More $CD4^+$ T cells migrated towards media containing CCL20 than to control media without CCL20 Figure 37. The experiment revealed that $CD4^+$ T cell migration was increased in untreated RA patients whereas it was reduced in RA patients treated with IL-6 receptor blocking antibodies (Figure 38), regarding the migration of effector $CD4^+$ T cells, no significant difference was found before and after specific blockade of p-VASP (Ser 157) in healthy individuals, untreated RA patients, and RA patients treated with IL-6 receptor blockers (Figure 39) (Yan, Golumba-Nagy, et al. 2021).

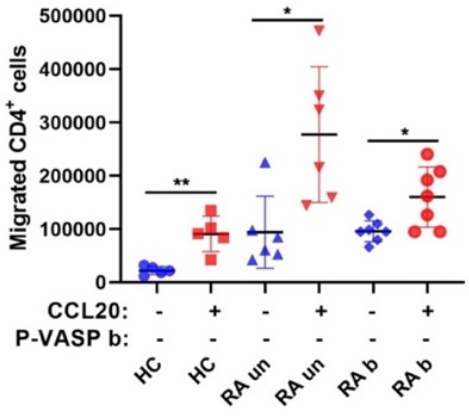

Figure 37 Transwell migration results of CD4⁺ T cells as compared to negative control

Shown is the absolute number of migrated *total* CD4⁺ T cells (including Treg cells) in the negative control group (without 50ng/ml CCL20 in the lower chamber) and positive control group (with 50ng/ml CCL20 in the lower chamber) in a chemo-attractant transwell system (HC, healthy controls; RA un, untreated RA patients; RA b, RA patients treated with IL-6 receptor blocking antibodies). Statistical analysis was performed using a two-tailed Student's t-test (*p < 0.05, **p < 0.01, ***p < 0.001). This diagram was adapted from the publication of Yan et al, 2021.

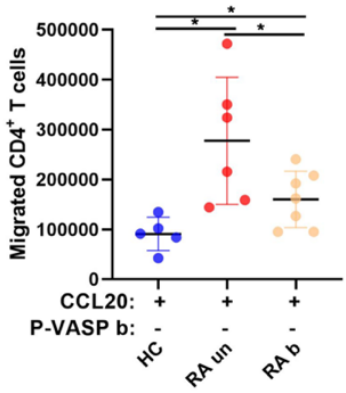

Figure 38 Absolute number of migrated *total* CD4⁺ T cells (including Treg cells) in healthy individuals, untreated RA patients, and RA patients treated with an IL-6R inhibitor

The absolute number of migrated *total* CD4⁺ T cells (including Treg cells) is shown in Figure 37. For clarity, the data from Figure 37 is presented in a different manner to show the differences between HC, untreated RA, and RA blocked patients in the CCL20 group. Statistical analysis was performed using a One-way ANOVA analysis is performed in more than two groups (*p < 0.05, **p < 0.01, ***p < 0.001). This diagram was adapted from the publication of Yan et al, 2021.

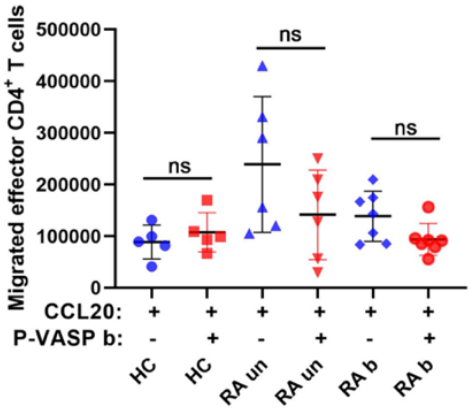

Figure 39 Absolute number of migrated *effector* CD4⁺ T cells (without Treg cells) after specific blockade of p-VASP in healthy individuals, untreated RA and IL-6R blocked RA patients

Absolute number of migrated *effector* CD4⁺ T cells (without Treg cells) after specific blockade of p-VASP in HC, untreated RA and IL-6R blocked RA patients. Statistical analysis was performed using a two-tailed Student's t-test (*p < 0.05, **p < 0.01, ***p < 0.001). This diagram was adapted from the publication of Yan et al, 2021.

4.4.2 Treg cells migration is impaired by specifically blocking p-VASP

We analyzed the effects of p-VASP phosphorylation at Ser157 on Treg cell migration. Representative flow cytometric analysis of migrated $CD25^{high}CD127^{low}FoxP3^{+}$ Treg cells from healthy individuals, untreated RA patients, and RA patients treated with IL-6 receptor blocking antibodies with or without specific p-VASP blocking antibodies are displayed in Figure 40-Figure 42, respectively. In RA patients, more migrated Treg cells were found as compared to healthy individuals. In healthy individuals, no difference before and after the blockade of p-VASP can be observed (Figure 42). The absolute number of migrated Treg cells decreases after the specific blockade of p-VASP (Ser 157) in untreated RA patients and RA patients treated with anti-IL-6 receptor antibodies. These results show that p-VASP is implicated in Treg cell migration in RA (Yan, Golumba-Nagy, et al. 2021).

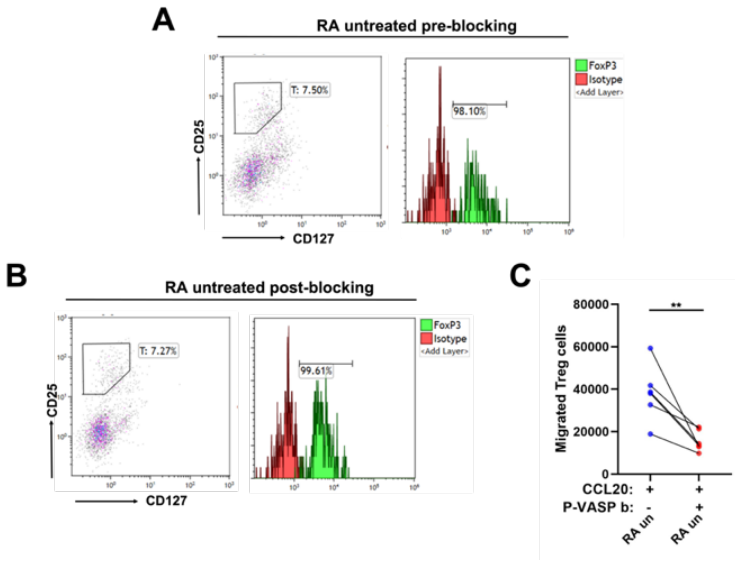

Figure 40 Transwell migration results of Treg cells in RA untreated patients

(A) Representative example of flow cytometric analysis of migrated Treg cells without p-VASP blocking antibodies in untreated RA patients. (B) Same cells as in (A), but after incubation with p-VASP blocking antibodies. (C) The absolute number of migrated Treg cells is decreased as measured by flow cytometry in untreated RA patients after the specific blockade of p-VASP. Statistical analysis was performed using a two-tailed Student's t-test (*p < 0.05, **p < 0.01, ***p < 0.001). This diagram was adapted from the publication of Yan et al, 2021.

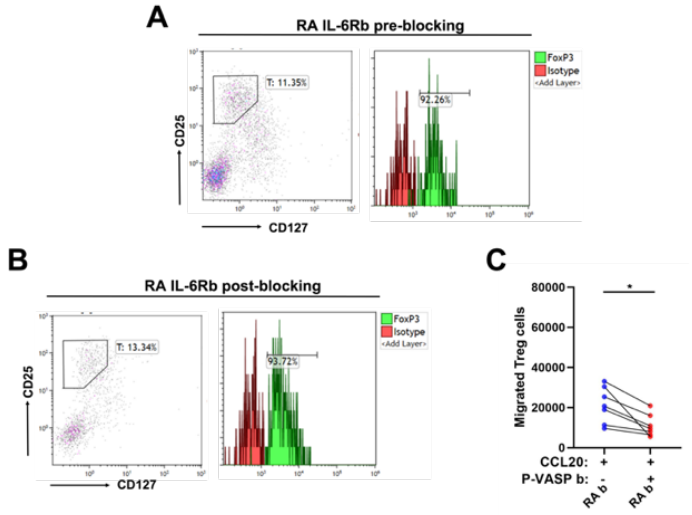

Figure 41 Transwell migration results of Treg cells in RA patients treated with an IL-6R inhibitor

(A) Representative example of flow cytometric analysis of migrated Treg cells without p-VASP blocking antibodies in RA patients treated with an IL-6R blocker. (B) Same cells as in (A), but after incubation with p-VASP blocking antibodies. (C) The absolute number of migrated Treg cells is decreased as measured by flow cytometry in RA patients treated with IL-6R blocker after the p-VASP specifical blockade. Statistical analysis was performed using a two-tailed Student's t-test (*p < 0.05, **p < 0.01, ***p < 0.001). This diagram was adapted from the publication of Yan et al, 2021.

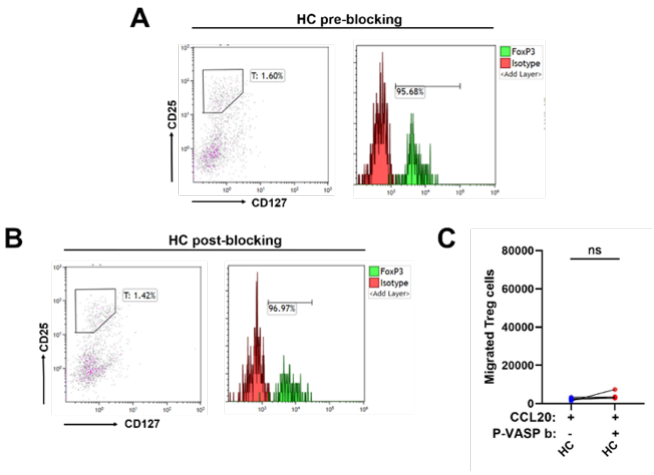

Figure 42 Transwell migration results of Treg cells in healthy individuals

(A) Representative example of flow cytometric analysis of migrated Treg cells without p-VASP blocking antibodies in healthy individuals. (B) Same cells as in (A), but after incubation with p-VASP blocking antibodies. (C) The absolute number of migrated Treg cells as assessed by flow cytometry in healthy individuals. Statistical analysis was performed using a two-tailed Student's t-test (*p < 0.05, **p < 0.01, ***p < 0.001). This diagram was adapted from the publication of Yan et al, 2021.

5 DISCUSSION

IL-6R blocking antibodies have been established as an efficient treatment for RA. However, the exact role of mIL-6R mediated IL-6 signaling in RA remains unclear. Especially, the influence of the mIL-6R on the balance between Th17 cells and Treg cells still needs to be elucidated. Th17 cells are an important inflammation-inducing cell population involved in the pathogenesis of RA. A better understanding of Th17 cell regulation might therefore help us to improve RA treatment.

In the first step, we established CIA in the DBA1/J mouse model in our lab. The mice in the CIA group developed inflammation in their paws and had an increased clinical score when comparted to control mice as shown previously by other research groups (Rosloniec et al. 2021; Ho et al. 2010; Sekine et al. 2008). H&E staining revealed synovial hyperplasia and increased inflammation in murine in the CIA group as compared to the control group, as well as pathological characteristics also shared by human RA patients (Orange et al. 2018; Lewis et al. 2019; Triaille et al. 2020). Interestingly, three independent phenotypes of RA have been suggested based on machine learning integration of synovial histologic features and RNA sequencing: a high inflammation type characterized by leukocytes infiltration, a low inflammation type and a mixed type (Orange et al. 2018). However, it is not clear whether there are also comparable subtypes of arthritis in CIA mice. These differences between human and murine arthritis, and the fact that experimental autoimmune arthritis is induced by collagen injection in mice, show the limitations of the CIA mouse model. As an alternative to CIA, humanized mouse models of arthritis can be obtained by introducing human transgenes or transferring human cells or tissues into immunodeficient mice (Lin et al. 2021; Schinnerling et al. 2019; Margheri et al. 2021). However, further investigations are needed to determine if the pathogenesis of these humanized mouse models share similarities with the development of RA.

Th17 cell numbers were increased in the spleen and this cell type significantly accumulated in inflamed joints of CIA mice, thereby indicating an involvement of the Th17 cell subset in the pathology of CIA (Gaffen 2009; Sarkar and Fox 2010; Pickens et al. 2010). In addition, IL-17 deficient mouse are resistant to collagen induced arthritis (Nakae et al. 2003). Our results and evidence from other research groups indicate that Th17 cells play a pathological role in murine autoimmune arthritis. It remains unclear if this is also the case in human suffering from RA, as anti-IL-17A treatment failed to induce an efficient response in RA patients in clinical trials (Koenders and van den Berg 2016; Pavelka et al. 2015). However, IL-17F and other IL-17

subtypes which are also produced by Th17 cells are significantly upregulated in the synovium and plasma (Jain et al. 2015; Zrioual et al. 2009) of RA patients and could play a major role in RA.

To explore the interaction between Treg cells and Th17 cells in CIA, we stained purified splenic $CD4^+$ T cells with the Treg cell marker FoxP3 and found that Treg cells were significantly decreased in the CIA group (Figure 11) (Yan, Golumba-Nagy, et al. 2021). This implies that the immune suppressive function in CIA mice may be disturbed due to the reduction of absolute Treg cell numbers, as Treg cells are crucial for the maintenance of immune homeostasis. This finding is also in accordance with our previous research showing that the Treg frequency is significantly decreased in untreated RA patients as compared to healthy individuals (Meyer et al. 2021).

To further investigate whether the immune surveillance role of Treg cells is disrupted in the CIA mouse model, we performed immunofluorescence staining to detect the production of TGF-β by Treg cells. What we found is that there are no Treg cells in control mouse joints (Figure 12) (Yan, Golumba-Nagy, et al. 2021), which might be because the synovial tissue is too thin in control mouse joints. This can be explained by the structure of the synovial tissue in joints, due to there being only 1-3 layers of synovial tissue under healthy conditions. As a results, there are few fibroblasts and small amounts of macrophages in the synovium (Smith et al. 2003). However, Treg cells are found to be present in CIA mouse joints and are characterized by the secretion of TGF-β (Yan, Golumba-Nagy, et al. 2021). Due to it not being possible to directly compare the Treg cell immune surveillance role in mouse joints, we performed IHF staining with lymph nodes from control mice and CIA mice. We found $FoxP3^+$ Treg cells present both in the lymph nodes of control mice and CIA mice, but a significant amount of Treg cells in CIA mice did not produce TGF-β (Figure 13) (Yan, Golumba-Nagy, et al. 2021). This is remarkable because TGF-β produced by Treg cells promotes the expression of Foxp3 and thereby controls immune homeostasis *in vivo* (Marie et al. 2005). Moreover, it also contributes to the inhibition of effector T cells activation and proliferation in both, human and mice (Bennett et al. 2001; Nakamura, Kitani, and Strober 2001). The evidence of our immunofluorescence staining supports the notion that Treg cell functions is impaired in CIA mice by reducing the production of TGF-β.

Moreover, the balance between Treg and Th17 cells was evaluated in the CIA mouse model. We found that the balance between these two populations was shifted towards Th17 cells in CIA mice (Figure 14) (Yan, Golumba-Nagy, et al. 2021). This dysregulation was also observed

by other groups (Jin et al. 2018; Bakheet et al. 2019) and might result from an over-activation of the Th17 subset as well as a decrease in Treg cells. Considering the imbalance between both subsets and impaired suppression ability of Treg cells, further investigation of both subsets is needed in order to improve our understanding of the pathogenesis of this disease.

In order to gain an insight into the characteristics of Th17 cells in CIA mice and control mice, we measured mIL-6R expression on Th17 cells by flow cytometry and observed a significant increase of mIL-6R in CIA mice (Yan, Golumba-Nagy, et al. 2021). This is an interesting finding as mIL-6R on $CD4^+$ T cells was significantly decreased once the cells are activated (Nowell et al. 2009). However, what we observed in this study in regards to RA-like mouse models seems to be, at least partially in disagreement with previous publications. As a subpopulation of $CD4^+$ T cells, Th17 cells show different characteristics when compared to other $CD4^+$ T cells. The increased membrane-bound IL-6R on Th17 cells may represent a regulation mechanism that differs from other $CD4^+$ T cell subsets. Recently, a group (Harbour et al. 2020) described that persistent IL-6 signaling through ongoing classical IL-6 receptor activation is required to retain the transcriptional and functional identity of Th17 cells in two mouse models of colitis. Therefore, the membrane-bound IL-6R expression might represent an potential mechanism regulating the pathological role of Th17 cells and the balance between both subsets.

To determine the characteristics of increased mIL-6R on Th17 cells and its role in the development of CIA, a dynamic evaluation of Th17 cells, serum IL-17, mIL-6R expression on Th17 cells, as well as serum IL-6 were performed (Yan, Golumba-Nagy, et al. 2021). This is the first time that a dynamic characterization of Th17 cells and mIL-6R was performed ex vivo by flow cytometry in CIA mice. This helps to reveal potential dynamic variations in mIL-6 receptor expression as well as possible effects of altered classical IL-6 receptor signaling on Th17 and Treg cell functions. The experimental workflow of CIA induction is displayed in Figure 16. The results show that Th17 cell frequency retains rather stable with higher levels CIA mice, but no statistically significant difference was found between the two groups (Figure 17). The Th17 frequency in the CIA group seems contradictory to our flow cytometry results as shown in Figure 10C, which might be due to the limited number of mice in each group (n=5) in our dynamic evaluation experiment. The effect size is too low to reach statistically significance between the two groups.

Even though the absolute number of Th17 cells does not vary a lot in the development of CIA, that does not necessarily mean that Th17 cells do not play an important role in the

development of CIA. In a next step, we performed analysis by ELISA to see the dynamic serum IL-17 levels. Importantly, there exists a significant increase in the IL-17 concentration (Figure 18) when compared to the control group, which indicates the Th17 cells pathological role is enhanced in the development of CIA through an increased production of the inflammatory cytokine IL-17, while its absolute number remains stable (Yan, Golumba-Nagy, et al. 2021). Recently, it has been reported that continuous IL-6 signaling mediated by the mIL-6R is necessary for Th17 cells to maintain IL-17 production in mouse models of colitis (Harbour et al. 2020). Therefore, mIL-6R on Th17 cells may be involved in enhancing Th17 cells function through an increasing in the production of IL-17 in the CIA mouse model.

Next, we monitored the mIL-6R expression on Th17 cells and found that mIL-6R on Th17 cells is significantly elevated in the CIA group starting with the 42nd-day after the first immunization (Figure 19). Interestingly, as the ligand of IL-6R, serum IL-6 is increased, but only in the early stage of CIA development (until day 42 after the first immunization) (Figure 20) (Yan, Golumba-Nagy, et al. 2021). Therefore, the upregulation of mIL-6R on Th17 cells could be an important mechanism contributing to the maintenance of Th17 cell functions in autoimmune arthritis where the serum level of IL-6 decreases. This is the first report revealing the dynamic characteristics of mIL-6R on Th17 cells and IL-6 in the serum. Our data provides evidence of a possible link between IL-6 serum levels and IL-6 receptor expression on Th17 cells, thereby suggesting that IL-6 receptor upregulation is a pathological mechanism contributing to the maintenance of pathological functioning of Th17 cells in autoimmune arthritis. Furthermore, given the IL-6 concentration elevation in the early stage of CIA and mIL-6 receptor increase in the late stages of CIA it might be interesting to observe the clinical effects caused by IL-6 blockade in early-stage and IL-6R blockade in RA patients respectively, which requires further investigation.

The dynamic evaluation of Treg cells showed that Treg cells frequency retained at a lower level in the development of CIA (Figure 21), in the early stage of CIA Treg frequency retained stable, but increased 42 days after the first immunization in the CIA group (Figure 22). This might be the decreased IL-6 in the serum (Figure 20) as IL-6 was reported to prevent Treg cell induction in the gut in a recent study (Yan, Ramanan, et al. 2021). The balance between Th17 cells and Treg cells is shifted to Th17 cells in CIA mice during the development of arthritis (Figure 23). At Day 42 after the first immunization, the Th17/Treg ratio reached its peak due to low Treg frequencies at this point in time (Yan, Golumba-Nagy, et al. 2021). Concurrently, the mean clinical score of CIA mice almost reached its highest level (Figure 9C), indicating that the Th17/Treg ratio is related to the clinical score of CIA mice.

VASP phosphorylation is an important post-translational modification that is shown to have a negative interaction with SH3 domains and regulates localization of VASP, which is thought to be involved in cell motility (Döppler et al. 2013; Lambrechts et al. 2000). Furthermore, Henes et al. showed that the expression level of VASP was decreased *in vitro* by IL-6 in endothelial HMEC-1 cells (Henes et al. 2009). Considering both, the roles of p-VASP in cell migration and the influence of IL-6 on p-VASP levels, we performed western blot analysis to measure the expression level of p-VASP in purified $CD4^+$ T cells in CIA mice and found that VASP phosphorylated at Ser157 was significantly decreased in CIA mice as compared to the control group (Figure 26) (Yan, Golumba-Nagy, et al. 2021). However, we wanted to further assess if the downregulation of p-VASP (Ser157) is specifically related to IL-6 signaling in CIA mice. To address this question, we used a mouse line (C57BL/6-Tg(H2-L-IL-6)1Kish/J) that overexpresses human IL-6 to evaluate the p-VASP (Ser157) expression level. Previous studies demonstrated a link between IL-6 and JAK/STAT3 pathway. First, we verified if the STAT3 pathway is activated in the transgenic mouse line. The western blot results show that p-STAT3 was significantly increased in the IL-6 overexpression mice (Yan, Golumba-Nagy, et al. 2021). Subsequently, the VASP phosphorylation at Ser157 as determined by western blot in IL-6 overexpression mouse was assessed and found to be specifically downregulated when compared to wild-type mice (Figure 27) (Yan, Golumba-Nagy, et al. 2021). This is direct evidence showing the regulation of p-VASP (Ser157) expression by IL-6 signaling. Interestingly, IL-6 does not only reduce VASP expression level at Ser157 but also total VASP expression (Figure 27A) (Yan, Golumba-Nagy, et al. 2021). Whether IL-6 regulates the expression level of p-VASP by activating the STAT3 pathway requires further investigation.

As the results displayed above are all established in RA-like mouse models *in vivo*, it is necessary to verify them with human RA samples in order to acquire knowledge on which to base further translational research in this field. Consistent with our findings in $CD4^+$ T cells from CIA mice, mIL-6R expression on Th17 cells is significantly upregulated in untreated RA patients when compared to healthy individuals (Figure 24D), and importantly RA patients treated with tocilizumab have a lower level of the mIL-6 receptor on Th17 cells as compared to untreated RA patients (Yan, Golumba-Nagy, et al. 2021). The reason for the mIL-6-R downregulation after the treatment with tocilizumab might be that tocilizumab prevents the binding of the antibody for flow cytometry, IL-6 signaling mediated by the mIL-6R may also be downregulated on Th17 cells as a consequence of the treatment with tocilizumab. In addition, we wanted to investigate the expression level of IL-6R mRNA level. PCR results showed that mRNA of the IL-6R in $CD4^+$ T cells is significantly increased in untreated RA patients as

compared to healthy individuals (Figure 25) (Yan, Golumba-Nagy, et al. 2021). However, we failed to obtain PCR results from peripheral Th17 cells from RA patients due to the limited number of these cells that can be isolated from the peripheral blood. In addition, we were able to show that p-VASP (Ser157) in $CD4^+$ T cells is dramatically downregulated in untreated RA patients when compared to healthy individuals (Figure 31). Importantly, the phosphorylation level of p-VASP (Ser157) is specifically restored by tocilizumab treatment. Therefore, p-VASP (Ser157) is specifically downregulated by extensive IL-6 signaling both in the CIA mouse model as well as in human RA samples and is upregulated by treatment with tocilizumab (Yan, Golumba-Nagy, et al. 2021). In addition, we also performed correlation analysis between p-VASP and IL-6R and found that their expression is negatively correlated (Figure 30) (Yan, Golumba-Nagy, et al. 2021).

We performed proteomics based analysis on purified $CD4^+$ T cells from healthy individuals, untreated RA patients and RA patients treated with tocilizumab to identify pathways that might be affected by changes in phosphorylation of VASP. Figure 32 shows three groups of DEPs. In a next step, gene ontology (GO) and KEGG pathway analysis based on DEPs was performed (Figure 33 & Figure 34). Our results highlight the role of integrin signaling as the activation of related pathways was significantly enriched in the group with reduced expression levels of p-VASP (Ser157) (Yan, Golumba-Nagy, et al. 2021). Furthermore, the reversibility of reduced p-VASP expression in RA patients achieved through IL-6 receptor inhibition confirms a possible link between IL-6 and p-VASP, and GSEA confirmed the enrichment of integrin signaling and related pathways in $CD4^+$ T cells with low p-VASP (Ser 157) levels (Figure 35) (Yan, Golumba-Nagy, et al. 2021). Consistent with our results, previous evidence suggests that integrin signaling implies cell adhesion to the extracellular matrix and to other cells (Horton et al. 2015; Horton et al. 2016; Zaidel-Bar et al. 2007). Additionally, integrin signaling has been shown to be important for the migration of leukocytes into inflamed joints response and of inflammatory mediators (Ley et al. 2007; Nourshargh and Alon 2014). Collectively, this data indicates p-VASP may play a role in $CD4^+$ T cell migration in autoimmune arthritis.

To further determine whether the expression of p-VASP (Ser157) correlates with the ability of cells to migrate in RA, we specifically blocked p-VASP in purified human $CD4^+$ T cells in vitro and performed flow cytometric analysis of migrated CD4+ effector T cells and Treg cells (Figure 36). More $CD4^+$ T cells migrated to the lower chamber in untreated RA patients when compared with healthy individuals and RA patients treated with tocilizumab (Figure 38) (Yan, Golumba-Nagy, et al. 2021). These findings are in line with previous findings published in this field (Tang et al. 2017; Petrasca et al. 2020; Tran et al. 2007). They show that more

inflammatory cells accumulate in inflamed joints, thereby indicating increased migratory ability of these inflammatory cells. After receiving treatment with tocilizumab, RA patients showed a reduced number of migrated $CD4^+$ T cells, which means that tocilizumab treatment can reduce the migration of inflammatory $CD4^+$ T cells in RA (Yan, Golumba-Nagy, et al. 2021). Our study shows that the specific blockade of p-VASP has no influence on $CD4^+$ effector T cell migration (Figure 39). In contrast, Treg cell migration is significantly reduced by specific inhibition of p-VASP (Ser 157) through blocking antibodies in untreated RA patients (Figure 40) as well as IL-6 receptor blocking antibodies in RA patients (Figure 41) (Yan, Golumba-Nagy, et al. 2021). The observed increase in Treg cell migration in RA explains why Treg cell frequencies are elevated in the synovial fluid of RA patients in some studies (Moradi et al. 2014; Cao et al. 2003; Dejaco et al. 2010). In contrast to Treg cells from RA patients, no reduction in cell migration was observed in Treg cells from healthy individuals following the specific blockade of VASP (Figure 42), and this effect seems to exceed the relative increase in Treg cell migration in RA patients when compared to healthy individuals (Yan, Golumba-Nagy, et al. 2021). This is a very interesting point because both healthy individuals and RA patients treated with the IL-6R inhibitor tocilizumab express a higher level of p-VASP (Ser157). However, they show different migration levels of Treg cells. This difference might be explained by the autoimmune state present in RA patients. In addition, we also found a reduced Treg cell number (Figure 28) and reduced TGF-β1 production (Figure 29) in IL-6 overexpression mouse line (Yan, Golumba-Nagy, et al. 2021), but it is not clear if the reduction of Treg and impaired Treg functions are directly related to IL-6 signaling mediated p-VASP deficiency. Further investigation is required regarding the influence of p-VASP's on Treg cell's differentiation and migratory ability, especially in transgenic p-VASP (Ser157) knockout RA mouse models.

One of the limitations of this study is that the functional role of VASP in Treg cell migration is not studied in VASP knock-out mice. This approach is hampered by the fact that the knock-out of VASP in mice affects the cortical development and leads to the absence of major cortical axon tracs. VASP knock-out mice therefore die during embryogenesis (Kwiatkowski et al. 2007). Despite the lack of in vivo data, we believe that the results of our ex vivo and in vitro analysis of murine and human $CD4^+$ T cells strongly support a role of VASP in Treg cell migration.

To sum up, our study provides new insights into the role of a dynamic elevation of mIL-6 receptor expression on Th17 cells in autoimmune arthritis and links IL-6 receptor signaling to reduced migration of Treg cells. Modification of Treg cell migration is induced by IL-6-mediated reduction in the post-translational phosphorylation of VASP. Our findings identify impaired

VASP phosphorylation as an important process contributing to deficient Treg cell migration and thereby to the pathogenesis of RA. Modification of VASP phosphorylation may be a promising therapeutic strategy to ameliorate autoimmune arthritis by enhancing Treg cell migration into inflamed joints.

6 REFERENCES

Almutairi, K., J. Nossent, D. Preen, H. Keen, and C. Inderjeeth. 2021. 'The global prevalence of rheumatoid arthritis: a meta-analysis based on a systematic review', *Rheumatol Int*, 41: 863-77.

Alpizar-Rodriguez, D., L. Brulhart, R. B. Mueller, B. Möller, J. Dudler, A. Ciurea, U. A. Walker, I. Von Mühlenen, D. Kyburz, P. Zufferey, M. Mahler, S. Bas, D. Gascon, C. Lamacchia, P. Roux-Lombard, K. Lauper, M. J. Nissen, D. S. Courvoisier, C. Gabay, and A. Finckh. 2017. 'The prevalence of anticitrullinated protein antibodies increases with age in healthy individuals at risk for rheumatoid arthritis', *Clin Rheumatol*, 36: 677-82.

Arnold, P., W. Luckstadt, W. Li, I. Boll, J. Lokau, C. Garbers, R. Lucius, S. Rose-John, and C. Becker-Pauly. 2020. 'Joint Reconstituted Signaling of the IL-6 Receptor via Extracellular Vesicles', *Cells*, 9.

Avci, A. B., E. Feist, and G. R. Burmester. 2018. 'Targeting IL-6 or IL-6 Receptor in Rheumatoid Arthritis: What's the Difference?', *BioDrugs*, 32: 531-46.

Azizi, G., F. Jadidi-Niaragh, and A. Mirshafiey. 2013. 'Th17 Cells in Immunopathogenesis and treatment of rheumatoid arthritis', *Int J Rheum Dis*, 16: 243-53.

Bakheet, S. A., M. A. Ansari, A. Nadeem, S. M. Attia, A. R. Alhoshani, G. Gul, Q. H. Al-Qahtani, N. A. Albekairi, K. E. Ibrahim, and S. F. Ahmad. 2019. 'CXCR3 antagonist AMG487 suppresses rheumatoid arthritis pathogenesis and progression by shifting the Th17/Treg cell balance', *Cell Signal*, 64: 109395.

Behrens, F., A. Himsel, S. Rehart, J. Stanczyk, B. Beutel, S. Y. Zimmermann, U. Koehl, B. Möller, S. Gay, J. P. Kaltwasser, J. M. Pfeilschifter, and H. H. Radeke. 2007. 'Imbalance in distribution of functional autologous regulatory T cells in rheumatoid arthritis', *Ann Rheum Dis*, 66: 1151-6.

Bennett, C. L., J. Christie, F. Ramsdell, M. E. Brunkow, P. J. Ferguson, L. Whitesell, T. E. Kelly, F. T. Saulsbury, P. F. Chance, and H. D. Ochs. 2001. 'The immune dysregulation, polyendocrinopathy, enteropathy, X-linked syndrome (IPEX) is caused by mutations of FOXP3', *Nat Genet*, 27: 20-1.

Bettelli, E., Y. Carrier, W. Gao, T. Korn, T. B. Strom, M. Oukka, H. L. Weiner, and V. K. Kuchroo. 2006. 'Reciprocal developmental pathways for the generation of pathogenic effector TH17 and regulatory T cells', *Nature*, 441: 235-8.

Blume, C., P. M. Benz, U. Walter, J. Ha, B. E. Kemp, and T. Renné. 2007. 'AMP-activated protein kinase impairs endothelial actin cytoskeleton assembly by phosphorylating vasodilator-stimulated phosphoprotein', *J Biol Chem*, 282: 4601-12.

Bo, M., G. L. Erre, M. Niegowska, M. Piras, L. Taras, M. G. Longu, G. Passiu, and L. A. Sechi. 2018. 'Interferon regulatory factor 5 is a potential target of autoimmune response triggered by Epstein-barr virus and Mycobacterium avium subsp. paratuberculosis in rheumatoid arthritis: investigating a mechanism of molecular mimicry', *Clin Exp Rheumatol*, 36: 376-81.

Bopp, T., C. Becker, M. Klein, S. Klein-Hessling, A. Palmetshofer, E. Serfling, V. Heib, M. Becker, J. Kubach, S. Schmitt, S. Stoll, H. Schild, M. S. Staege, M. Stassen, H. Jonuleit, and E. Schmitt. 2007. 'Cyclic adenosine monophosphate is a key component of regulatory T cell-mediated suppression', *J Exp Med*, 204: 1303-10.

Borsellino, G., M. Kleinewietfeld, D. Di Mitri, A. Sternjak, A. Diamantini, R. Giometto, S. Höpner, D. Centonze, G. Bernardi, M. L. Dell'Acqua, P. M. Rossini, L. Battistini, O. Rötzschke, and K. Falk. 2007. 'Expression of ectonucleotidase CD39 by Foxp3+ Treg cells: hydrolysis of extracellular ATP and immune suppression', *Blood*, 110: 1225-32.

Bours, M. J., E. L. Swennen, F. Di Virgilio, B. N. Cronstein, and P. C. Dagnelie. 2006. 'Adenosine 5'-triphosphate and adenosine as endogenous signaling molecules in immunity and inflammation', *Pharmacol Ther*, 112: 358-404.

Brand, D. D., K. A. Latham, and E. F. Rosloniec. 2007. 'Collagen-induced arthritis', *Nat Protoc*, 2: 1269-75.

Breedveld, F. C., M. H. Weisman, A. F. Kavanaugh, S. B. Cohen, K. Pavelka, R. van Vollenhoven, J. Sharp, J. L. Perez, and G. T. Spencer-Green. 2006. 'The PREMIER study: A multicenter, randomized, double-blind clinical trial of combination therapy with adalimumab plus methotrexate versus methotrexate alone or adalimumab alone in patients with early, aggressive rheumatoid arthritis who had not had previous methotrexate treatment', *Arthritis Rheum*, 54: 26-37.

Butler, D. M., A. M. Malfait, L. J. Mason, P. J. Warden, G. Kollias, R. N. Maini, M. Feldmann, and F. M. Brennan. 1997. 'DBA/1 mice expressing the human TNF-alpha transgene develop a severe, erosive arthritis: characterization of the cytokine cascade and cellular composition', *J Immunol*, 159: 2867-76.

Campbell, D. J., and M. A. Koch. 2011. 'Phenotypical and functional specialization of FOXP3+ regulatory T cells', *Nat Rev Immunol*, 11: 119-30.

Camps, M., T. Rückle, H. Ji, V. Ardissone, F. Rintelen, J. Shaw, C. Ferrandi, C. Chabert, C. Gillieron, B. Françon, T. Martin, D. Gretener, D. Perrin, D. Leroy, P. A. Vitte, E. Hirsch, M. P. Wymann, R. Cirillo, M. K. Schwarz, and C. Rommel. 2005. 'Blockade of PI3Kgamma suppresses joint inflammation and damage in mouse models of rheumatoid arthritis', *Nat Med*, 11: 936-43.

Cao, D., V. Malmström, C. Baecher-Allan, D. Hafler, L. Klareskog, and C. Trollmo. 2003. 'Isolation and functional characterization of regulatory CD25brightCD4+ T cells from the target organ of patients with rheumatoid arthritis', *Eur J Immunol*, 33: 215-23.

Chang, M. H., and P. A. Nigrovic. 2019. 'Antibody-dependent and -independent mechanisms of inflammatory arthritis', *JCI Insight*, 4.

Chen, W., W. Jin, N. Hardegen, K. J. Lei, L. Li, N. Marinos, G. McGrady, and S. M. Wahl. 2003. 'Conversion of peripheral CD4+CD25- naive T cells to CD4+CD25+ regulatory T cells by TGF-beta induction of transcription factor Foxp3', *J Exp Med*, 198: 1875-86.

Cohen, S., E. Hurd, J. Cush, M. Schiff, M. E. Weinblatt, L. W. Moreland, J. Kremer, M. B. Bear, W. J. Rich, and D. McCabe. 2002. 'Treatment of rheumatoid arthritis with anakinra, a recombinant human interleukin-1 receptor antagonist, in combination with methotrexate: results of a twenty-four-week, multicenter, randomized, double-blind, placebo-controlled trial', *Arthritis Rheum*, 46: 614-24.

Cross, M., E. Smith, D. Hoy, L. Carmona, F. Wolfe, T. Vos, B. Williams, S. Gabriel, M. Lassere, N. Johns, R. Buchbinder, A. Woolf, and L. March. 2014. 'The global burden of rheumatoid arthritis: estimates from the global burden of disease 2010 study', *Ann Rheum Dis*, 73: 1316-22.

Dar, L., S. Tiosano, A. Watad, N. L. Bragazzi, D. Zisman, D. Comaneshter, A. Cohen, and H. Amital. 2018. 'Are obesity and rheumatoid arthritis interrelated?', *Int J Clin Pract*, 72.

De Benedetti, F., N. Rucci, A. Del Fattore, B. Peruzzi, R. Paro, M. Longo, M. Vivarelli, F. Muratori, S. Berni, P. Ballanti, S. Ferrari, and A. Teti. 2006. 'Impaired skeletal development in interleukin-6-transgenic mice: a model for the impact of chronic inflammation on the growing skeletal system', *Arthritis Rheum*, 54: 3551-63.

de la Rosa, M., S. Rutz, H. Dorninger, and A. Scheffold. 2004. 'Interleukin-2 is essential for CD4+CD25+ regulatory T cell function', *Eur J Immunol*, 34: 2480-8.

Dejaco, C., C. Duftner, A. Klauser, and M. Schirmer. 2010. 'Altered T-cell subtypes in spondyloarthritis, rheumatoid arthritis and polymyalgia rheumatica', *Rheumatol Int*, 30: 297-303.

Döppler, H. R., L. I. Bastea, L. J. Lewis-Tuffin, P. Z. Anastasiadis, and P. Storz. 2013. 'Protein kinase D1-mediated phosphorylations regulate vasodilator-stimulated phosphoprotein (VASP) localization and cell migration', *J Biol Chem*, 288: 24382-93.

Döppler, H., and P. Storz. 2013. 'Regulation of VASP by phosphorylation: consequences for cell migration', *Cell Adh Migr*, 7: 482-6.

Dougados, M., P. Emery, E. M. Lemmel, R. de la Serna, C. A. Zerbini, S. Brin, and P. van Riel. 2003. 'Efficacy and safety of leflunomide and predisposing factors for treatment response in patients with active rheumatoid arthritis: RELIEF 6-month data', *J Rheumatol*, 30: 2572-9.

Downs-Canner, S., S. Berkey, G. M. Delgoffe, R. P. Edwards, T. Curiel, K. Odunsi, D. L. Bartlett, and N. Obermajer. 2017. 'Suppressive IL-17A(+)Foxp3(+) and ex-Th17 IL-17A(neg)Foxp3(+) T(reg) cells are a source of tumour-associated T(reg) cells', *Nat Commun*, 8: 14649.

Emery, P., F. C. Breedveld, S. Hall, P. Durez, D. J. Chang, D. Robertson, A. Singh, R. D. Pedersen, A. S. Koenig, and B. Freundlich. 2008. 'Comparison of methotrexate monotherapy with a combination of methotrexate and etanercept in active, early, moderate to severe rheumatoid arthritis (COMET): a randomised, double-blind, parallel treatment trial', *Lancet*, 372: 375-82.

Emery, P., E. Keystone, H. P. Tony, A. Cantagrel, R. van Vollenhoven, A. Sanchez, E. Alecock, J. Lee, and J. Kremer. 2008. 'IL-6 receptor inhibition with tocilizumab improves treatment outcomes in patients with rheumatoid arthritis refractory to anti-tumour necrosis factor biologicals: results from a 24-week multicentre randomised placebo-controlled trial', *Ann Rheum Dis*, 67: 1516-23.

Feldmann, M., and R. N. Maini. 2003. 'Lasker Clinical Medical Research Award. TNF defined as a therapeutic target for rheumatoid arthritis and other autoimmune diseases', *Nat Med*, 9: 1245-50.

Fife, B. T., and K. E. Pauken. 2011. 'The role of the PD-1 pathway in autoimmunity and peripheral tolerance', *Ann N Y Acad Sci*, 1217: 45-59.

Flores-Borja, F., E. C. Jury, C. Mauri, and M. R. Ehrenstein. 2008. 'Defects in CTLA-4 are associated with abnormal regulatory T cell function in rheumatoid arthritis', *Proc Natl Acad Sci U S A*, 105: 19396-401.

Fujimoto, M., S. Serada, M. Mihara, Y. Uchiyama, H. Yoshida, N. Koike, Y. Ohsugi, T. Nishikawa, B. Ripley, A. Kimura, T. Kishimoto, and T. Naka. 2008. 'Interleukin-6 blockade suppresses autoimmune arthritis in mice by the inhibition of inflammatory Th17 responses', *Arthritis Rheum*, 58: 3710-9.

Gaffen, S. L. 2009. 'The role of interleukin-17 in the pathogenesis of rheumatoid arthritis', *Curr Rheumatol Rep*, 11: 365-70.

Gaffo, A., K. G. Saag, and J. R. Curtis. 2006. 'Treatment of rheumatoid arthritis', *Am J Health Syst Pharm*, 63: 2451-65.

Gambaryan, S., W. Hauser, A. Kobsar, M. Glazova, and U. Walter. 2001. 'Distribution, cellular localization, and postnatal development of VASP and Mena expression in mouse tissues', *Histochem Cell Biol*, 116: 535-43.

Gartlehner, G., R. A. Hansen, B. L. Jonas, P. Thieda, and K. N. Lohr. 2006. 'The comparative efficacy and safety of biologics for the treatment of rheumatoid arthritis: a systematic review and metaanalysis', *J Rheumatol*, 33: 2398-408.

Gauldie, S. D., D. S. McQueen, C. J. Clarke, and I. P. Chessell. 2004. 'A robust model of adjuvant-induced chronic unilateral arthritis in two mouse strains', *J Neurosci Methods*, 139: 281-91.

Gewiese-Rabsch, J., C. Drucker, S. Malchow, J. Scheller, and S. Rose-John. 2010. 'Role of IL-6 trans-signaling in CCl_4induced liver damage', *Biochim Biophys Acta*, 1802: 1054-61.

Glant, T. T., K. Mikecz, A. Arzoumanian, and A. R. Poole. 1987. 'Proteoglycan-induced arthritis in BALB/c mice. Clinical features and histopathology', *Arthritis Rheum*, 30: 201-12.

Goekoop-Ruiterman, Y. P., J. K. de Vries-Bouwstra, C. F. Allaart, D. van Zeben, P. J. Kerstens, J. M. Hazes, A. H. Zwinderman, A. J. Peeters, J. M. de Jonge-Bok, C. Mallée, W. M. de Beus, P. B. de Sonnaville, J. A. Ewals, F. C. Breedveld, and B. A. Dijkmans. 2007. 'Comparison of treatment strategies in early rheumatoid arthritis: a randomized trial', *Ann Intern Med*, 146: 406-15.

Gondek, D. C., L. F. Lu, S. A. Quezada, S. Sakaguchi, and R. J. Noelle. 2005. 'Cutting edge: contact-mediated suppression by CD4+CD25+ regulatory cells involves a granzyme B-dependent, perforin-independent mechanism', *J Immunol*, 174: 1783-6.

Grossman, W. J., J. W. Verbsky, B. L. Tollefsen, C. Kemper, J. P. Atkinson, and T. J. Ley. 2004. 'Differential expression of granzymes A and B in human cytotoxic lymphocyte subsets and T regulatory cells', *Blood*, 104: 2840-8.

Halbrügge, M., and U. Walter. 1989. 'Purification of a vasodilator-regulated phosphoprotein from human platelets', *Eur J Biochem*, 185: 41-50.

Hammer, J., F. Gallazzi, E. Bono, R. W. Karr, J. Guenot, P. Valsasnini, Z. A. Nagy, and F. Sinigaglia. 1995. 'Peptide binding specificity of HLA-DR4 molecules: correlation with rheumatoid arthritis association', *J Exp Med*, 181: 1847-55.

Harbour, S. N., D. F. DiToro, S. J. Witte, C. L. Zindl, M. Gao, T. R. Schoeb, G. W. Jones, S. A. Jones, R. D. Hatton, and C. T. Weaver. 2020. 'TH17 cells require ongoing classic IL-6 receptor signaling to retain transcriptional and functional identity', *Sci Immunol*, 5.

Harrington, L. E., R. D. Hatton, P. R. Mangan, H. Turner, T. L. Murphy, K. M. Murphy, and C. T. Weaver. 2005. 'Interleukin 17-producing CD4+ effector T cells develop via a lineage distinct from the T helper type 1 and 2 lineages', *Nat Immunol*, 6: 1123-32.

Hashizume, M., N. Hayakawa, and M. Mihara. 2008. 'IL-6 trans-signalling directly induces RANKL on fibroblast-like synovial cells and is involved in RANKL induction by TNF-alpha and IL-17', *Rheumatology (Oxford)*, 47: 1635-40.

Hegen, M., J. C. Keith, Jr., M. Collins, and C. L. Nickerson-Nutter. 2008. 'Utility of animal models for identification of potential therapeutics for rheumatoid arthritis', *Ann Rheum Dis*, 67: 1505-15.

Heink, S., N. Yogev, C. Garbers, M. Herwerth, L. Aly, C. Gasperi, V. Husterer, A. L. Croxford, K. Möller-Hackbarth, H. S. Bartsch, K. Sotlar, S. Krebs, T. Regen, H. Blum, B. Hemmer, T. Misgeld, T. F. Wunderlich, J. Hidalgo, M. Oukka, S. Rose-John, M. Schmidt-Supprian, A. Waisman, and T. Korn. 2017. 'Trans-presentation of IL-6 by dendritic cells is required for the priming of pathogenic T(H)17 cells', *Nat Immunol*, 18: 74-85.

Helmick, C. G., D. T. Felson, R. C. Lawrence, S. Gabriel, R. Hirsch, C. K. Kwoh, M. H. Liang, H. M. Kremers, M. D. Mayes, P. A. Merkel, S. R. Pillemer, J. D. Reveille, and J. H. Stone. 2008. 'Estimates of the prevalence of arthritis and other rheumatic conditions in the United States. Part I', *Arthritis Rheum*, 58: 15-25.

Henes, J., M. A. Schmit, J. C. Morote-Garcia, V. Mirakaj, D. Kohler, L. Glover, T. Eldh, U. Walter, J. Karhausen, S. P. Colgan, and P. Rosenberger. 2009. 'Inflammation-associated repression of vasodilator-stimulated phosphoprotein (VASP) reduces alveolar-capillary barrier function during acute lung injury', *FASEB J*, 23: 4244-55.

Hennigan, S., and A. Kavanaugh. 2008. 'Interleukin-6 inhibitors in the treatment of rheumatoid arthritis', *Ther Clin Risk Manag*, 4: 767-75.

Hibi, M., M. Murakami, M. Saito, T. Hirano, T. Taga, and T. Kishimoto. 1990. 'Molecular cloning and expression of an IL-6 signal transducer, gp130', *Cell*, 63: 1149-57.

Ho, P. P., L. Y. Lee, X. Zhao, B. H. Tomooka, R. T. Paniagua, O. Sharpe, M. J. BenBarak, P. E. Chandra, W. Hueber, L. Steinman, and W. H. Robinson. 2010. 'Autoimmunity against fibrinogen mediates inflammatory arthritis in mice', *J Immunol*, 184: 379-90.

Hoes, J. N., J. W. Jacobs, S. M. Verstappen, J. W. Bijlsma, and G. J. Van der Heijden. 2009. 'Adverse events of low-to medium-dose oral glucocorticoids in inflammatory diseases: a meta-analysis', *Ann Rheum Dis*, 68: 1833-8.

Holmdahl, R. 2006. 'Dissection of the genetic complexity of arthritis using animal models', *Immunol Lett*, 103: 86-91.

Holmdahl, R., T. J. Goldschmidt, S. Kleinau, C. Kvick, and R. Jonsson. 1992. 'Arthritis induced in rats with adjuvant oil is a genetically restricted, alpha beta T-cell dependent autoimmune disease', *Immunology*, 76: 197-202.

Horai, R., A. Nakajima, K. Habiro, M. Kotani, S. Nakae, T. Matsuki, A. Nambu, S. Saijo, H. Kotaki, K. Sudo, A. Okahara, H. Tanioka, T. Ikuse, N. Ishii, P. L. Schwartzberg, R. Abe, and Y. Iwakura. 2004. 'TNF-alpha is crucial for the development of autoimmune arthritis in IL-1 receptor antagonist-deficient mice', *J Clin Invest*, 114: 1603-11.

Horai, R., S. Saijo, H. Tanioka, S. Nakae, K. Sudo, A. Okahara, T. Ikuse, M. Asano, and Y. Iwakura. 2000. 'Development of chronic inflammatory arthropathy resembling rheumatoid arthritis in interleukin 1 receptor antagonist-deficient mice', *J Exp Med*, 191: 313-20.

Horton, E. R., A. Byron, J. A. Askari, D. H. J. Ng, A. Millon-Fremillon, J. Robertson, E. J. Koper, N. R. Paul, S. Warwood, D. Knight, J. D. Humphries, and M. J. Humphries. 2015. 'Definition of a consensus integrin adhesome and its dynamics during adhesion complex assembly and disassembly', *Nat Cell Biol*, 17: 1577-87.

Horton, E. R., J. D. Humphries, J. James, M. C. Jones, J. A. Askari, and M. J. Humphries. 2016. 'The integrin adhesome network at a glance', *J Cell Sci*, 129: 4159-63.

Howe, A. K. 2004. 'Regulation of actin-based cell migration by cAMP/PKA', *Biochim Biophys Acta*, 1692: 159-74.

Hsieh, C. S., S. E. Macatonia, C. S. Tripp, S. F. Wolf, A. O'Garra, and K. M. Murphy. 1993. 'Development of TH1 CD4+ T cells through IL-12 produced by Listeria-induced macrophages', *Science*, 260: 547-9.

Huizinga, T. W., C. I. Amos, A. H. van der Helm-van Mil, W. Chen, F. A. van Gaalen, D. Jawaheer, G. M. Schreuder, M. Wener, F. C. Breedveld, N. Ahmad, R. F. Lum, R. R. de Vries, P. K. Gregersen, R. E. Toes, and L. A. Criswell. 2005. 'Refining the complex rheumatoid arthritis phenotype based on specificity of the HLA-DRB1 shared epitope for antibodies to citrullinated proteins', *Arthritis Rheum*, 52: 3433-8.

Hunter, C. A., and S. A. Jones. 2015. 'IL-6 as a keystone cytokine in health and disease', *Nat Immunol*, 16: 448-57.

Huter, E. N., G. A. Punkosdy, D. D. Glass, L. I. Cheng, J. M. Ward, and E. M. Shevach. 2008. 'TGF-beta-induced Foxp3+ regulatory T cells rescue scurfy mice', *Eur J Immunol*, 38: 1814-21.

Jain, M., M. Attur, V. Furer, J. Todd, R. Ramirez, M. Lock, Q. A. Lu, S. B. Abramson, and J. D. Greenberg. 2015. 'Increased plasma IL-17F levels in rheumatoid arthritis patients are responsive to methotrexate, anti-TNF, and T cell costimulatory modulation', *Inflammation*, 38: 180-6.

Jiao, Z., W. Wang, R. Jia, J. Li, H. You, L. Chen, and Y. Wang. 2007. 'Accumulation of FoxP3-expressing CD4+CD25+ T cells with distinct chemokine receptors in synovial fluid of patients with active rheumatoid arthritis', *Scand J Rheumatol*, 36: 428-33.

Jin, S., H. Chen, Y. Li, H. Zhong, W. Sun, J. Wang, T. Zhang, J. Ma, S. Yan, J. Zhang, Q. Tian, X. Yang, and J. Wang. 2018. 'Maresin 1 improves the Treg/Th17 imbalance in rheumatoid arthritis through miR-21', *Ann Rheum Dis*, 77: 1644-52.

Jones, G., A. Sebba, J. Gu, M. B. Lowenstein, A. Calvo, J. J. Gomez-Reino, D. A. Siri, M. Tomsic, E. Alecock, T. Woodworth, and M. C. Genovese. 2010. 'Comparison of tocilizumab monotherapy versus methotrexate monotherapy in patients with moderate to severe rheumatoid arthritis: the AMBITION study', *Ann Rheum Dis*, 69: 88-96.

Kadowaki, K. M., H. Matsuno, H. Tsuji, and I. Tunru. 1994. 'CD4+ T cells from collagen-induced arthritic mice are essential to transfer arthritis into severe combined immunodeficient mice', *Clin Exp Immunol*, 97: 212-8.

Kaneko, S., Y. Kondo, M. Yokosawa, K. Furuyama, S. Segawa, H. Tsuboi, A. Kanamori, I. Matsumoto, M. Yamazaki, and T. Sumida. 2018. 'The RORγt-CCR6-CCL20 axis augments Th17 cells invasion into the synovia of rheumatoid arthritis patients', *Mod Rheumatol*, 28: 814-25.

Kaplan, M. J. 2013. 'Role of neutrophils in systemic autoimmune diseases', *Arthritis Res Ther*, 15: 219.

Keystone, E. C., M. C. Genovese, D. E. Schlichting, I. de la Torre, S. D. Beattie, T. P. Rooney, and P. C. Taylor. 2018. 'Safety and Efficacy of Baricitinib Through 128 Weeks in an Open-label, Longterm Extension Study in Patients with Rheumatoid Arthritis', *J Rheumatol*, 45: 14-21.

Kim, E. Y., and K. D. Moudgil. 2009. 'The determinants of susceptibility/resistance to adjuvant arthritis in rats', *Arthritis Res Ther*, 11: 239.

Kimura, A., and T. Kishimoto. 2010. 'IL-6: regulator of Treg/Th17 balance', *Eur J Immunol*, 40: 1830-5.

Kishimoto, T., S. Akira, and T. Taga. 1992. 'Interleukin-6 and its receptor: a paradigm for cytokines', *Science*, 258: 593-7.

Klareskog, L., D. van der Heijde, J. P. de Jager, A. Gough, J. Kalden, M. Malaise, E. Martín Mola, K. Pavelka, J. Sany, L. Settas, J. Wajdula, R. Pedersen, S. Fatenejad, and M. Sanda. 2004. 'Therapeutic effect of the combination of etanercept and methotrexate compared with each treatment alone in patients with rheumatoid arthritis: double-blind randomised controlled trial', *Lancet*, 363: 675-81.

Knochelmann, H. M., C. J. Dwyer, S. R. Bailey, S. M. Amaya, D. M. Elston, J. M. Mazza-McCrann, and C. M. Paulos. 2018. 'When worlds collide: Th17 and Treg cells in cancer and autoimmunity', *Cell Mol Immunol*, 15: 458-69.

Koenders, M. I., and W. B. van den Berg. 2016. 'Secukinumab for rheumatology: development and its potential place in therapy', *Drug Des Devel Ther*, 10: 2069-80.

Kotschenreuther, K., I. Waque, S. Yan, A. Meyer, T. Haak, J. von Tresckow, J. Schiller, L. Gloyer, M. Dittrich-Salamon, and D. M. Kofler. 2021. 'Cannabinoids drive Th17 cell differentiation in patients with rheumatic autoimmune diseases', *Cell Mol Immunol*, 18: 764-66.

Kraakman, M. J., H. L. Kammoun, T. L. Allen, V. Deswaerte, D. C. Henstridge, E. Estevez, V. B. Matthews, B. Neill, D. A. White, A. J. Murphy, L. Peijs, C. Yang, S. Risis, C. R. Bruce, X. J. Du, A. Bobik, R. S. Lee-Young, B. A. Kingwell, A. Vasanthakumar, W. Shi, A. Kallies, G. I. Lancaster, S. Rose-John, and M. A. Febbraio. 2015. 'Blocking IL-6 trans-signaling prevents high-fat diet-induced adipose tissue macrophage recruitment but does not improve insulin resistance', *Cell Metab*, 21: 403-16.

Krause, M., and A. Gautreau. 2014. 'Steering cell migration: lamellipodium dynamics and the regulation of directional persistence', *Nat Rev Mol Cell Biol*, 15: 577-90.

Kumar, B. V., T. J. Connors, and D. L. Farber. 2018. 'Human T Cell Development, Localization, and Function throughout Life', *Immunity*, 48: 202-13.

Kwiatkowski, A. V., D. A. Rubinson, E. W. Dent, J. Edward van Veen, J. D. Leslie, J. Zhang, L. M. Mebane, U. Philippar, E. M. Pinheiro, A. A. Burds, R. T. Bronson, S. Mori, R. Fässler, and F. B. Gertler. 2007. 'Ena/VASP Is Required for neuritogenesis in the developing cortex', *Neuron*, 56: 441-55.

Laban, H., A. Weigert, J. Zink, A. Elgheznawy, C. Schurmann, L. Gunther, R. Abdel Malik, S. Bothur, S. Wingert, R. Bremer, M. A. Rieger, B. Brune, R. P. Brandes, I. Fleming, and P. M. Benz. 2018. 'VASP regulates leukocyte infiltration, polarization, and vascular repair after ischemia', *J Cell Biol*, 217: 1503-19.

Laban, H., A. Weigert, J. Zink, A. Elgheznawy, C. Schürmann, L. Günther, R. Abdel Malik, S. Bothur, S. Wingert, R. Bremer, M. A. Rieger, B. Brüne, R. P. Brandes, I. Fleming, and P. M. Benz. 2018. 'VASP regulates leukocyte infiltration, polarization, and vascular repair after ischemia', *J Cell Biol*, 217: 1503-19.

Lambrechts, A., A. V. Kwiatkowski, L. M. Lanier, J. E. Bear, J. Vandekerckhove, C. Ampe, and F. B. Gertler. 2000. 'cAMP-dependent protein kinase phosphorylation of EVL, a Mena/VASP relative, regulates its interaction with actin and SH3 domains', *J Biol Chem*, 275: 36143-51.

Lard, L. R., H. Visser, I. Speyer, I. E. vander Horst-Bruinsma, A. H. Zwinderman, F. C. Breedveld, and J. M. Hazes. 2001. 'Early versus delayed treatment in patients with recent-onset rheumatoid arthritis: comparison of two cohorts who received different treatment strategies', *Am J Med*, 111: 446-51.

Lawson, C. A., A. K. Brown, V. Bejarano, S. H. Douglas, C. H. Burgoyne, A. S. Greenstein, A. W. Boylston, P. Emery, F. Ponchel, and J. D. Isaacs. 2006. 'Early rheumatoid arthritis is associated with a deficit in the CD4+CD25high regulatory T cell population in peripheral blood', *Rheumatology (Oxford)*, 45: 1210-7.

Leipe, J., M. Grunke, C. Dechant, C. Reindl, U. Kerzendorf, H. Schulze-Koops, and A. Skapenko. 2010. 'Role of Th17 cells in human autoimmune arthritis', *Arthritis Rheum*, 62: 2876-85.

Lewis, M. J., M. R. Barnes, K. Blighe, K. Goldmann, S. Rana, J. A. Hackney, N. Ramamoorthi, C. R. John, D. S. Watson, S. K. Kummerfeld, R. Hands, S. Riahi, V. Rocher-Ros, F. Rivellese, F. Humby, S. Kelly, M. Bombardieri, N. Ng, M. DiCicco, D. van der Heijde, R. Landewé, A. van der Helm-van Mil, A. Cauli, I. B. McInnes, C. D. Buckley, E. Choy, P. C. Taylor, M. J. Townsend, and C. Pitzalis. 2019. 'Molecular Portraits of Early Rheumatoid Arthritis Identify Clinical and Treatment Response Phenotypes', *Cell Rep*, 28: 2455-70.e5.

Ley, K., C. Laudanna, M. I. Cybulsky, and S. Nourshargh. 2007. 'Getting to the site of inflammation: the leukocyte adhesion cascade updated', *Nat Rev Immunol*, 7: 678-89.

Li, S., H. Yin, K. Zhang, T. Wang, Y. Yang, X. Liu, X. Chang, M. Zhang, X. Yan, Y. Ren, W. Pan, and L. Zhang. 2017. 'Effector T helper cell populations are elevated in the bone marrow of rheumatoid arthritis patients and correlate with disease severity', *Sci Rep*, 7: 4776.

Liang, B., C. Workman, J. Lee, C. Chew, B. M. Dale, L. Colonna, M. Flores, N. Li, E. Schweighoffer, S. Greenberg, V. Tybulewicz, D. Vignali, and R. Clynes. 2008. 'Regulatory T cells inhibit dendritic cells by lymphocyte activation gene-3 engagement of MHC class II', *J Immunol*, 180: 5916-26.

Lin, L., W. Xuan, D. Luckey, S. Wang, F. Wang, J. Lau, K. J. Warrington, E. L. Matteson, R. Vassallo, and V. Taneja. 2021. 'A novel humanized model of rheumatoid arthritis associated lung disease', *Clin Immunol*, 230: 108813.

Madhok, R., A. Crilly, J. Watson, and H. A. Capell. 1993. 'Serum interleukin 6 levels in rheumatoid arthritis: correlations with clinical and laboratory indices of disease activity', *Ann Rheum Dis*, 52: 232-4.

Maini, R. N., F. C. Breedveld, J. R. Kalden, J. S. Smolen, D. Davis, J. D. Macfarlane, C. Antoni, B. Leeb, M. J. Elliott, J. N. Woody, T. F. Schaible, and M. Feldmann. 1998. 'Therapeutic efficacy of multiple intravenous infusions of anti-tumor necrosis factor alpha monoclonal antibody combined with low-dose weekly methotrexate in rheumatoid arthritis', *Arthritis Rheum*, 41: 1552-63.

Maini, R. N., P. C. Taylor, J. Szechinski, K. Pavelka, J. Bröll, G. Balint, P. Emery, F. Raemen, J. Petersen, J. Smolen, D. Thomson, and T. Kishimoto. 2006. 'Double-blind randomized controlled clinical trial of the interleukin-6 receptor antagonist, tocilizumab, in European patients with rheumatoid arthritis who had an incomplete response to methotrexate', *Arthritis Rheum*, 54: 2817-29.

Margheri, F., L. Maggi, A. Biagioni, A. Chillà, A. Laurenzana, F. Bianchini, D. Bani, M. Capone, A. Mazzoni, M. C. Rossi, F. Liotta, L. Cosmi, T. Giani, R. Cimaz, G. Fibbi, F. Annunziato, and M. Del Rosso. 2021. 'Th17 lymphocyte-dependent degradation of joint cartilage by synovial fibroblasts in a humanized mouse model of arthritis and reversal by secukinumab', *Eur J Immunol*, 51: 220-30.

Marie, J. C., J. J. Letterio, M. Gavin, and A. Y. Rudensky. 2005. 'TGF-beta1 maintains suppressor function and Foxp3 expression in CD4+CD25+ regulatory T cells', *J Exp Med*, 201: 1061-7.

Martin, D. A., J. E. Towne, G. Kricorian, P. Klekotka, J. E. Gudjonsson, J. G. Krueger, and C. B. Russell. 2013. 'The emerging role of IL-17 in the pathogenesis of psoriasis: preclinical and clinical findings', *J Invest Dermatol*, 133: 17-26.

Martin, J. C., D. L. Baeten, and R. Josien. 2014. 'Emerging role of IL-17 and Th17 cells in systemic lupus erythematosus', *Clin Immunol*, 154: 1-12.

McNamee, K., R. Williams, and M. Seed. 2015. 'Animal models of rheumatoid arthritis: How informative are they?', *Eur J Pharmacol*, 759: 278-86.

Meyer, A., P. S. Wittekind, K. Kotschenreuther, J. Schiller, J. von Tresckow, T. H. Haak, and D. M. Kofler. 2021. 'Regulatory T cell frequencies in patients with rheumatoid arthritis are increased by conventional and biological DMARDs but not by JAK inhibitors', *Ann Rheum Dis*, 80: e196.

Moradi, B., P. Schnatzer, S. Hagmann, N. Rosshirt, T. Gotterbarm, J. P. Kretzer, M. Thomsen, H. M. Lorenz, F. Zeifang, and T. Tretter. 2014. 'CD4^{+}CD25^{+}/highCD127low/$^{-}$ regulatory T cells are enriched in rheumatoid arthritis and osteoarthritis joints--analysis of frequency and phenotype in synovial membrane, synovial fluid and peripheral blood', *Arthritis Res Ther*, 16: R97.

Möttönen, M., J. Heikkinen, L. Mustonen, P. Isomäki, R. Luukkainen, and O. Lassila. 2005. 'CD4+ CD25+ T cells with the phenotypic and functional characteristics of regulatory T cells are enriched in the synovial fluid of patients with rheumatoid arthritis', *Clin Exp Immunol*, 140: 360-7.

Möttönen, T., P. Hannonen, M. Leirisalo-Repo, M. Nissilä, H. Kautiainen, M. Korpela, L. Laasonen, H. Julkunen, R. Luukkainen, K. Vuori, L. Paimela, H. Blåfield, M. Hakala, K. Ilva, U. Yli-Kerttula, K. Puolakka, P. Järvinen, M. Hakola, H. Piirainen, J. Ahonen, I. Pälvimäki, S. Forsberg, K. Koota, and C. Friman. 1999. 'Comparison of combination therapy with single-drug therapy in early rheumatoid arthritis: a randomised trial. FIN-RACo trial group', *Lancet*, 353: 1568-73.

Murphy, C. A., C. L. Langrish, Y. Chen, W. Blumenschein, T. McClanahan, R. A. Kastelein, J. D. Sedgwick, and D. J. Cua. 2003. 'Divergent pro- and antiinflammatory roles for IL-23 and IL-12 in joint autoimmune inflammation', *J Exp Med*, 198: 1951-7.

Nakae, S., A. Nambu, K. Sudo, and Y. Iwakura. 2003. 'Suppression of immune induction of collagen-induced arthritis in IL-17-deficient mice', *J Immunol*, 171: 6173-7.

Nakamura, K., A. Kitani, and W. Strober. 2001. 'Cell contact-dependent immunosuppression by CD4(+)CD25(+) regulatory T cells is mediated by cell surface-bound transforming growth factor beta', *J Exp Med*, 194: 629-44.

Nandi, P., G. H. Kingsley, and D. L. Scott. 2008. 'Disease-modifying antirheumatic drugs other than methotrexate in rheumatoid arthritis and seronegative arthritis', *Curr Opin Rheumatol*, 20: 251-6.

Niki, Y., H. Yamada, S. Seki, T. Kikuchi, H. Takaishi, Y. Toyama, K. Fujikawa, and N. Tada. 2001. 'Macrophage- and neutrophil-dominant arthritis in human IL-1 alpha transgenic mice', *J Clin Invest*, 107: 1127-35.

Nishimoto, N., J. Hashimoto, N. Miyasaka, K. Yamamoto, S. Kawai, T. Takeuchi, N. Murata, D. van der Heijde, and T. Kishimoto. 2007. 'Study of active controlled monotherapy used for rheumatoid arthritis, an IL-6 inhibitor (SAMURAI): evidence of clinical and radiographic benefit from an x ray reader-blinded randomised controlled trial of tocilizumab', *Ann Rheum Dis*, 66: 1162-7.

Nishimoto, N., K. Yoshizaki, N. Miyasaka, K. Yamamoto, S. Kawai, T. Takeuchi, J. Hashimoto, J. Azuma, and T. Kishimoto. 2004. 'Treatment of rheumatoid arthritis with humanized anti-interleukin-6 receptor antibody: a multicenter, double-blind, placebo-controlled trial', *Arthritis Rheum*, 50: 1761-9.

Noack, M., and P. Miossec. 2014. 'Th17 and regulatory T cell balance in autoimmune and inflammatory diseases', *Autoimmun Rev*, 13: 668-77.

Nourshargh, S., and R. Alon. 2014. 'Leukocyte migration into inflamed tissues', *Immunity*, 41: 694-707.

Nowell, M. A., A. S. Williams, S. A. Carty, J. Scheller, A. J. Hayes, G. W. Jones, P. J. Richards, S. Slinn, M. Ernst, B. J. Jenkins, N. Topley, S. Rose-John, and S. A. Jones. 2009. 'Therapeutic targeting of IL-6 trans signaling counteracts STAT3 control of experimental inflammatory arthritis', *J Immunol*, 182: 613-22.

O'Shea, J. J., and W. E. Paul. 2010. 'Mechanisms underlying lineage commitment and plasticity of helper CD4+ T cells', *Science*, 327: 1098-102.

Ohshima, S., Y. Saeki, T. Mima, M. Sasai, K. Nishioka, S. Nomura, M. Kopf, Y. Katada, T. Tanaka, M. Suemura, and T. Kishimoto. 1998. 'Interleukin 6 plays a key role in the development of antigen-induced arthritis', *Proc Natl Acad Sci U S A*, 95: 8222-6.

Ohta, A., and M. Sitkovsky. 2001. 'Role of G-protein-coupled adenosine receptors in downregulation of inflammation and protection from tissue damage', *Nature*, 414: 916-20.

Okada, Y., D. Wu, G. Trynka, T. Raj, C. Terao, K. Ikari, Y. Kochi, K. Ohmura, A. Suzuki, S. Yoshida, R. R. Graham, A. Manoharan, W. Ortmann, T. Bhangale, J. C. Denny, R. J. Carroll, A. E. Eyler, J. D. Greenberg, J. M. Kremer, D. A. Pappas, L. Jiang, J. Yin, L. Ye, D. F. Su, J. Yang, G. Xie, E. Keystone, H. J. Westra, T. Esko, A. Metspalu, X. Zhou, N. Gupta, D. Mirel, E. A. Stahl, D. Diogo, J. Cui, K. Liao, M. H. Guo, K. Myouzen, T. Kawaguchi, M. J. Coenen, P. L. van Riel, M. A. van de Laar, H. J. Guchelaar, T. W. Huizinga, P. Dieudé, X. Mariette, S. L. Bridges, Jr., A. Zhernakova, R. E. Toes, P. P. Tak, C. Miceli-Richard, S. Y. Bang, H. S. Lee, J. Martin, M. A. Gonzalez-Gay, L. Rodriguez-Rodriguez, S. Rantapää-Dahlqvist, L. Arlestig, H. K. Choi, Y. Kamatani, P. Galan, M. Lathrop, S. Eyre, J. Bowes, A. Barton, N. de Vries, L. W. Moreland, L. A. Criswell, E. W. Karlson, A. Taniguchi, R. Yamada, M. Kubo, J. S. Liu, S. C. Bae, J. Worthington, L. Padyukov, L. Klareskog, P. K. Gregersen, S. Raychaudhuri, B. E. Stranger, P. L. De Jager, L. Franke, P. M. Visscher, M. A. Brown, H. Yamanaka, T. Mimori, A. Takahashi, H. Xu, T. W. Behrens, K. A. Siminovitch, S. Momohara, F. Matsuda, K. Yamamoto, and R. M. Plenge. 2014. 'Genetics of rheumatoid arthritis contributes to biology and drug discovery', *Nature*, 506: 376-81.

Okeke, E. B., and J. E. Uzonna. 2019. 'The Pivotal Role of Regulatory T Cells in the Regulation of Innate Immune Cells', *Front Immunol*, 10: 680.

Onishi, Y., Z. Fehervari, T. Yamaguchi, and S. Sakaguchi. 2008. 'Foxp3+ natural regulatory T cells preferentially form aggregates on dendritic cells in vitro and actively inhibit their maturation', *Proc Natl Acad Sci U S A*, 105: 10113-8.

Orange, D. E., P. Agius, E. F. DiCarlo, N. Robine, H. Geiger, J. Szymonifka, M. McNamara, R. Cummings, K. M. Andersen, S. Mirza, M. Figgie, L. B. Ivashkiv, A. B. Pernis, C. S. Jiang, M. O. Frank, R. B. Darnell, N. Lingampali, W. H. Robinson, E. Gravallese, V. P. Bykerk, S. M. Goodman, and L. T. Donlin. 2018.

'Identification of Three Rheumatoid Arthritis Disease Subtypes by Machine Learning Integration of Synovial Histologic Features and RNA Sequencing Data', *Arthritis Rheumatol*, 70: 690-701.

Ospelt, C., H. Bang, E. Feist, G. Camici, S. Keller, J. Detert, A. Krämer, S. Gay, K. Ghannam, and G. R. Burmester. 2017. 'Carbamylation of vimentin is inducible by smoking and represents an independent autoantigen in rheumatoid arthritis', *Ann Rheum Dis*, 76: 1176-83.

Park, H., Z. Li, X. O. Yang, S. H. Chang, R. Nurieva, Y. H. Wang, Y. Wang, L. Hood, Z. Zhu, Q. Tian, and C. Dong. 2005. 'A distinct lineage of CD4 T cells regulates tissue inflammation by producing interleukin 17', *Nat Immunol*, 6: 1133-41.

Pavelka, K., Y. Chon, R. Newmark, S. L. Lin, S. Baumgartner, and N. Erondu. 2015. 'A study to evaluate the safety, tolerability, and efficacy of brodalumab in subjects with rheumatoid arthritis and an inadequate response to methotrexate', *J Rheumatol*, 42: 912-9.

Penatti, A., F. Facciotti, R. De Matteis, P. Larghi, M. Paroni, A. Murgo, O. De Lucia, M. Pagani, L. Pierannunzii, M. Truzzi, A. Ioan-Facsinay, S. Abrignani, J. Geginat, and P. L. Meroni. 2017. 'Differences in serum and synovial CD4+ T cells and cytokine profiles to stratify patients with inflammatory osteoarthritis and rheumatoid arthritis', *Arthritis Res Ther*, 19: 103.

Petrasca, A., J. J. Phelan, S. Ansboro, D. J. Veale, U. Fearon, and J. M. Fletcher. 2020. 'Targeting bioenergetics prevents CD4 T cell-mediated activation of synovial fibroblasts in rheumatoid arthritis', *Rheumatology (Oxford)*, 59: 2816-28.

Pickens, S. R., M. V. Volin, A. M. Mandelin, 2nd, J. K. Kolls, R. M. Pope, and S. Shahrara. 2010. 'IL-17 contributes to angiogenesis in rheumatoid arthritis', *J Immunol*, 184: 3233-41.

Plosker, G. L., and K. F. Croom. 2005. 'Sulfasalazine: a review of its use in the management of rheumatoid arthritis', *Drugs*, 65: 1825-49.

Putnam, A. L., T. M. Brusko, M. R. Lee, W. Liu, G. L. Szot, T. Ghosh, M. A. Atkinson, and J. A. Bluestone. 2009. 'Expansion of human regulatory T-cells from patients with type 1 diabetes', *Diabetes*, 58: 652-62.

Raphael, I., S. Nalawade, T. N. Eagar, and T. G. Forsthuber. 2015. 'T cell subsets and their signature cytokines in autoimmune and inflammatory diseases', *Cytokine*, 74: 5-17.

Rosloniec, E. F., D. D. Brand, L. K. Myers, K. B. Whittington, M. Gumanovskaya, D. M. Zaller, A. Woods, D. M. Altmann, J. M. Stuart, and A. H. Kang. 1997. 'An HLA-DR1 transgene confers susceptibility to collagen-induced arthritis elicited with human type II collagen', *J Exp Med*, 185: 1113-22.

Rosloniec, E. F., K. Whittington, A. Proslovsky, and D. D. Brand. 2021. 'Collagen-Induced Arthritis Mouse Model', *Curr Protoc*, 1: e313.

Sack, U., R. W. Kinne, T. Marx, P. Heppt, S. Bender, and F. Emmrich. 1993. 'Interleukin-6 in synovial fluid is closely associated with chronic synovitis in rheumatoid arthritis', *Rheumatol Int*, 13: 45-51.

Saini, C., R. K. Srivastava, M. Tarique, S. Kurra, N. Khanna, V. Ramesh, and A. Sharma. 2020. 'Elevated IL-6R on CD4(+) T cells promotes IL-6 driven Th17 cell responses in patients with T1R leprosy reactions', *Sci Rep*, 10: 15143.

Sakaguchi, N., T. Takahashi, H. Hata, T. Nomura, T. Tagami, S. Yamazaki, T. Sakihama, T. Matsutani, I. Negishi, S. Nakatsuru, and S. Sakaguchi. 2003. 'Altered thymic T-cell selection due to a mutation of the ZAP-70 gene causes autoimmune arthritis in mice', *Nature*, 426: 454-60.

Sarkar, S., and D. A. Fox. 2010. 'Targeting IL-17 and Th17 cells in rheumatoid arthritis', *Rheum Dis Clin North Am*, 36: 345-66.

Scherer, H. U., T. Häupl, and G. R. Burmester. 2020. 'The etiology of rheumatoid arthritis', *J Autoimmun*, 110: 102400.

Schinnerling, K., C. Rosas, L. Soto, R. Thomas, and J. C. Aguillón. 2019. 'Humanized Mouse Models of Rheumatoid Arthritis for Studies on Immunopathogenesis and Preclinical Testing of Cell-Based Therapies', *Front Immunol*, 10: 203.

Sechi, A. S., and J. Wehland. 2004. 'ENA/VASP proteins: multifunctional regulators of actin cytoskeleton dynamics', *Front Biosci*, 9: 1294-310.

Sekine, C., T. Sugihara, S. Miyake, H. Hirai, M. Yoshida, N. Miyasaka, and H. Kohsaka. 2008. 'Successful treatment of animal models of rheumatoid arthritis with small-molecule cyclin-dependent kinase inhibitors', *J Immunol*, 180: 1954-61.

Shevach, E. M. 2009. 'Mechanisms of foxp3+ T regulatory cell-mediated suppression', *Immunity*, 30: 636-45.

Skroza, N., I. Proietti, R. Pampena, G. La Viola, N. Bernardini, F. Nicolucci, E. Tolino, S. Zuber, V. Soccodato, and C. Potenza. 2013. 'Correlations between psoriasis and inflammatory bowel diseases', *Biomed Res Int*, 2013: 983902.

Smith, M. D., E. Barg, H. Weedon, V. Papengelis, T. Smeets, P. P. Tak, M. Kraan, M. Coleman, and M. J. Ahern. 2003. 'Microarchitecture and protective mechanisms in synovial tissue from clinically and arthroscopically normal knee joints', *Ann Rheum Dis*, 62: 303-7.

Smolen, J. S., D. Aletaha, J. W. Bijlsma, F. C. Breedveld, D. Boumpas, G. Burmester, B. Combe, M. Cutolo, M. de Wit, M. Dougados, P. Emery, A. Gibofsky, J. J. Gomez-Reino, B. Haraoui, J. Kalden, E. C. Keystone, T. K. Kvien, I. McInnes, E. Martin-Mola, C. Montecucco, M. Schoels, and D. van der Heijde. 2010. 'Treating rheumatoid arthritis to target: recommendations of an international task force', *Ann Rheum Dis*, 69: 631-7.

Smolen, J. S., R. B. M. Landewé, J. W. J. Bijlsma, G. R. Burmester, M. Dougados, A. Kerschbaumer, I. B. McInnes, A. Sepriano, R. F. van Vollenhoven, M. de Wit, D. Aletaha, M. Aringer, J. Askling, A. Balsa, M. Boers, A. A. den Broeder, M. H. Buch, F. Buttgereit, R. Caporali, M. H. Cardiel, D. De Cock, C. Codreanu, M. Cutolo, C. J. Edwards, Y. van Eijk-Hustings, P. Emery, A. Finckh, L. Gossec, J. E. Gottenberg, M. L. Hetland, T. W. J. Huizinga, M. Koloumas, Z. Li, X. Mariette, U. Müller-Ladner, E. F. Mysler, J. A. P. da Silva, G. Poór, J. E. Pope, A. Rubbert-Roth, A. Ruyssen-Witrand, K. G. Saag, A. Strangfeld, T. Takeuchi, M. Voshaar, R. Westhovens, and D. van der Heijde. 2020. 'EULAR recommendations for the management of rheumatoid arthritis with synthetic and biological disease-modifying antirheumatic drugs: 2019 update', *Ann Rheum Dis*, 79: 685-99.

Smolen, Josef S., Daniel Aletaha, and Iain B. McInnes. 2016. 'Rheumatoid arthritis', *The Lancet*, 388: 2023-38.

Sokol, C. L., G. M. Barton, A. G. Farr, and R. Medzhitov. 2008. 'A mechanism for the initiation of allergen-induced T helper type 2 responses', *Nat Immunol*, 9: 310-8.

Stastny, P. 1978. 'Association of the B-cell alloantigen DRw4 with rheumatoid arthritis', *N Engl J Med*, 298: 869-71.

Stockinger, B., and S. Omenetti. 2017. 'The dichotomous nature of T helper 17 cells', *Nat Rev Immunol*, 17: 535-44.

Su, Q., J. Jing, W. Li, J. Ma, X. Zhang, Z. Wang, Z. Zhou, L. Dai, and L. Shao. 2019. 'Impaired Tip60-mediated Foxp3 acetylation attenuates regulatory T cell development in rheumatoid arthritis', *J Autoimmun*, 100: 27-39.

Suzuki, M., M. Hashizume, H. Yoshida, M. Shiina, and M. Mihara. 2010. 'IL-6 and IL-1 synergistically enhanced the production of MMPs from synovial cells by up-regulating IL-6 production and IL-1 receptor I expression', *Cytokine*, 51: 178-83.

Tang, Y., B. Wang, X. Sun, H. Li, X. Ouyang, J. Wei, B. Dai, Y. Zhang, and X. Li. 2017. 'Rheumatoid arthritis fibroblast-like synoviocytes co-cultured with PBMC increased peripheral CD4(+) CXCR5(+) ICOS(+) T cell numbers', *Clin Exp Immunol*, 190: 384-93.

Taniguchi, K., L. W. Wu, S. I. Grivennikov, P. R. de Jong, I. Lian, F. X. Yu, K. Wang, S. B. Ho, B. S. Boland, J. T. Chang, W. J. Sandborn, G. Hardiman, E. Raz, Y. Maehara, A. Yoshimura, J. Zucman-Rossi, K. L. Guan, and M. Karin. 2015. 'A gp130-Src-YAP module links inflammation to epithelial regeneration', *Nature*, 519: 57-62.

Taylor, P. C., M. E. Weinblatt, G. R. Burmester, T. P. Rooney, S. Witt, C. D. Walls, M. Issa, C. A. Salinas, C. Saifan, X. Zhang, A. Cardoso, M. A. González-Gay, and T. Takeuchi. 2019. 'Cardiovascular Safety During Treatment With Baricitinib in Rheumatoid Arthritis', *Arthritis Rheumatol*, 71: 1042-55.

Terao, C., K. Ohmura, K. Ikari, T. Kawaguchi, M. Takahashi, K. Setoh, T. Nakayama, S. Kosugi, A. Sekine, Y. Tabara, A. Taniguchi, S. Momohara, H. Yamanaka, R. Yamada, F. Matsuda, and T. Mimori. 2014. 'Effects of smoking and shared epitope on the production of anti-citrullinated peptide antibody in a Japanese adult population', *Arthritis Care Res (Hoboken)*, 66: 1818-27.

Thome, J. J., K. L. Bickham, Y. Ohmura, M. Kubota, N. Matsuoka, C. Gordon, T. Granot, A. Griesemer, H. Lerner, T. Kato, and D. L. Farber. 2016. 'Early-life compartmentalization of human T cell differentiation and regulatory function in mucosal and lymphoid tissues', *Nat Med*, 22: 72-7.

Thornton, A. M., and E. M. Shevach. 1998. 'CD4+CD25+ immunoregulatory T cells suppress polyclonal T cell activation in vitro by inhibiting interleukin 2 production', *J Exp Med*, 188: 287-96.

Timper, K., J. L. Denson, S. M. Steculorum, C. Heilinger, L. Engström-Ruud, C. M. Wunderlich, S. Rose-John, F. T. Wunderlich, and J. C. Brüning. 2017. 'IL-6 Improves Energy and Glucose Homeostasis in Obesity via Enhanced Central IL-6 trans-Signaling', *Cell Rep*, 19: 267-80.

Tran, C. N., S. K. Lundy, P. T. White, J. L. Endres, C. D. Motyl, R. Gupta, C. M. Wilke, E. A. Shelden, K. C. Chung, A. G. Urquhart, and D. A. Fox. 2007. 'Molecular interactions between T cells and fibroblast-like synoviocytes: role of membrane tumor necrosis factor-alpha on cytokine-activated T cells', *Am J Pathol*, 171: 1588-98.

Trentham, D. E., A. S. Townes, and A. H. Kang. 1977. 'Autoimmunity to type II collagen an experimental model of arthritis', *J Exp Med*, 146: 857-68.

Triaille, C., L. Vansteenkiste, M. Constant, J. Ambroise, L. Méric de Bellefon, A. Nzeusseu Toukap, T. Sokolova, C. Galant, P. Coulie, J. Carrasco, P. Durez, and B. R. Lauwerys. 2020. 'Paired Rheumatoid Arthritis Synovial Biopsies From Small and Large Joints Show Similar Global Transcriptomic Patterns With Enrichment of Private Specificity TCRB and TCR Signaling Pathways', *Front Immunol*, 11: 593083.

Trichet, L., C. Sykes, and J. Plastino. 2008. 'Relaxing the actin cytoskeleton for adhesion and movement with Ena/VASP', *J Cell Biol*, 181: 19-25.

Tripathi, S. K., and R. Lahesmaa. 2014. 'Transcriptional and epigenetic regulation of T-helper lineage specification', *Immunol Rev*, 261: 62-83.

van Amelsfort, J. M., K. M. Jacobs, J. W. Bijlsma, F. P. Lafeber, and L. S. Taams. 2004. 'CD4(+)CD25(+) regulatory T cells in rheumatoid arthritis: differences in the presence, phenotype, and function between peripheral blood and synovial fluid', *Arthritis Rheum*, 50: 2775-85.

van den Berg, W. B. 2009. 'Lessons from animal models of arthritis over the past decade', *Arthritis Res Ther*, 11: 250.

van der Linden, M. P., R. Knevel, T. W. Huizinga, and A. H. van der Helm-van Mil. 2011. 'Classification of rheumatoid arthritis: comparison of the 1987 American College of Rheumatology criteria and the 2010

American College of Rheumatology/European League Against Rheumatism criteria', *Arthritis Rheum*, 63: 37-42.

van Hamburg, J. P., P. S. Asmawidjaja, N. Davelaar, A. M. Mus, E. M. Colin, J. M. Hazes, R. J. Dolhain, and E. Lubberts. 2011. 'Th17 cells, but not Th1 cells, from patients with early rheumatoid arthritis are potent inducers of matrix metalloproteinases and proinflammatory cytokines upon synovial fibroblast interaction, including autocrine interleukin-17A production', *Arthritis Rheum*, 63: 73-83.

van Hamburg, J. P., and S. W. Tas. 2018. 'Molecular mechanisms underpinning T helper 17 cell heterogeneity and functions in rheumatoid arthritis', *J Autoimmun*, 87: 69-81.

van Wesemael, T. J., S. Ajeganova, J. Humphreys, C. Terao, A. Muhammad, D. P. Symmons, A. J. MacGregor, I. Hafström, L. A. Trouw, A. H. van der Helm-van Mil, T. W. Huizinga, T. Mimori, R. E. Toes, F. Matsuda, B. Svensson, S. M. Verstappen, and D. van der Woude. 2016. 'Smoking is associated with the concurrent presence of multiple autoantibodies in rheumatoid arthritis rather than with anti-citrullinated protein antibodies per se: a multicenter cohort study', *Arthritis Res Ther*, 18: 285.

Veldhoen, M., R. J. Hocking, C. J. Atkins, R. M. Locksley, and B. Stockinger. 2006. 'TGFbeta in the context of an inflammatory cytokine milieu supports de novo differentiation of IL-17-producing T cells', *Immunity*, 24: 179-89.

Verpoort, K. N., F. A. van Gaalen, A. H. van der Helm-van Mil, G. M. Schreuder, F. C. Breedveld, T. W. Huizinga, R. R. de Vries, and R. E. Toes. 2005. 'Association of HLA-DR3 with anti-cyclic citrullinated peptide antibody-negative rheumatoid arthritis', *Arthritis Rheum*, 52: 3058-62.

Viglietta, V., C. Baecher-Allan, H. L. Weiner, and D. A. Hafler. 2004. 'Loss of functional suppression by CD4+CD25+ regulatory T cells in patients with multiple sclerosis', *J Exp Med*, 199: 971-9.

Vignali, D. A., L. W. Collison, and C. J. Workman. 2008. 'How regulatory T cells work', *Nat Rev Immunol*, 8: 523-32.

Vincent, T. L., R. O. Williams, R. Maciewicz, A. Silman, and P. Garside. 2012. 'Mapping pathogenesis of arthritis through small animal models', *Rheumatology (Oxford)*, 51: 1931-41.

Wang, T., X. Sun, J. Zhao, J. Zhang, H. Zhu, C. Li, N. Gao, Y. Jia, D. Xu, F. P. Huang, N. Li, L. Lu, and Z. G. Li. 2015. 'Regulatory T cells in rheumatoid arthritis showed increased plasticity toward Th17 but retained suppressive function in peripheral blood', *Ann Rheum Dis*, 74: 1293-301.

Weaver, C. T., R. D. Hatton, P. R. Mangan, and L. E. Harrington. 2007. 'IL-17 family cytokines and the expanding diversity of effector T cell lineages', *Annu Rev Immunol*, 25: 821-52.

Wing, J. B., and S. Sakaguchi. 2012. 'Multiple treg suppressive modules and their adaptability', *Front Immunol*, 3: 178.

Wing, K., Y. Onishi, P. Prieto-Martin, T. Yamaguchi, M. Miyara, Z. Fehervari, T. Nomura, and S. Sakaguchi. 2008. 'CTLA-4 control over Foxp3+ regulatory T cell function', *Science*, 322: 271-5.

Wollenhaupt, J., E. B. Lee, J. R. Curtis, J. Silverfield, K. Terry, K. Soma, C. Mojcik, R. DeMasi, S. Strengholt, K. Kwok, I. Lazariciu, L. Wang, and S. Cohen. 2019. 'Safety and efficacy of tofacitinib for up to 9.5 years in the treatment of rheumatoid arthritis: final results of a global, open-label, long-term extension study', *Arthritis Res Ther*, 21: 89.

Yan, Shuaifeng, Viktoria Golumba-Nagy, Konstantin Kotschenreuther, Jan Thiele, Nasrin Refaian, Deng Shuya, Lydia Gloyer, Mara Dittrich-Salamon, Anja Meyer, Ludwig M. Heindl, and David M. Kofler. 2021. 'Membrane-bound IL-6R is upregulated on Th17 cells and inhibits Treg cell migration by regulating post-translational modification of VASP in autoimmune arthritis', *Cellular and Molecular Life Sciences*, 79: 3.

Yan, Y., D. Ramanan, M. Rozenberg, K. McGovern, D. Rastelli, B. Vijaykumar, O. Yaghi, T. Voisin, M. Mosaheb, I. Chiu, S. Itzkovitz, M. Rao, D. Mathis, and C. Benoist. 2021. 'Interleukin-6 produced by enteric neurons regulates the number and phenotype of microbe-responsive regulatory T cells in the gut', *Immunity*, 54: 499-513.e5.

Zaidel-Bar, R., S. Itzkovitz, A. Ma'ayan, R. Iyengar, and B. Geiger. 2007. 'Functional atlas of the integrin adhesome', *Nat Cell Biol*, 9: 858-67.

Zheng, Y., S. Josefowicz, A. Chaudhry, X. P. Peng, K. Forbush, and A. Y. Rudensky. 2010. 'Role of conserved non-coding DNA elements in the Foxp3 gene in regulatory T-cell fate', *Nature*, 463: 808-12.

Zhou, L., Ivanov, II, R. Spolski, R. Min, K. Shenderov, T. Egawa, D. E. Levy, W. J. Leonard, and D. R. Littman. 2007. 'IL-6 programs T(H)-17 cell differentiation by promoting sequential engagement of the IL-21 and IL-23 pathways', *Nat Immunol*, 8: 967-74.

Zhou, Y., and M. Sun. 2018. 'A meta-analysis of the relationship between body mass index and risk of rheumatoid arthritis', *Excli j*, 17: 1079-89.

Zizzo, G., M. De Santis, S. L. Bosello, A. L. Fedele, G. Peluso, E. Gremese, B. Tolusso, and G. Ferraccioli. 2011. 'Synovial fluid-derived T helper 17 cells correlate with inflammatory activity in arthritis, irrespectively of diagnosis', *Clin Immunol*, 138: 107-16.

Zrioual, S., R. Ecochard, A. Tournadre, V. Lenief, M. A. Cazalis, and P. Miossec. 2009. 'Genome-wide comparison between IL-17A- and IL-17F-induced effects in human rheumatoid arthritis synoviocytes', *J Immunol*, 182: 3112-20.

Zúñiga-Pflücker, J. C. 2004. 'T-cell development made simple', *Nat Rev Immunol*, 4: 67-72.

7 PUBLICATION

Shuaifeng Yan, Viktoria Golumba-Nagy, Konstantin Kotschenreuther, et al. Membrane-bound IL-6R is upregulated on Th17 cells and inhibits Treg cell migration by regulating post-translational modification of VASP in autoimmune arthritis. Cell. Mol. Life Sci. 79, 3 (2022). https://doi.org/10.1007/s00018-021-04076-2

Shuaifeng Yan, Konstantin Kotschenreuther, Shuya Deng, et al. Regulatory T cells in rheumatoid arthritis: function, development, regulation, and therapeutic potential. (Under revision)

8 ERKLÄRUNG

Ich versichere, dass ich die von mir vorgelegt Dissertation selbstständig angefertigt, die benutzten Quellen und Hilfsmittel vollständig angegeben und die Stellen der Arbeit- einschließlich Tabellen, Karten und Abbildungen-, die anderen Werken im Wortlaut oder dem Sinn nach entnommen sind, in jedem Einzelfall als Entlehnung kenntlich gemacht habe; dass diese Dissertation noch keiner anderen Fakultät oder Universität zur Prüfung vorgelegen hat; dass sie - abgesehen von unten angegebenen Teilpublikationen – noch nicht veröffentlicht worden ist sowie, dass ich eine solche Veröffentlichung vor Abschluss des Promotionsverfahrens nicht vornehmen werde.

Die Bestimmungen dieser Promotionsordnung sind mir bekannt. Die von mir vorgelegte Dissertation ist von PD Dr. med. David Kofler betreut worden.

Übersicht der Publikationen:

Shuaifeng Yan, Viktoria Golumba-Nagy, Konstantin Kotschenreuther, et al. Membrane-bound IL-6R is upregulated on Th17 cells and inhibits Treg cell migration by regulating post-translational modification of VASP in autoimmune arthritis. Cell Mol Life Sci. 2021 Dec 16;79(1):3.

Shuaifeng Yan, Konstantin Kotschenreuther, Shuya Deng, et al. Regulatory T cells in rheumatoid arthritis: function, development, regulation, and therapeutic potential. (Under revision)

Ich versichere, dass ich alle Angaben wahrheitsgemäß nach bestem Wissen und Gewissen gemacht habe und verpflichte mich, jedmögliche, die obigen Angaben betreffenden Veränderungen, dem Promotionsausschuss unverzüglich mitzuteilen.

09.2022 Shuaifeng Yan